Author's response to referee comments on "Historical and Future changes in Air pollutants from CMIP6 Models"

Steven T. Turnock et al.
Correspondence to: Steven T. Turnock
(steven.turnock@metoffice.gov.uk)

We would like to thank both of the reviewers for their helpful and constructive comments. Below we have responded to each comment in turn and made alterations to the manuscript where appropriate (shown enclosed in "*speech marks and italic font" and any deletions from the manuscript shown with a strikethrough "~~example~~"*). The referee comments are shown first in grey shading and the author's response is shown below in normal font.

We would like to note that all analyses have been updated based on current model availability to aid in the response to the reviewers comments below. Minor changes to the text and figures have been made to reflect this. This includes the addition of both surface O_3 and $PM_{2.5}$ data from a new CMIP6 model, MRI-ESM2-0. Furthermore, the use of data from the GISS-E2-1-H model has been replaced by that from GISS-E2-1-G, as data is available from both future and historical scenarios with this configuration of the GISS model. A different ocean is coupled to the same atmosphere in the two versions of the GISS-E2-1 model, which does not make any significant changes to the regional simulation of air pollutants. Additional data has also now been included for more future scenarios from CMIP6 models already included within the manuscript. The overall results and conclusions of the paper remain unchanged.

Response to Referee 1

This comprehensive manuscript interrogates past and future changes to surface ozone and PM2.5 air pollution in state-of-the-science multi-model simulations from AerChemMIP/CMIP6 using updated historical and future emissions datasets. The manuscript is thorough and extremely clear and represents a very large simulation and analyses workload involving multiple international institutes. It is important to document the validation of the state of the science global Earth system models and assess the surface air quality responses to past and future global change for new updated emission scenarios. The methodology is sound and the Figures are clear. It may be possible to slightly reduce the number of Figures in the main manuscript further. The multi-model evaluation of surface ozone and PM2.5 is highly valuable to the entire chemistry-climate scientific community. The manuscript discusses changes to both emissions climate, but these are mostly qualitative, and even intuitive, rather than quantitative because none of the applied simulation protocols formally separate out climate change versus emissions change impacts. The authors have done an excellent job with the available datasets and from this perspective the paper is appropriate for publication. However, the results raise some challenging questions about the usage of these global models for surface air quality research. For instance, human health effects calculations depend explicitly on absolute concentrations for exposure. There are some more detailed comments/questions to consider below.

1. The systematic model overestimate of surface ozone across all models is striking (e.g. Fig. 3(c) and (f)). From Fig. 4 for the NAM and EU where there is by far the most data, all models are unable to reproduce the seasonal dynamics (maximum in NH spring and gradually decreasing through the summer months). The authors offer some possible explanations: "The overestimation in the CMIP6 models analysed here could be due to the coarse resolution of the ESMs, an excess of O3 chemical production (potentially due to an overabundance of NOx and/or VOCs) and weak O3 deposition.". If possible, it would be good to have a more robust and clear explanation and

understanding of the systematic overestimate and poor seasonal dynamics? Is the coarse resolution problem related to directly injecting the NOx emissions across the large spatial extent ~2degx2deg (~200km) grid cells? Where the ozone production regime will be highly NOx-limited at this scale? What is needed from the community to improve/address the systematic positive bias in surface ozone simulations in global models?

I would like to thank the reviewer for their comment on the discrepancies between models and observations, which is an ongoing topic of research within the global chemistry climate modelling community. The simulated overestimation of surface O_3 concentrations by CMIP6 models presented in this manuscript is consistent with those from previous work in the comparison of 15 ACCMIP models against TOAR observations by Young et al., (2018). Young et al., (2018) (and references therein to other previous model evaluation studies) also found that ACCMIP models overestimated observed surface O_3 concentrations, as well as simulated peak surface O_3 concentrations later in the year than observations, which is consistent with the seasonality simulated by the CMIP6 models (Fig. 4). The overestimation of observed surface O_3 concentrations in the northern hemisphere is common across global models and is a persistent feature in model evaluations across numerous different generations of models. Therefore, it is most likely that the overestimation is due to an issue that is commonplace across all models, such as uncertainties in emission inventories or processes that are represented in a similar way in models e.g. deposition. Performing additional sensitivity experiments using a range of emission inventories or deposition schemes would aid in the understanding if these were key issues in contributing to the model biases.

One such way to identify drivers of uncertainties in models is to conduct a sensitivity analysis on global chemistry-climate models by analysing the sensitivity of O_3 to variations in different model parameters (Wild et al., 2020). Tropospheric O_3 was found in the study of Wild et al. (2020) to show a large sensitivity to atmospheric water vapour, precursor emissions and dry deposition processes in three global chemistry-climate models. A more detailed global sensitivity study applied specifically to surface O_3 formation, would have the potential to highlight where key areas of research are needed to improve model simulations. Additionally if the sensitivity study were to be combined with observational constraint, as done in other studies for aerosols (Johnson et al., 2019), then this work has the potential to further identify the reasons for model uncertainties and highlight where improvements are needed in the simulation of ozone formation.

When considering the impact that horizontal resolution could have, model evaluation studies using regional composition models (with finer horizontal resolution than global models) across Europe, North America and East Asia have reported improvements in the simulation of surface O_3 when compared to observations, but also that certain models overestimate surface O_3 (Gao et al., 2018; Im et al., 2018). Analysing the impacts of model resolution on tropospheric O_3 production shows improvements in the simulation of O_3 going from ~600 km to 120 km horizontal resolution (reduced O_3 production over polluted regions), but also finds that this resolution is still too coarse to sufficiently resolve regional O_3 production (Wild and Prather, 2006). In addition, a comparison of the simulation of air pollutants using different model resolutions in Neal et al., (2017), highlighted benefits in using higher resolution modelling in the simulation of primary pollutants from improved emissions, but only modest improvements for secondary pollutants like O_3 and $PM_{2.5}$. Enhancing the relatively coarse resolution of global models, and the benefits of higher resolution emissions and other processes, might improve the simulation of surface O_3 but would not necessarily account for all of the model-observational discrepancies.

Whilst the aim of the current study was to highlight discrepancies in surface O_3 between the latest generation of CMIP6 models and observations, it was not intended to provide a detailed explanation

of the causes of this discrepancy within individual models. Further work is required to explore the reasons for the differences between individual CMIP6 models and observations, which would need to be the subject of future research, potentially using global sensitivity analysis, process studies and simulations at finer resolution.

However, a couple of changes to the manuscript have been included below to improve the description of the evaluation work.

The sentences on Page 9 line 266-268 have been amended to the following:

"*The model observational comparison of CMIP6 models to the TOAR observations are consistent across all models and with the previous evaluation of ACCMIP models (*Young et al., 2018) *. This indicates a common source of error within models, for example uncertainties in emission inventories, deposition processes or vertical mixing (Wild et al., 2020). In addition, the coarse resolution of the ESMs could lead to an overproduction of O_3 across polluted regions, with finer resolutions exhibiting improvements in the simulation of surface O_3 (Wild and Prather, 2006; Neal et al., 2017).*"

A new sentence has been included on page 30 line 640:

"*The comparison of surface O_3 and $PM_{2.5}$ simulated by CMIP6 models to observations shows similar biases to previous generations of global composition-climate models. Further studies are required (e.g. global sensitivity or process studies) to explore the uncertainties in models and the differences with observations.*"

2. The systematic underestimate in monthly PM2.5 in NAM, EU and EAS (Fig. 6) is troubling. Can it really be explained only by the missing nitrate component? Are there other fundamental missing or misrepresented processes? Output from these models is more frequently being used to assess health impacts, for example, premature mortality due to outdoor air pollution exposure (PM2.5 and ozone) but such application would not be justified based on the model/measurement comparison here. It could be argued from the model/measurement evaluation that the models cannot be applied as tools to study the surface air quality?

The reviewer is correct in that the underestimation of observed $PM_{2.5}$ by the CMIP6 models cannot be solely attributed to the exclusion of nitrate aerosol mass but is potentially due to a number of issues, which are also found in other model evaluation studies. Figure S12 (now S13) shows that the surface mass concentrations of nitrate aerosols from two CMIP6 models could make a small contribution to the total $PM_{2.5}$ concentrations, particularly in northern hemisphere winter months (Bauer et al., 2016). On page 13 lines 326 to 328 we mention that including the nitrate aerosol mass fraction could account for some, but not all of the discrepancy in $PM_{2.5}$ between models and observations. In addition, the MERRA-2 reanalysis product has been constructed in the same way as $PM_{2.5}$ has been computed from the CMIP6 models, by not including the mass from nitrate aerosols. Page 13 lines 328 to 330 makes the point that the CMIP6 models still show an underestimation of the MERRA-2 product, and that differences are due to errors in other aerosol sources and processes.

Other studies performing single and multi-model evaluation of global and regional models against observations across North America, Europe and Asia found that simulated concentrations of fine mode aerosols tended to be underestimated due to a number of possible reasons including: errors in emissions, simulated meteorology and aerosol formation mechanisms for both inorganic and secondary organic aerosols (Tsigaridis et al., 2014; Pan et al., 2015; Glotfelty et al., 2017; Solazzo et al., 2017; Im et al., 2018). On page 12 lines 313 to 317 of the manuscript we highlighted the potential

reasons for some of the model-observational discrepancy and the similarity to other studies. This text has now been slightly modified to the following:

"*Nevertheless, the evaluation highlights that fine particulate matter ($PM_{2.5}$) is generally underrepresented in the CMIP6 models across North America, Europe and parts of Asia for which observations are available; a similar result to other studies evaluating global and regional models (Tsigaridis et al., 2014; Pan et al., 2015; Glotfelty et al., 2017; Solazzo et al., 2017; Im et al., 2018). Numerous reasons potentially exist for the model observation discrepancy shown here and in other studies including uncertainties in emissions inventories (e.g. local dust sources), errors in wet/dry deposition, the absence/underrepresentation of aerosol formation processes (e.g. organic aerosols) and the coarse resolution of global models leading to errors in emissions and simulated meteorology. Understanding the causes of model observational discrepancies is an area of active research and should be explored in further research, for example in a global multi-model sensitivity study that explores model uncertainties.*"

The reviewer points out that the underestimation of $PM_{2.5}$ by CMIP6 models might preclude their use for studying the health impacts of air quality. Air pollutant concentrations from coarser resolution models have previously been shown to produce lower health impacts than those from models with a finer horizontal resolution (Punger and West, 2013; Li et al., 2016; Silva et al., 2016a). However, air pollutant concentrations from global model simulations (including those of CMIP5 models) have been successfully utilised in health impact studies by using the change in concentrations between the future and present day (as they are able to reproduce the relationship between concentrations and emissions/climate, see response to point 3 below) or applying correction factors to account for the anticipated underestimations in concentrations in the present day, particularly across urban areas (Silva et al., 2016b; Butt et al., 2017; Chowdhury et al., 2018; Bauer et al., 2019). It should also be noted that there are large uncertainties in the exposure response functions used in health impact studies that relate exposure of air pollutants to human health impacts (Jerrett et al., 2009; Burnett et al., 2014). Health impact studies, including those used within the global burden of disease assessment, have used a combination of global modelling, satellite remote sensing products and ground based observations to generate $PM_{2.5}$ concentrations with greater precision, reducing some of the simulated biases from global composition models (van Donkelaar et al., 2010; Brauer et al., 2016; Jerrett et al., 2017). We would therefore recommend that any studies wanting to use output from CMIP6 models to study the future health impacts from changes in air quality consider the different techniques and methods outlined in some of the above studies.

3. How reliable are the model simulations of past and future changes when the monthly mean surface air quality concentrations cannot be reproduced by the models and there are clear systematic biases?

Whilst there are model observational biases in the absolute magnitude of the present day simulations of both surface O_3 and $PM_{2.5}$ in the CMIP6 models, there is some confidence in the ability of models to simulate temporal changes when compared to long-term historical observations.

Long term changes in surface O_3 concentrations from CMIP6 models have been evaluated in the tropospheric O_3 CMIP6 companion paper of Griffiths et al., (2019) at four remote locations with the longest observational record over the second half of the twentieth century. Figure 4 of Griffiths et al., (2019) shows that the CMIP6 models are able to reproduce the observed multi-decadal changes in surface O_3, providing some confidence in the ability of CMIP6 models to simulate future changes. Young et al., (2018) presented a summary of the ability of the previous generation of global chemistry

climate models to simulate long term changes in surface O_3 based on the comparisons in Parrish et al., (2014). This showed that selected CMIP5 models had areas of agreement and disagreement with long-term measurements of O_3 concentrations at northern midlatitudes. However, the models were reported to underestimate the observed long-term changes in surface O_3 by ~50%. The evaluation highlighted a number of limitations in long-term comparisons from uncertainties in emission changes, observational records, sampling biases and low frequency variability influencing observed O_3 concentrations that is not simulated by models. Therefore, any future predictions of changes in surface O_3 by CMIP6 models could be similarly uncertain and represent a conservative estimate of change. The long-term comparison of models and observations is an area of active research and is currently being undertaken in other studies using output from CMIP6 models, with any results from this providing information on the ability of CMIP6 models to simulate changes in surface O_3.

The absence of long historical records of fine particulate matter concentrations at the surface have limited the ability to evaluate any changes simulated by models over a multi-decadal period. The longest records of such data exist over Europe and North America and this is where long-term evaluations have tended to be focussed. Studies evaluating global composition models over these regions and at other locations have tended to show that models are able to reproduce the multi-decadal trends in aerosol components, particularly sulphate, and aerosol optical depth (AOD) (Lamarque et al., 2010; Pozzoli et al., 2011; Leibensperger et al., 2012; Chin et al., 2014; Turnock et al., 2015; Aas et al., 2019). CMIP5 models were previously shown to have a reasonable reproduction of satellite trends in AOD since the 1980s (Shindell et al., 2013). Simulated aerosol trends in AOD, sulphate and particulate matter from global composition models, including a number of CMIP6 models, have been shown to be able to reproduce observed changes over the last two decades (Mortier et al., 2020). These studies all provide confidence in the simulation of past and future changes in fine particulate matter within global composition models, even though the magnitude of present day concentrations is underestimated.

There is some confidence in the ability of global models to reproduce long term observed changes in air pollutants from previous studies, although this will require further research using the latest generation of models contributing to CMIP6 to understand the reasons for any discrepancies. Nevertheless, multi-decadal changes in air pollutants simulated by CMIP6 models in different future scenarios provide a useful indication of future changes in air pollutants under different pathways of emissions and climate change, even if there are potential uncertainties associated with the projections.

The ability of CMIP6 models to reproduce long term changes in surface O_3 was mentioned on p18, lines 384-386. We have amended this sentence to that below for additional clarity.

"An evaluation of the long-term changes in surface O_3 over the historical period simulated by the CMIP6 models at specific measurement locations is presented separately in the tropospheric O_3 CMIP6 companion paper of Griffiths et al., (2019). This shows that the CMIP6 models can reasonably represent long term changes in surface ozone since the 1960s, providing a degree of confidence in the future projection of changes in the CMIP6 scenarios. However, long term changes in simulated surface O_3 from the previous generation of global composition climate models (CMIP5) were found to underestimate the observed trend at northern hemisphere monitoring locations (Parrish et al., 2014). Further comparisons of long-term historical observations of surface O_3 with that simulated by CMIP6 models is outside the scope of the current work but will be the subject of future research."

The sentence on page 20 lines 416-418 has been replaced with the following:

"*There is limited long-term multi-decadal observational data available to assess changes in aerosols simulated by global models. Previous studies using long-term data since the 1980s, mainly over Europe and North America, have found that global models are able to reproduce the observed multi-decadal changes in aerosols relatively well (Pozzoli et al., 2011; Leibensperger et al., 2012; Tørseth et al., 2012; Chin et al., 2014; Turnock et al., 2015; Aas et al., 2019). More recently, global composition models, including some CMIP6 models, were shown to be able to reproduce the observed changes in AOD, sulphate and particulate matter over the last two decades (Mortier et al., 2020). The ability of global composition models to reproduce historical changes in aerosols provides a degree of confidence in the future projections under the CMIP6 scenarios. Further model observational comparisons of multi-decadal changes in aerosols will need to be undertaken to improve the understanding of changing aerosol properties and processes.*"

4. Fig. 9. I find this Figure also striking in the diversity of model results for historical surface ozone evolution. Why does the GISS model have such large changes/sensitivities to the PI-PD? Esp. for Europe, S. Asia and E. Asia (but not SE Asia + less polluted SH regions)? Does the GISS model gas-phase chemistry have a larger sensitivity to NOx changes than other models and why? The GISS model is also an outlier in Fig. 10 for evolution of PM2.5 over S. Asia region specifically? What is the value of the multimodel mean in e.g. Fig. 13 when there is such large diversity of sensitivities shown in Figs. 9&10?

As the reviewer points out, Figure 9 shows that there is a large diversity in the regional surface O_3 response over the historical period across the CMIP6 models. In the revised manuscript the regional surface O_3 response from an additional model (MRI-ESM2-0) has been included on Figure 9, which doesn't change the overall result but adds to the multi-model mean.

Further investigation has been undertaken into the different historical changes in surface O_3 concentrations from CMIP6 models with the regional annual mean absolute concentrations over the historical period shown in a new Figure S15 below and the spatial annual mean concentrations in 2005-2014, 1980-1989 and 1850-159 shown in a new Figure S14 below. Figure S14 and S15 show that there is a range of surface O_3 concentrations simulated by CMIP6 models over different regions particularly in 1850, with more agreement between models towards the present day. However, there is a noticeable difference in the regional change of simulated surface O_3 concentrations over the historical period in different models (Fig. S15). Out of all the CMIP6 models, UKESM1 tends to simulate some of the smallest changes in regional annual mean surface O_3 concentrations over the historical period due to having larger concentrations in the 1850s and some of the smallest concentrations in recent decades. Whilst the opposite response is true for simulated regional annual mean surface O_3 concentrations in the GISS-E2-1-G model (smallest 1850 and largest 2015 concentrations), resulting in some of the largest regional mean changes in annual mean surface O_3 shown on Figure 9.

Uncertainties in the simulation of pre-industrial O_3 concentrations across models is one of the contributing factors to the diversity of the response in historical surface O_3 across models. Figure S14 shows that there is significant diversity in the simulated pre-industrial O_3 concentrations across CMIP6 models due to the lack of observation data for validation purposes. Uncertainties arise in the simulation of the pre-industrial O_3 state due to differences in meteorology and chemical mechanisms, in particularly the simulation of NOx and natural emission sources of O_3 precursors (isoprene) in this period, which can dominate O_3 formation.

In addition, the difference in the historical simulation of surface O_3 concentrations across CMIP6 models could be due to the chemical sensitivity of each model to NOx concentrations in the different time periods and the change in concentrations between them. A comparison of the regional annual

mean surface O_3 concentrations and regional annual mean NOx (NO + NO_2) concentrations for three time periods (new Figure S17 as shown below) highlights the different chemical sensitivities of O_3 formation to NOx across models. Across most regions the higher NOx concentrations in UKESM1 have tended to result in higher surface O_3 concentrations in the 1850s and lower in the present day. Whereas for GISS-E2-1-G the lower NOx concentrations have tended to result in the lower surface O_3 concentrations in the 1850s and higher concentrations in the present day period, indicating a shift in chemical environments over time. The large sensitivity of O_3 formation to surface NOx concentrations in the GISS model was also shown in the global sensitivity study of Wild et al., (2020). The sensitivity of surface O_3 formation to different historical NOx concentrations is particularly noticeable in most models over South Asia (due to the large regional changes in NOx) but especially evident in GISS-E2-1-G, which results in its large surface O_3 response over this region. Additionally, the large increase in $PM_{2.5}$ over the historical period in South Asia (Fig. S18 below) could also influence the heterogeneous loss of radicals to aerosols and therefore also changes to O_3.

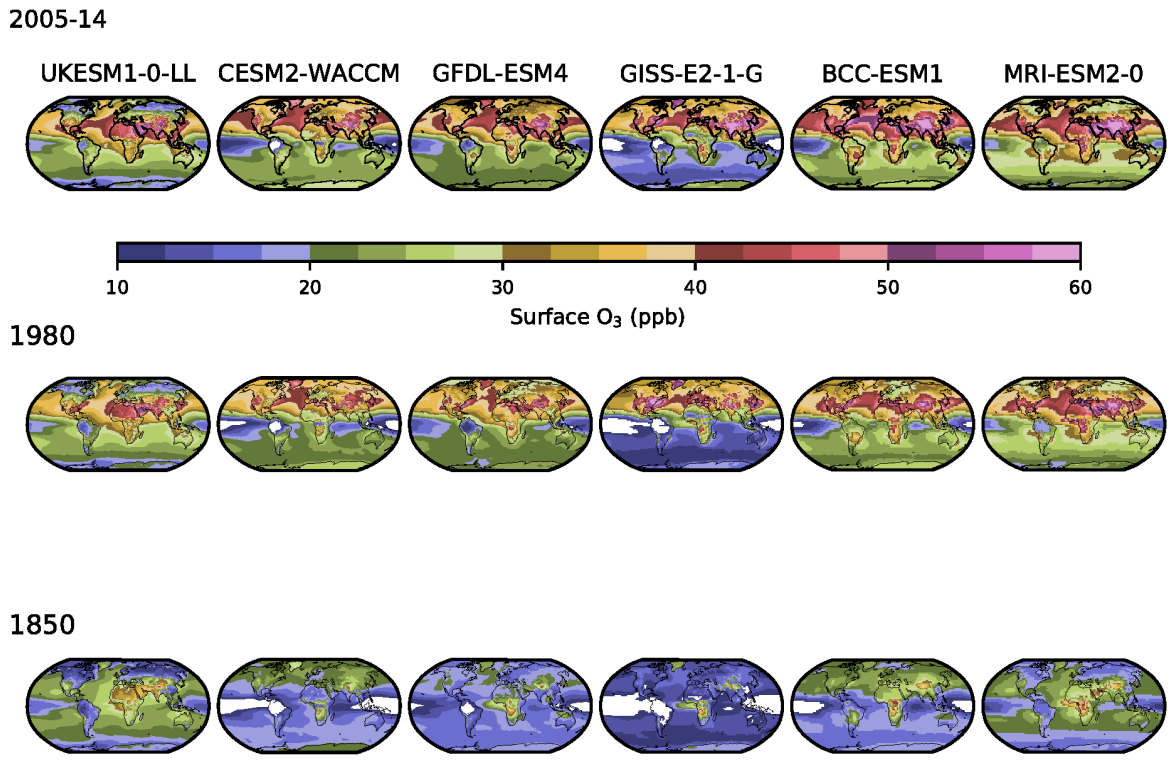

Figure S14 - Annual mean surface O_3 concentrations across 6 CMIP6 models over the period 2005-2014 (top row), 1980-1989 (middle row) and 1850-1859 (bottom row).

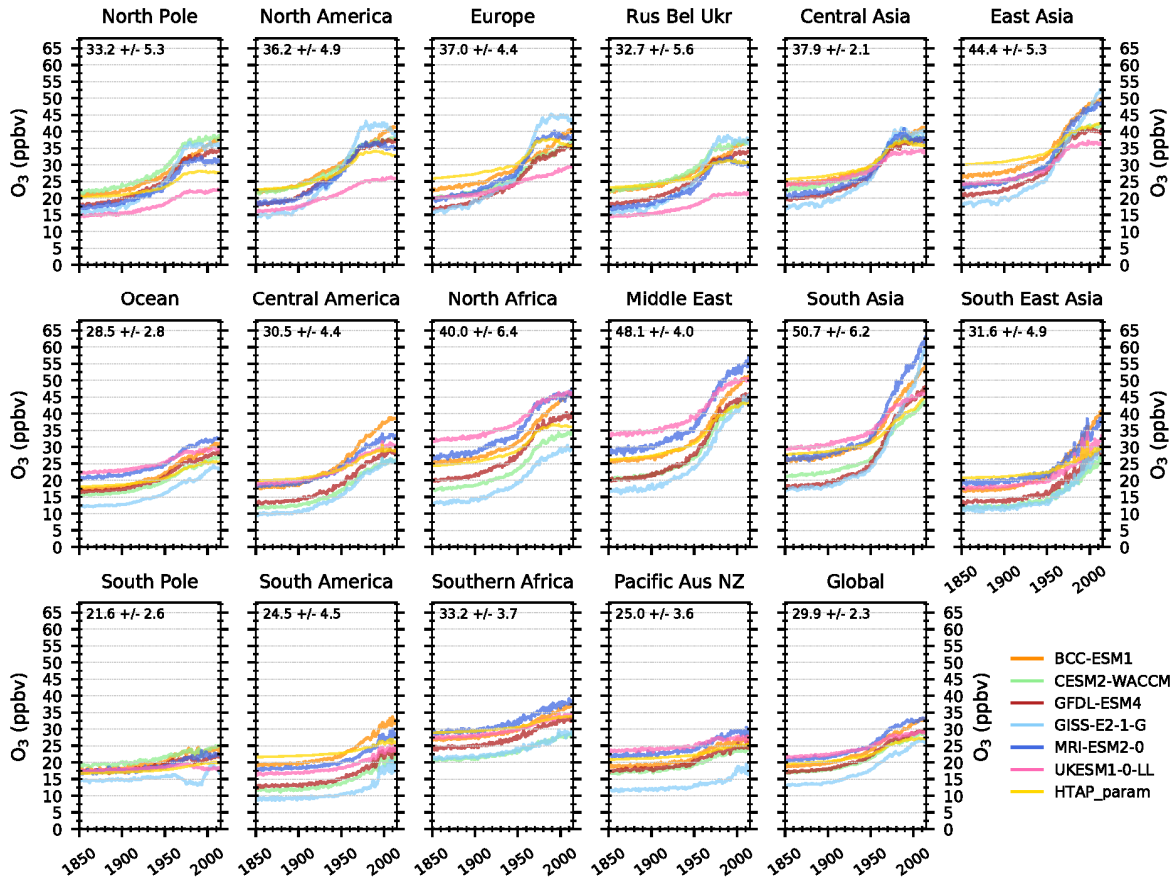

Figure S15 - Regional and global annual mean surface O_3 concentrations across 6 CMIP6 models and the HTAP_param. The multi-model annual mean year 2005-2014 surface O_3 concentrations (+/- 1 standard deviation) are shown in the top left of each panel. Regions are defined in Figure S1.

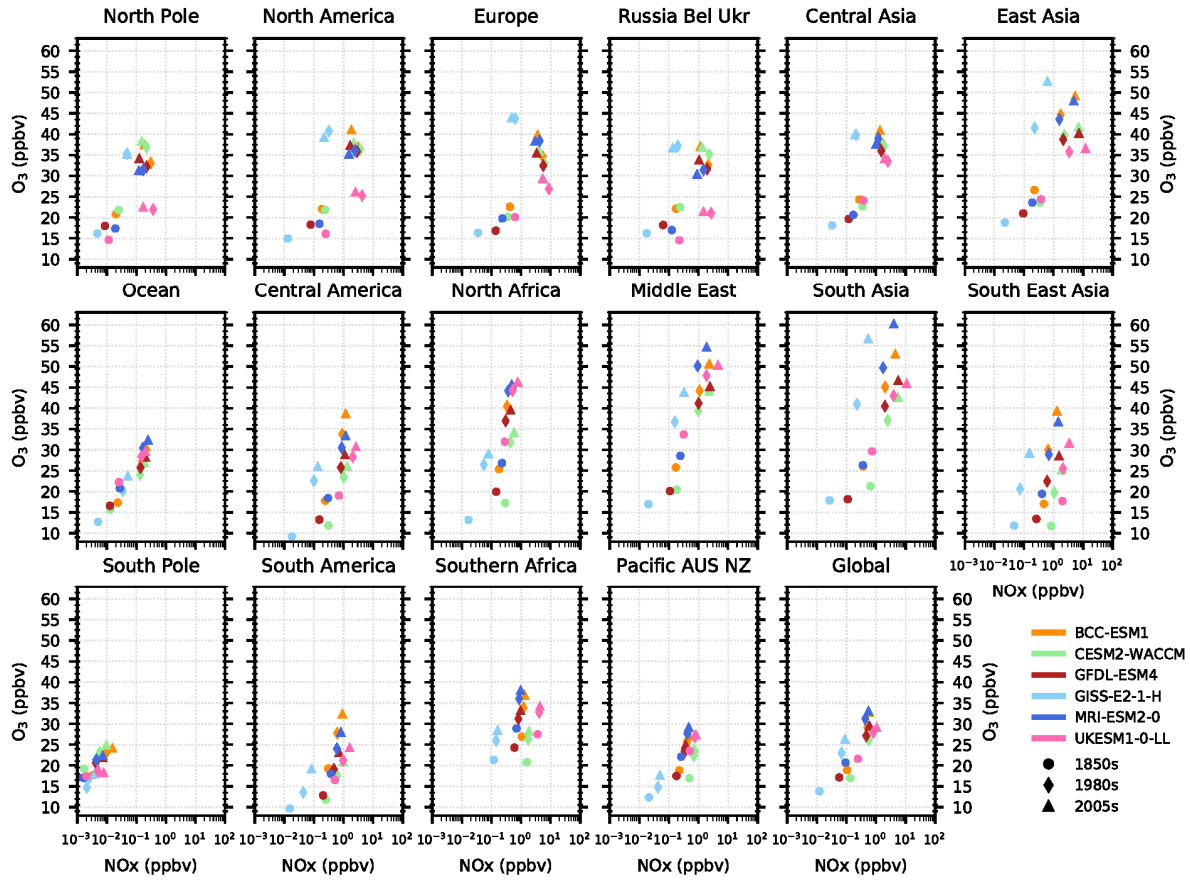

Figure S17 – Annual mean regional surface O_3 concentrations compared to regional annual mean surface NOx ($NO + NO_2$) concentrations across 6 CMIP6 models over three ten-year periods of 1850-1859 (circles), 1980-1989 (diamonds) and 2005-2014 (triangle).

As the reviewer points out the change in historical surface $PM_{2.5}$ from GISS-E2-1-G on Figure 10 is also shown to be smaller than other CMIP6 models over South Asia. Like for surface O_3, a revised Figure 10 has now been produced to include the additional model results from MRI-ESM2-0, which hasn't altered the overall result. A new Figure S18 below shows the pre-industrial to present day change in total annual mean surface $PM_{2.5}$ and from each individual component. Looking at the historical change in each aerosol component highlights that over South Asia, the response in GISS-E2-1-G is the smallest from all CMIP6 models for sulphate and one of the smallest for black carbon and organic aerosol. The combination of the smaller response in all anthropogenic aerosol components from GISS-E2-1-G over South Asia results in the smaller response in historical total $PM_{2.5}$ concentrations shown on Figure 10 and below.

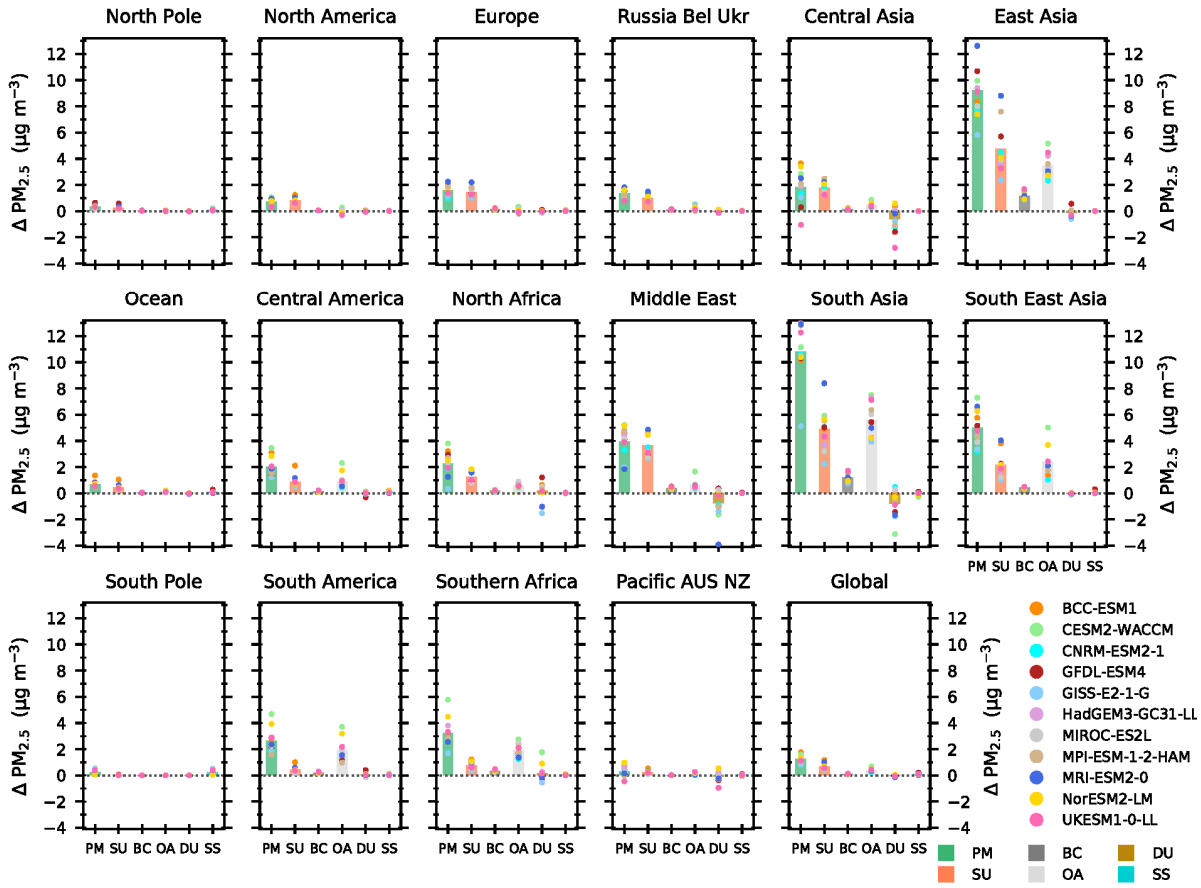

Figure S18 – Pre-industrial (1850-1859 mean) to present day (2005-2014 mean) changes in the regional and global annual mean surface total $PM_{2.5}$ concentrations (PM) and that from each individual component (BC – black carbon, DU – dust, SU – sulphate, OA – organic aerosol and SS – sea salt). Individual circles represent each annual and seasonal mean changes from the 11 individual CMIP6 models, with the multi-model mean represented by the solid bar. The. Regions are defined in Figure S1.

Showing the diversity in response across CMIP6 models is useful as this identifies where the models (with different chemistry and meteorology) agree but also where there is disagreement and uncertainties in the simulated surface O_3 response. This could help identify further research priorities to understand the differences between models. The multi-model means shown on Figure 11 and 13 (now Fig. 14) also contain a shaded area which shows the diversity in the simulated response across CMIP6 models (+ 1 standard deviation of the multi-model mean). We feel that it is useful to show the multi-model mean as it provides a degree of confidence in the future projections and allows the reader to identify where there is agreement between models in the simulated future response (such as Europe) but also where there is disagreement and uncertainty in the range of potential future model responses (e.g. over South Asia in ssp370). Where there is significant model diversity, we feel that including a multi-model mean with a degree of uncertainty provides useful information on the confidence in future predictions of surface air pollutants across different CMIP6 models.

We have made the following changes to the manuscript to reflect the above discussion on historical changes in surface O_3 and $PM_{2.5}$.

The sentence on page 17, line 379 has been amended as follow:

"*The simulated changes in surface O_3 across 6 CMIP6 models and the HTAP_param are shown in Figure 9 and Figure S14-S15 over the historical period of 1850 to 2014.*"

A new sentence has been inserted on Page 18, line 388.

"*The large diversity across CMIP6 models in the surface O_3 response over the historical period can be attributed to the different magnitude of simulated O_3 concentrations in the 1850 period (Figure S14) and the rate of change in regional mean O_3 concentrations (Figure S15), which is related to the different chemical sensitivity of O_3 formation in each model to changing NOx concentrations over the historical period (Figure S17).*"

The sentence on page 18, line 391 has been amended to the following:

"*South Asia is the region with the largest diversity in simulated historical changes in surface O_3 of between 16 and 40 ppb, with a larger range in DJF (10-40 ppb) than in JJA (19-36 ppb). The large diversity in CMIP6 models is attributed to the large differences in simulated NOx concentrations, and hence chemical sensitivities of O_3 formation, occurring across South Asia (Figure S17). In addition, the large historical change in $PM_{2.5}$ over this region* (Fig. S18) *could alter the heterogeneous loss rate of radicals to aerosols and therefore also affect O_3 formation.*"

The sentence on Page 19, line 410-412 has been amended as follows:

"*The largest model diversity is also exhibited over the Asian regions with variations in the response between models of up to 50%, ~~potentially simulation dust emissions and simulation of organic aerosols~~ with larger differences between models in DJF than JJA (Figure S16), reflecting the differences shown in the present day model evaluation (Fig. 6). The inter-model differences can be attributed to the different simulation of historical changes in the anthropogenic components sulphate, black carbon and organic aerosols (Figure S18).*"

5. "Surface O3 increases across most world regions in this scenario can be attributed to the large increase in global CH4 abundances (80%) and the large predicted increase in surface temperatures". Why do increases in surface temperature increase surface ozone concentrations independent of emissions? What is the mechanism? Is it temperature, or co-varying stagnation or light/downward SW? How do we know it is temperature with 100% certainty as stated here?

We thank the reviewer for the comment on this particular sentence, which was an attempt to identify the importance of changes in CH_4 and climate on regional surface O_3 concentrations in the ssp370 scenario, despite the reductions in precursor emissions over certain regions. Previous work has shown that climate change can have an important impact on surface and tropospheric O_3 concentrations; the ozone climate penalty (Rasmussen et al., 2013; Stevenson et al., 2013; Colette et al., 2015). In addition, the importance of future changes in global CH_4 abundance for surface O_3 concentrations has been previously shown (Fiore et al., 2009; Wild et al., 2012; Young et al., 2013; Turnock et al., 2019). Therefore, the purpose of the sentence mentioned by the reviewer was to highlight the continued importance of these drivers in the SSPs used in CMIP6 models, although we appreciate that the sentence needs to be clearer.

Therefore, the sentence on P21 line 443 has been amended to improve its clarity as follow:

"*Despite the reductions in O_3 precursor emissions across North America, Europe and East Asia by 2100 (Fig. 2) surface O_3 concentrations have continued to increase up to the end of this period, indicating the importance of future changes in chemistry, global CH_4 abundances and climate on the response of surface O_3 in ssp370* (Wild et al., 2012; Gao et al., 2013; Rasmussen et al., 2013; Young et al., 2013; Colette et al., 2015; Fortems-Cheiney et al., 2017; Li et al., 2017; Turnock et al., 2019)."

In addition, future model experiments utilising a fixed climate signal, as well sensitivity studies involving CH_4, are currently being undertaken by the Aerosol Chemistry Model Intercomparison Project (AerChemMIP). This will enable the quantification of the impact from changes in climate and CH_4 on future air pollutants, which will inform future studies on the importance of these processes.

6. "across East Asia the additional precursor emission reductions in ssp370-lowNTCF have made little difference to surface O3 concentrations predicted by the CMIP6 models, indicating that other factors are more important over this region (chemistry or climate change)." This result is critically important. So, aggressive mitigation of ozone precursors has no impact on the surface ozone concentrations in this region relative to a scenario with those precursors? What is the reason for surface ozone in East Asia to be independent of ozone precursor emission changes under this level of global change? Further explanation is needed. Are there climatic feedbacks from the precursors themselves that are offsetting the changes?

The apparent small change in surface O_3 for the ssp370-lowNTCF scenario over East Asia can be initially attributed to only having a three model ensemble of results available for this future scenario at the time of manuscript submission. One model (BCC-ESM1) shows a larger response of surface O_3 in 2050 in both the ssp370 (original Figure S14, now changed to S19) and ssp370-lowNTCF scenarios than the other two models, which had a disproportionate impact on the multi-model mean shown in Figure 11. Since submission of the original manuscript, surface O_3 concentrations have become available from an additional two CMIP6 models for ssp370-lowNTCF (MRI-ESM2-0 and UKESM1-0-LL) which have now been included in the analysis to provide additional information for the explanation of the different surface O_3 response over East Asia in the ssp370 and ssp370-lowNTCF scenarios.

A revised Figure S14 (shown below and now Figure S19) has been included in the manuscript along with a new Figure S20 (shown below) showing the change in surface O_3 in the ssp370-lowNTCF scenario from CMIP6 models. The surface O_3 change in the BCC-ESM1 model is larger in both of the scenarios compared to other CMIP6 models. The difference between the 2050 panels in both figures (Figure R1) shows that the more aggressive mitigation measures in ssp370-lowNTCF have reduced future increases in surface O_3 concentrations across most world regions, compared to the response in ssp370. The notable exception is across Eastern China, a part of the larger East Asian region defined in Figure S1, where surface O_3 concentrations increase in ssp370-lowNTCF consistently across all models compared to ssp370. The increase in surface O_3 in all models for ssp370-lowNTCF over Eastern China can be attributed to a small increase in NMVOC emissions (Fig. 2) and a large decrease in NOx emissions (from a high initial value), which reduces the NOx titration of O_3 over this area. The decrease in $PM_{2.5}$ concentrations over Eastern China (Figure R2) could also reduce the heterogeneous loss of radicals (e.g. N_2O_5, HO_2) to aerosols in ssp370-lowNTCF, compared to ssp370, and is another process that could be important in explaining the increase in surface O_3, but will need further investigation (Li et al., 2019). The increase in surface O_3 over Eastern China is responsible for the smaller benefits simulated in the ssp370-lowNTCF scenario over the larger East Asia region (where the averaging takes into account both increases and decreases across the region). Further sensitivity experiments will be required to allow for a full quantification of the impacts from changes in chemistry and climate across different models in the ssp370 and ssp370-lowNTCF over the East Asia region.

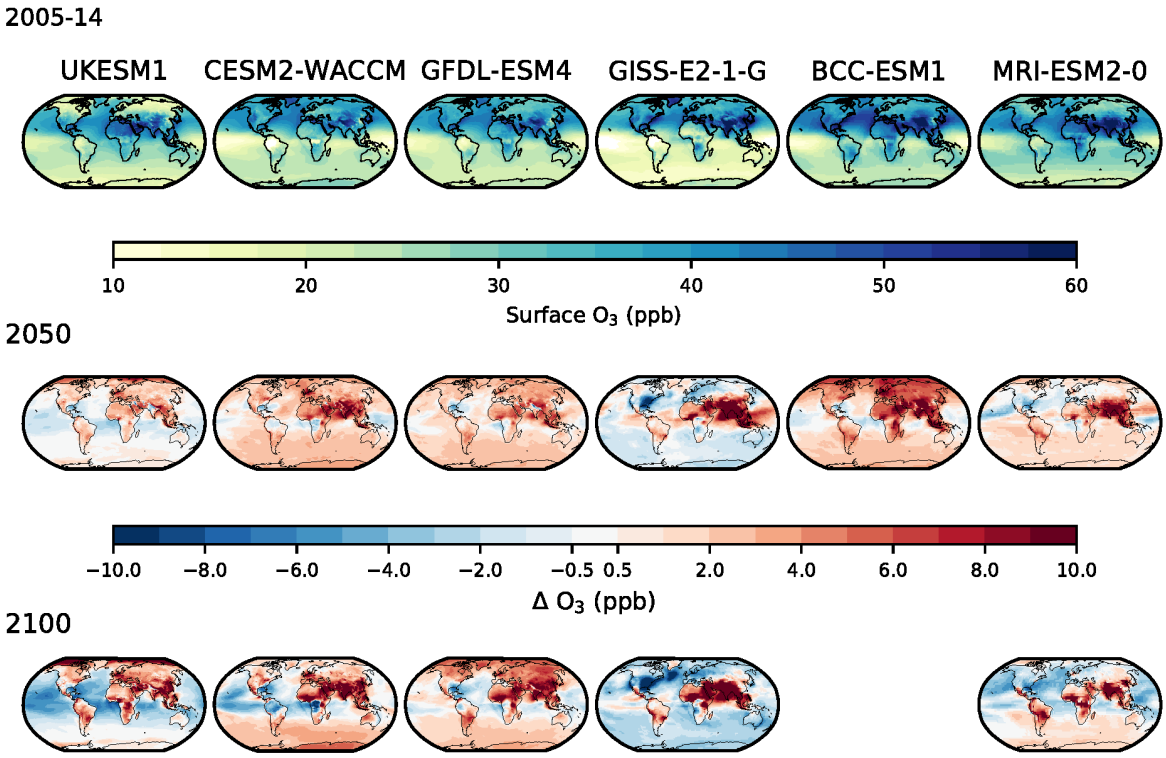

Figure S19 – Annual mean surface O_3 concentrations and future response in ssp370 across 6 different CMIP6 models. Top row shows the 2005-2014 annual mean surface O_3 concentrations in each model from the historical simulations. Middle row shows the surface O_3 response in 2050, relative to 2005-2014 mean, in each model for ssp370. Bottom row shows the same as the middle but for 2100. No data is presented in 2100 for BCC-ESM1 as data for ssp370 only extended out to 2055.

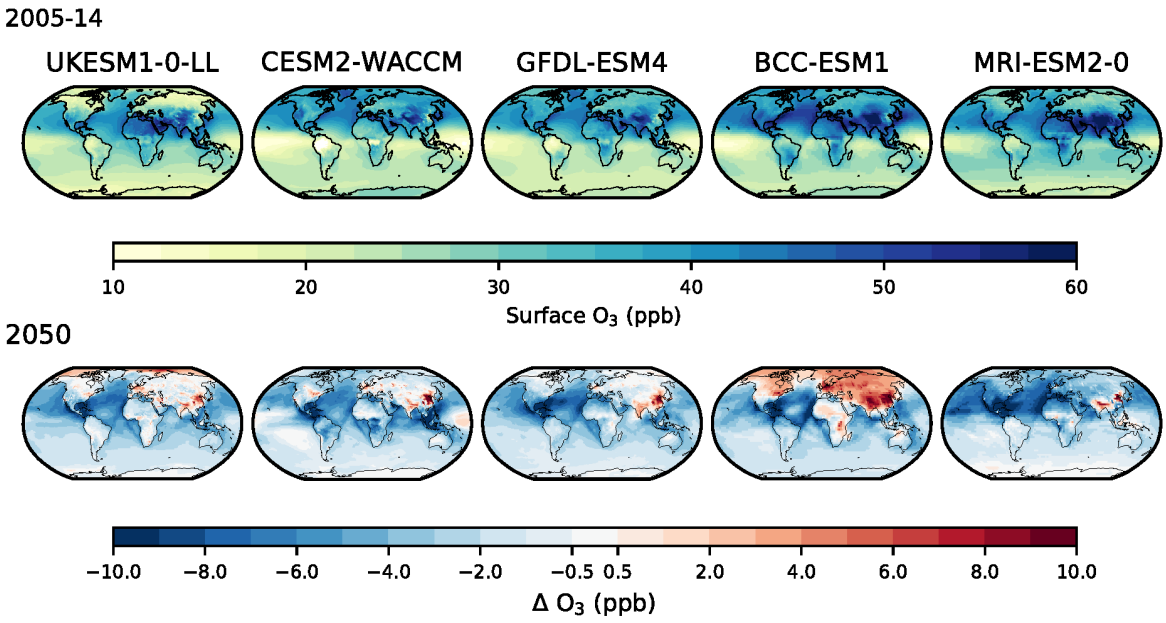

Figure S20 – Annual mean surface O_3 concentrations and future response in ssp370-lowNTCF across 5 different CMIP6 models. Top row shows the 2005-2014 annual mean surface O_3 concentrations in each model from the historical simulations. Bottom row shows the surface O_3 response in 2050, relative to 2005-2014 mean, in each model for ssp370-lowNTCF.

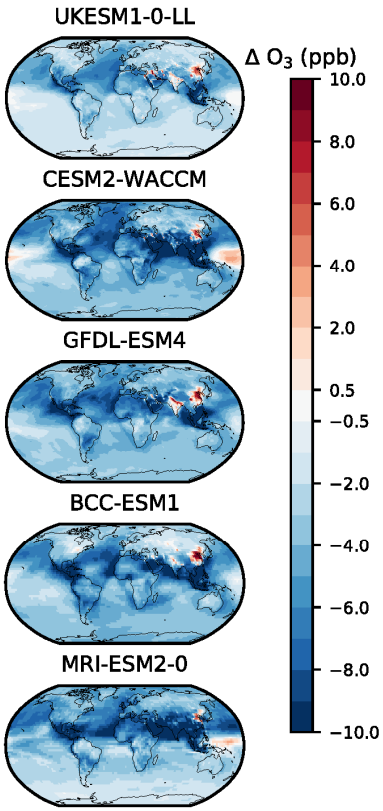

Figure R1 – Difference in annual mean surface O_3 for 5 CMIP6 models between ssp370-lowNTCF and ssp370 in 2050.

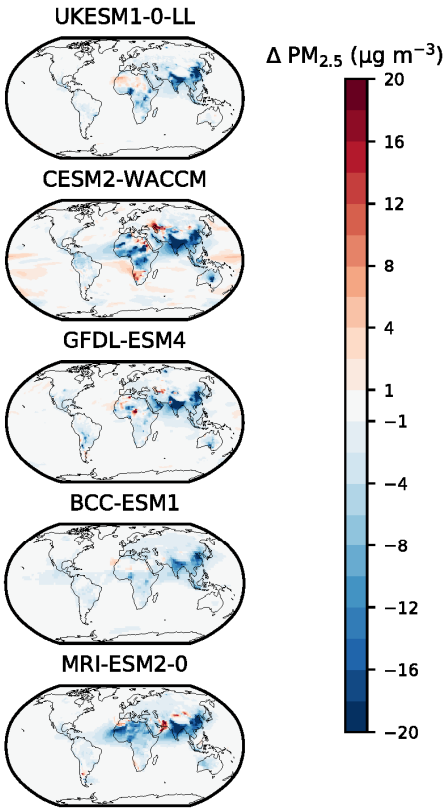

Figure R2 – Same as Fig. S1 but for surface $PM_{2.5}$.

An amended version of Figure 11 has now been included in the manuscript (and shown below) using the additional available model data. This shows a regional reduction in surface O_3 concentrations across East Asia in the ssp370-lowNTCF scenario compared to the ssp370, highlighting the benefit, albeit small, from the additional mitigation measures to O_3 precursors.

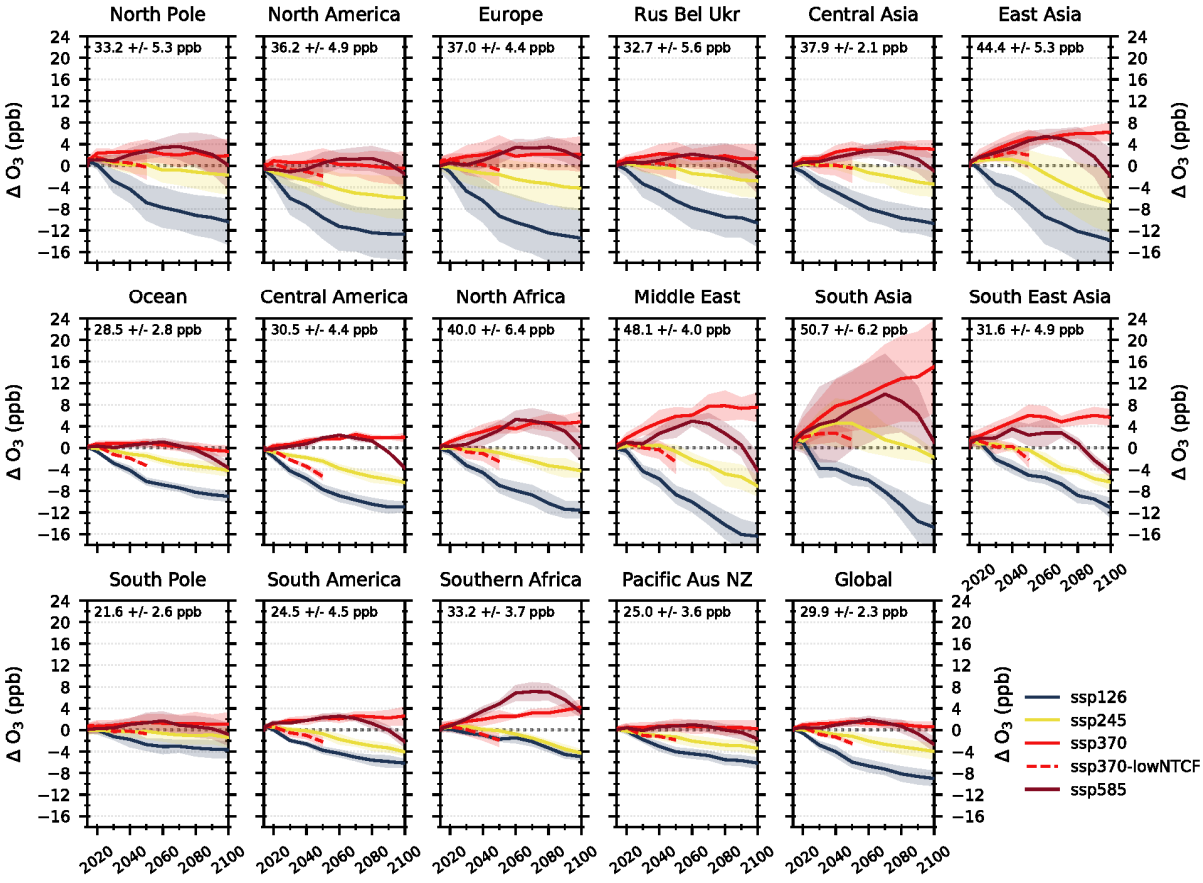

The following changes to the manuscript text have been made to reflect the above discussion of the reasons behind the changes in surface O_3 across East Asia in ssp370-lowNTCF:

P21, line 454 sentence amended to:

"*However, across East Asia the additional precursor emission reductions in ssp370-lowNTCF have resulted in smaller benefits to surface O_3 concentrations being simulated by the CMIP6 models than in other regions (Figure S20), which is attributed to an increase in surface O_3 concentrations over Eastern China (a part of the larger East Asian region shown in Fig. S1). This increase in surface O_3 results from the slight increase in NMVOC emissions (Fig. 2) and a reduction in the NOx titration of O_3 due to the large decreases in NOx emissions in ssp370-lowNTCF. In addition, a reduction in the heterogeneous loss of radicals due to decreases in $PM_{2.5}$ concentrations in ssp370-lowNTCF could also lead to increased surface O_3 concentrations* (Li et al., 2019)."

7. "Discrepancies in the magnitude of change in these emissions due to climate and *land-use change*". Please specify in similar to Table 1 the models for which the natural emissions and atmospheric chemistry are actually dynamically coupled with the climate model's land surface scheme and vegetation cover / Plant Functional Types (that are dynamically changing in the simulations due to human land use change). Which models have the BVOC emissions actually coupled to the climate model's internal land surface scheme? If uncertainty in the changes to

natural emissions is an important conclusion of the paper, there needs to be a separate Table describing the representation of those emissions in each model.

We would like to thank the reviewer for this useful comment. As part of the revision we have included a new table in the supplementary material (Table S1 shown below) that provides information on the chemistry and aerosol configuration within each model used in this study. In addition, a new Figure S23 has been included to show the emissions of isoprene from each model (in a similar way to Figure S15, revised now to S22). In direct response to the reviewers comment, the CMIP6 models that have interactive chemistry and emission of BVOCs coupled to the model's land surface scheme and a dynamic vegetation model are UKESM1-0-LL, GISS-E2-1-G (isoprene only), BCC-ESM1 and CESM2-WACCM. The number of BVOCs emitted from vegetation and involved in atmospheric chemistry varies within each of the CMIP6 models, leading to discrepancies in the total BVOC emissions in Fig S15 (now S22). GISS-E2-1-G interactively emits only isoprene, with no inhibition to CO_2 concentrations, whereas CESM2-WACCM emits isoprene (with inhibition to CO_2 concentrations), monoterpenes and many other short and long chained hydrocarbons. Emissions of BVOCs in these models will depend on the future climate and how the distribution of different vegetation types changes in each CMIP6 model in response to the future scenarios. This could lead to important differences in both O_3 and secondary organic aerosol formation, particularly over regions with large natural sources of BVOC emissions. Further discussion of these comparisons are also made in the response to reviewer 2 but some small changes to manuscript are shown below.

Page 24 Lines 501-509 have been amended as follows:

"*Over South America and Southern Africa, particularly the tropical areas (Fig. S194), larger future changes in surface O_3, particularly by 2100, are predicted by GFDL-ESM4 and UKESM1 than by CESM2-WACCM. Over this region, biogenic emissions (particularly isoprene) are an important source of O_3 formation. Discrepancies in the future response of these BVOC emissions between models could be occurring due to the differing magnitudes of climate and land-use change and how they are coupled within individual CMIP6 models (Table S1), which could affect future surface O_3. Future changes in the total emissions of BVOCs and solely from isoprene obtained from five CMIP6 models (Figure S22 and S2315) show that CESM2-WACCM has larger total BVOC emissions over the period 2005-2014 (due to the inclusion of more BVOCs), which then increase in the future ssp370 scenario, along with isoprene emissions, resulting in a smaller increase (and decreases over some parts of the region) in surface O_3. Whereas, ~~GFDL-ESM4 and~~ UKESM1-0-LL shows larger increases in O_3 and a reduction in BVOCs, mainly from isoprene (Fig. S23), over part of South America and tropical Africa. ~~have smaller increases in BVOC emissions with some emissions reducing over parts of Africa in UKESM1~~.*"

Page 28 Lines 586-590 have been amended as follows:

"*Over Southern Africa UKESM1-0-LL shows a reduction in future $PM_{2.5}$, in contrast to ~~the~~ other models, ~~This can again be attributed~~ due to a reduction in the BC, OA and dust aerosol components (Fig. S24, S26 and S27). UKESM1-0-LL exhibits particularly strong negative correlations for surface $PM_{2.5}$ when compared with temperature and precipitation. These relationships over Southern Africa are quite different to other CMIP6 models, which is also highlighted in the model evaluation over this region (Fig. 8) and indicates that climate change influences aerosol concentrations differently over this region in this model (Figure 16). In addition, there is a slight positive correlation of $PM_{2.5}$ with BVOC emissions in UKESM1-0-LL over Southern Africa. Future biogenic emissions (including monoterpenes) reduce here in ssp370 (Fig. S22), potentially due to land-use vegetation change as UKESM1-0-LL has dynamic vegetation coupled to BVOC emissions (Table S1). This could also reduce $PM_{2.5}$ concentrations over this*

region because monoterpene emissions are the main precursor to SOA formation in UKESM1-0-LL (Mulcahy et al., 2019)."

Table S1 – Brief descriptions of the chemistry and aerosol set up within CMIP6 models used in this study

CMIP6 Model	Horiz. Res.	Vert levels (top level)	Aerosol scheme	Aerosol Species	Natural Sources	Treatment of SOA	Chemistry Scheme	Chemistry reactions	BVOCs	Model Ref
BCC-ESM1	2.813° x 2.813°	L26 (2.914 hPa)	Mass-based aerosol scheme. Prescribed stratospheric aerosols.	SO_4, BC (hydrophilic and hydrophobic), OM (hydrophilic and hydrophobic, sea salt (4 size bins), dust (4 size bins). No nucleation or coagulation of aerosols	Prescribed DMS seawater concentrations with emissions dependent on wind speed. Online emissions of sea-salt and dust aerosols. NOx calculated from lightning.	Hydrophilic OC from anthropogenic emissions but also from natural sources calculated using a fixed yield, assumed to be equal to 10% of monoterpene emissions (from land surface model)	CAM-Chem (based on MOZART). Tropospheric only chemistry.	66 gas-phase chemical species with 33 photolytic reactions and 135 kinetic reactions.	Online biogenic emissions from dynamically evolving vegetation computed in the land model BCC-AVIM2.0 following the algorithm of MEGANv2.1 which has a dependence on light and temperature but also inhibits isoprene emissions based on CO_2.	(Wu et al., 2020)
CESM2-WACCM	0.9° x 1.25°	L70 ($6x10^{-6}$ hPa)	MAM4 (modal scheme, simulating mass and number concentrations) with VBS-SOA	SO_4, BC, OM (both primary and secondary), sea salt, dust	Prescribed climatology of DMS seawater concentrations and emissions. Online emissions of sea-salt and dust aerosols. NOx calculated from lightning. Soil NOx and ocean CO, VOCs from POET	Explicit calculation of SOA using volatility basis set (VBS) where aromatic species, terpenes and isoprene are oxidised to produce a range of gas-phase SOA precursors with different volatilities. Formation of SOA linked to BVOCs emissions from interactive land surface scheme.	MOZART-TSMLT1 covering troposphere, stratosphere, mesosphere and lower thermosphere	231 gas-phase species, 150 photolytic reactions, 403 kinetic reactions and 30 heterogeneous reactions involving ClOx, BrOx, NOx-HOx-Ox, CO, CH_4 and NMVOCs.	Online biogenic emissions (isoprene, monoterpenes, acetone, methanol, and other short and long-chained hydrocarbons) from dynamically evolving vegetation computed in the Community Land Model (CLM) using the MEGAN2.1 algorithm, which has dependence on light and temperature but also inhibits isoprene emissions based on CO_2.	(Gettelman et al., 2019; Tilmes et al., 2019; Emmons et al., 2020)
CNRM-ESM2-1	1.4° x 1.4°	L91 (80km)	TACTIC_v2. Tropospheric aerosols. Mass	SO_4, BC (hydrophilic and hydrophobic), OM (hydrophilic	Prescribed DMS seawater concentrations. Online	Prescribed SOA from monthly inventory	No representation of lower tropospheric	N/A	N/A	(Michou et al., 2019; Séférian et al., 2019)

CMIP6 Model	Horiz. Res.	Vert levels (top level)	Aerosol scheme	Aerosol Species	Natural Sources	Treatment of SOA	Chemistry Scheme	Chemistry reactions	BVOCs	Model Ref
			based aerosol scheme.	and hydrophobic), sea salt (3 size bins), dust (3 size bins)	emissions of sea-salt and dust aerosols		chemistry so not considered here.			
GFDL-ESM4	cubed-sphere (c96) grid, with ~100 km native resolution, regridded to 1.0° x 1.25°	L49 (0.01 hPa)	Bulk mass-based scheme. 5 size bins are used for sea salt and dust.	NH_4, SO_4, NO_3, NH_4, BC, OM, sea salt, dust	DMS and sea salt emissions calculated online as a function of wind speed (and a prescribed DMS seawater climatology). Dust emissions coupled to interactive vegetation. Lightning NOx calculated online as a function of convection. Natural emissions of NOx, CO, NMVOCs, H_2, and NH_3 from POET. NH_3 from seabird colonies. Two-way exchange of NH_3 with ocean.	SOA formed simulated using an anthropogenic source from oxidation of C_4H_{10} tracer and a tracer representing BVOC emissions from vegetation	Interactive stratosphere-troposphere	43 photolysis reactions, 190 gas-phase kinetic reationcs and 15 heterogeneous recations. NOx-HOx-Ox- chemical cycles and CO, CH_4 and NMVOC oxidation reactions	Online emissions of BVOCs (isoprene and monoterpenes) calculated from a prescribed vegetation cover using MEGAN2.1 algorithm, which has dependence on light and temperature but also inhibits isoprene emissions based on CO_2.	(Horowitz et al., 2019; Dunne et al., 2020)
GISS-E2-1-G	2° x 2.5°	L40 (0.1 hPa)	OMA (one moment aerosol scheme – mass based)	SO_4, NO_3, NH_4, BC, OM treated as externally mixed with prescribed and constant size distribution. Sea salt has two size classes. Sectional scheme for dust with 5 size bins that can be coated with SO_4 and NO_3 to increase solubility.	Sea salt, DMS, isoprene and dust emission fluxes are calculated interactively. Online NOx calculated from lightning. Soil NOx, ocean CO, VOCs from GEIA. NH_3 from oceans. SO_2 from volcanoes as in AeroCom.	Two-product model approximation to represent SOA formation from the oxidation of biogenic VOCs, including NOx dependent chemistry yields.	Coupled troposphere-stratosphere chemistry scheme. Modified Carbon Bond Mechanism 4 (CBM-4) chemical mechanism	inorganic chemistry of Ox, NOx, HOx, CO, and organic chemistry of CH_4 and lumped higher hydrocarbons (only isoprene and terpenes are explicitly taken into account), along with Cl and Br stratospheric chemistry and heterogenous reactions on PSCs and SO_4 aerosols.	Emissions of isoprene from dynamically evolving vegetation are calculated interactively using the algorithm of Guenther et al., (1995), which has dependence on light and temperature. Terpene emissions are prescribed.	(Bauer et al., 2020)
HadGEM3-GC31-LL	1.25° x 1.875°	L85 (85km)	GLOMAP-Mode. (Modal scheme,	SO_4, BC, OM, sea salt in 5 log-	Prescribed climatologies of DMS	Fixed yield of SOA of 26% calculated	Simplified sulphur	Oxidation for SO_4 and simplified	N/A	(Mulcahy et al., 2020)

CMIP6 Model	Horiz. Res.	Vert levels (top level)	Aerosol scheme	Aerosol Species	Natural Sources	Treatment of SOA	Chemistry Scheme	Chemistry reactions	BVOCs	Model Ref
			mass and number). Mass based bin scheme used for dust.	normal modes and dust in 6 bins	seawater concentrations and BVOC emissions. No marine source of primary organics. Online emissions of sea-salt and dust aerosols	from gas-phase oxidation reactions involving prescribed land-based monoterpene sources	chemistry for use with aerosol scheme	oxidation scheme (monoterpenes) for SOA		
MIROC6-ES2L	2.813° x 2.813°	L40 (3.0 hPa)	SPRINTAS.	SO_4, BC, OM, sea salt and dust in log-normal size distributions. External mixing assumed for SO_4, sea salt and dust aerosols.	Online emissions of DMS, sea-salt and dust aerosols. Primary marine organic aerosol emissions coupled to ocean biogeochemistry.	Prescribed emissions of isoprene and terpenes from GEIA used to convert to secondary organic carbon.	Simplified chemistry for use with aerosol scheme	Oxidation for SO_4 and simplified oxidation scheme (isoprene and monoterpenes) for SOA	Prescribed emissions of isoprene and terpenes from GEIA.	(Takemura, 2012; Hajima et al., 2020)
MPI-ESM1.2-HAM	1.875° x 1.875°	L47 (0.01 hPa)	HAM2.3 (Modal scheme, mass and number)	SO4, BC, OM, sea salt, dust in 7 log-normal modes	Interactive online emissions of DMS (using prescribed sea water concentrations), sea-salt and dust aerosols dependent on meteorology.	15% of natural terpene emissions at the surface (prescribed) form SOA. SOA have identical properties to primary organic aerosols	Simplified sulphur chemistry. Other fields prescribed.	Reactions involving SO_2, DMS and SO_4, including aqueous phase.	N/A	(Tegen et al., 2019)
MRI-ESM2-0	MRI-AGCM3.5: 1.125° x 1.125°, MASINGAR mk-2r4c: 1.875° x 1.875°, MRI-CCM2.1: 2.813° x 2.813°	L80 (0.01 hPa)	MASINGAR mk-2r4c	Mass-based scheme with externally mixed size distributions. SO4 (three categories), BC (hydrophilic and hydrophobic), OM (hydrophilic and hydrophobic), sea salt (10 size bins), dust (10 size bins).	Interactive online emissions of DMS (using prescribed Climatological DMS sea water concentrations), sea-salt, and dust aerosols dependent on meteorology. Online NOx calculated from lightning. Climatological soil NOx and ocean CO, VOCs emissions.	No explicit calculation: 14% of prescribed monoterpene and 1.68 % of isoprene emissions are assumed to form SOA.	Chemistry Climate Model version 2.1 (MRI-CCM2.1) covering troposphere, stratosphere, and mesosphere	90 chemical species and 259 chemical reactions (184 gas-phase reactions, 59 photolysis reactions, and 16 heterogeneous reactions) involving HOx-NOx-CH_4-CO cycles and NMVOC oxidation reactions, and halogen chemistry (Cl and Br)	Climatological BVOCs emissions	(Deushi and Shibata, 2011; Yukimoto et al., 2019)
NorESM2-LM	1.9° x 2.5°	L32 (3.64 hPa)	OsloAero6	SO4, BC, OM, sea salt, dust. (log-normal modes)	Interactive emissions for sea-salt, biogenic primary OM (including	Fixed SOA formation yields of 15% and 5% from	Simplified chemistry for use in aerosol	Oxidation for SO_4 and simplified oxidation scheme	Online biogenic emissions from dynamically evolving	(Kirkevåg et al., 2018;

CMIP6 Model	Horiz. Res.	Vert levels (top level)	Aerosol scheme	Aerosol Species	Natural Sources	Treatment of SOA	Chemistry Scheme	Chemistry reactions	BVOCs	Model Ref
					MSA) and DMS over oceans, and interactive mineral dust and BVOC over land	oxidation of monoterpenes and isoprene	scheme. Other fields prescribed.	(isoprene and monoterpenes) for SOA	vegetation computed in the Community Land Model (CLM) using the MEGAN2.1 algorithm, which has dependence on light and temperature but also inhibits isoprene emissions based on CO_2.	Seland et al., 2020)
UKESM1-0-LL	1.25° x 1.875°	L85 (85km)	GLOMAP-Mode. (Modal scheme, mass and number). Mass based bin scheme used for dust.	SO_4, BC, OM, sea salt in 5 log-normal modes and dust in 6 bins	Dynamic vegetation and interactive ocean biogeochemistry used for online emissions of DMS, sea-salt and dust aerosols, as well as emissions of primary marine organics and biogenic organic compounds. Online NOx calculated from lightning, soil NOx and ocean CO, VOCs from POET	Fixed SOA yield of 26% from gas-phase oxidation reactions involving interactive land-based monoterpene sources.	UKCA coupled stratosphere-troposphere. Interactive photolysis	84 chemical tracers. Simulates chemical cycles of Ox, HOx and NOx, as well as oxidation reactions of CO, CH_4 and NMVOCs. In addition, heterogeneous processes, Cl and Br chemistry are included.	Dynamic vegetation and land surface model used to calculate interactive emissions of Isoprene and monoterpenes using light and temperature, but isoprene emissions are inhibited based on CO_2. Isoprene emissions coupled to chemistry and affect tropospheric O_3 and methane lifetime. Monoterpenes only affect SOA.	(Archibald et al., 2020; Mulcahy et al., 2020)

Minor comments

I find Fig. 2 challenging to look at and wonder about for other readers. I appreciate it is difficult to show this Fig. 1 type information across multiple regions.

I would like to thank the reviewer for the comment on Figure 2., which has been reproduced in a different way to try and make it easy to view. The amended figure is shown below and have been used to replace the original Figure 2 in the manuscript.

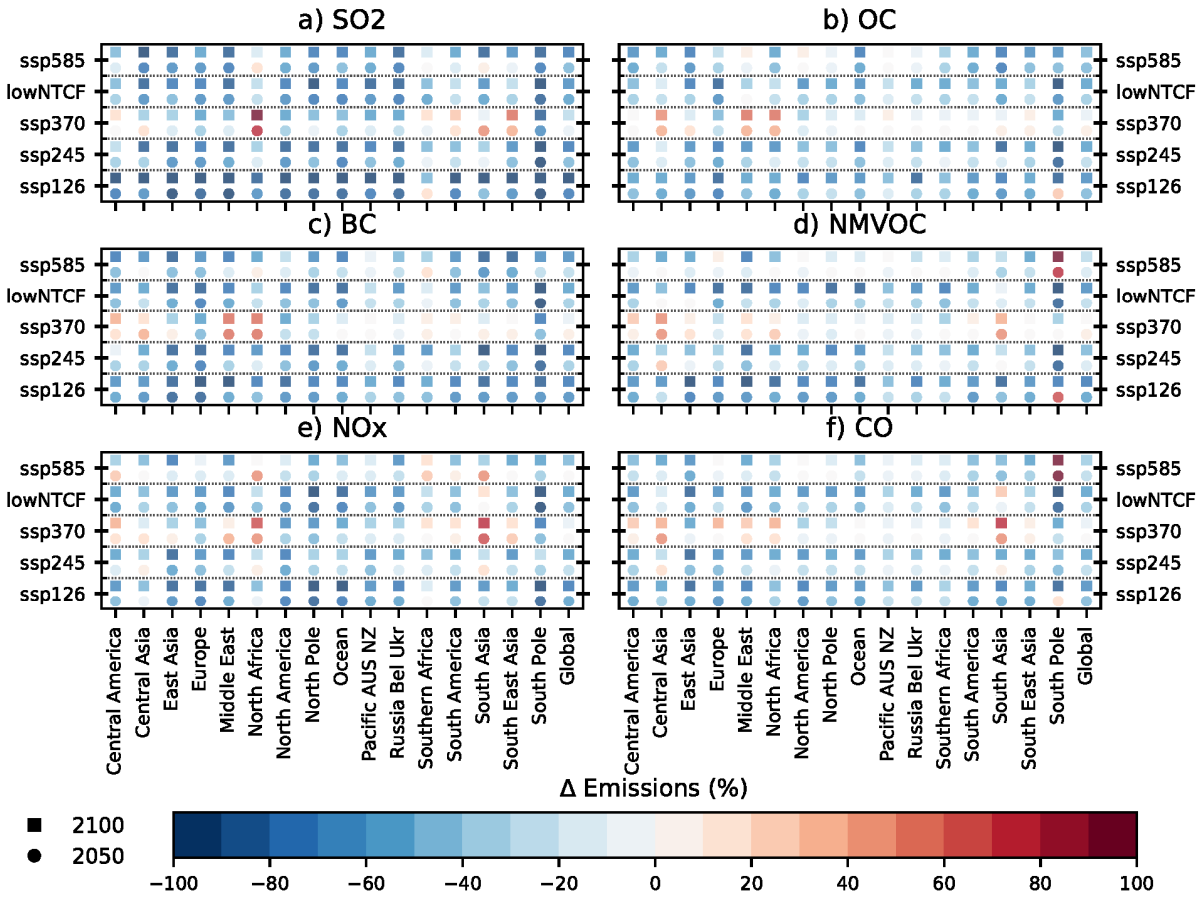

Is it necessary to have both Fig 6 and Fig 8 i.e. for the 2000-2010 and 2005 and 2014 periods? Could one of the plots go into SI?

We thank the author for the comments but whilst it appears that Figure 6 and 8 are showing similar results, there are key differences which means it is important to include both within the main text. Figure 6 shows a comparison of model vs observations at ground based monitoring locations, which are from specific spatial points within each region. The results for MERRA on Figure 6 are also shown at only these locations for the same time period (2000-2010) in order to directly compare the MERRA product with the ground based observations and CMIP6 models. This provides additional information for the evaluation of model biases (see response to comment 2 above). In figure 8 the regional means are calculated from MERRA based on all of the grid points within a particular region. The regional meaning therefore contains many more data points (see parenthesis on Figure 8) than is possible in Figure 6, which allows for improved statistics by using the reanalysis product. The comparison of Figure 6 and 8 therefore provides additional inter-comparison between the CMIP6 models, MERRA reanalysis product and ground based observations and we feel that it warrants a separate inclusion within the main text.

"Large regional historical changes are simulated for both pollutants, across East and South Asia, with an increase of up to 40 ppb for O3 and 12 µg m-3 for PM2.5." and similar sentences in abstract. Need to include the temporal averaging associated with those values in abstract (annual).

The following sentences have been changed within the abstract to include reference to the temporal averaging period:

"*Large regional historical changes are simulated for both pollutants, across East and South Asia, with an annual mean increase of up to 40 ppb for O_3 and 12 µg m^{-3} for $PM_{2.5}$. In future scenarios containing strong air quality and climate mitigation measures (ssp126), annual mean concentrations of air pollutants are substantially reduced across all regions by up to 15 ppb for O_3 and 12 µg m^{-3} for $PM_{2.5}$. However, for scenarios that encompass weak action on mitigating climate and reducing air pollutant emissions (ssp370), annual mean increases of both surface O_3 (up 10 ppb) and $PM_{2.5}$ (up to 8 µg m^{-3}) are simulated across most regions.*"

"Near Term Climate Forcers (NTCFs)." IPCC AR6 uses "Short-lived Climate Forcers (SLCFs)".

Changed all references to Near Term Climate Forcers in the manuscript to Short-lived Climate Forcers (SLFCs) to be consistent with IPCC AR6.

"Initial assessments have been made of future changes to air pollutants in the SSPs using simplified models." Need to add references here.

The sentence has been changed to the following to include additional references:

"*Initial assessments have been made of future changes to air pollutants in the SSPs using simplified models (Reis et al., 2018; Turnock et al., 2018, 2019)*"

"A particular climate mitigation target, in terms of an anthropogenic radiative forcing by 2100, is included on top of each SSP" What does "on top of" mean exactly?

The sentence has been amended as follows to improve clarity on this point:

"*A particular climate mitigation target, in terms of an anthropogenic radiative forcing by 2100, and the range of emission mitigation measures associated with achieving it are included in addition to the existing policy measures within each baseline SSP scenario.*"

"However, scenarios with large increases in global CH4 abundances, a large climate change signal and limited control of precursor emissions fail to restrict regional increases in surface O3, leading to poor future air quality and potential human health impacts (Silva et al., 2017)." Is this statement redundant/obvious? Where is the new science?

Thank you to reviewer for the comment on this sentence. The sentence has been rewritten to make it more relevant to differences in the new scenarios that have been used in CMIP6.

"However, scenarios with large climate signals (ssp370 and ssp585) but different post 2050 controls on O_3 precursors (most notably CH_4 and NOx), show different long-term changes in regional surface O_3 concentrations, which could have important consequences for impacts on human health."

"Whilst there is disagreements" sp. there are

Corrected mistake.

Response to Referee 2

This manuscript conducts an evaluation of surface PM2.5 and ozone with observations for the CMIP6 chemistry-climate models that participated in AerChemMIP. It also documents the simulated historical & future changes in annual mean ozone and PM2.5 in various regions around the globe. It's clear that an enormous amount of effort went in to preparing this manuscript. By detailing the performance of each individual model (10 for PM2.5; 5 for ozone) against the available observations, a major community service has been performed in the production of this detailed supplemental information.

The rather long paper documents the current status of O3 and PM2.5 in the latest versions of global chemistry-climate models. It does so, however, without much attempt to understand more deeply the inter-model differences, or the sources of agreement, beyond discussing qualitative links to the emission trajectories or referencing relationships identified in prior work. A stronger paper would be more cohesive throughout and communicate better the novelty of the work. Below I suggest ways to strengthen the paper in each of these two directions, followed by more detailed comments. I support the points made by the other reviewer and so try to avoid repeating those points here.

First, the model evaluation presented is not tied in a clear way to the past or future projections of the models. The evaluation focuses on monthly and seasonal data but then only annual mean concentrations are presented for the historical and future trends. It seems far more relevant to evaluate regional trends in annual mean concentrations where observations allow this, or to demonstrate some relationship between seasonal cycles and future changes across the models (and should one exist, this would be an exciting finding as it would open up the possibility of identifying a "best" model from the evaluation with observations). The evaluation shown in Figures 5 and 6 of the Mortier et al. paper or in Figure 4 of Griffiths et al. in this special issue seems more relevant, although the remote sites used in Griffiths et al. are not that relevant for the polluted regions examined in this study. One could tackle a similar type of evaluation for North America and Europe where there are at least two decades of long-term observations for ozone and PM2.5, and it should be particularly straightforward to do so with the gridded MERRA reanalysis product for PM2.5. An alternative angle could be to examine if the past or future trends are strongly seasonally dependent. If so, showing some of the seasonality in the projections would connect better to the seasonal evaluation included. If the authors choose to remove any of the current figures, they should be included in the supplemental material, as the general evaluation done here will certainly be of high value to the modeling community.

We thank the reviewer for this useful comment on trying to make the manuscript more quantitative and also to improve the connections between the model evaluation and historical/future projections. As the reviewer mentions an analysis of long-term changes in surface O_3 and aerosol properties has already been undertaken in other manuscripts within this special issue and was therefore considered outside of the scope of the current work (see response to point 3 of reviewer 1 for more details). Further work is ongoing to analyse long term surface O_3 changes from CMIP6 models at northern hemisphere continental observation locations. Therefore, we have made improvements throughout the manuscript to better connect the seasonal and annual mean aspects of the present day model evaluation with the historical and future simulations. Revised versions of Figures 3, 5 and 7 have been produced to include a comparison of the annual mean surface concentrations of O_3 and $PM_{2.5}$ with observations, in addition to the seasonal mean comparisons originally present. Figures S2 to S7 in the supplementary material showing individual CMIP6 model comparisons have also been updated to include annual mean comparisons. Numerous minor text changes to the manuscript have been made in section 3 to reflect the inclusion of the annual mean evaluation. An example of the revised Figure 3 for surface O_3 is shown below:

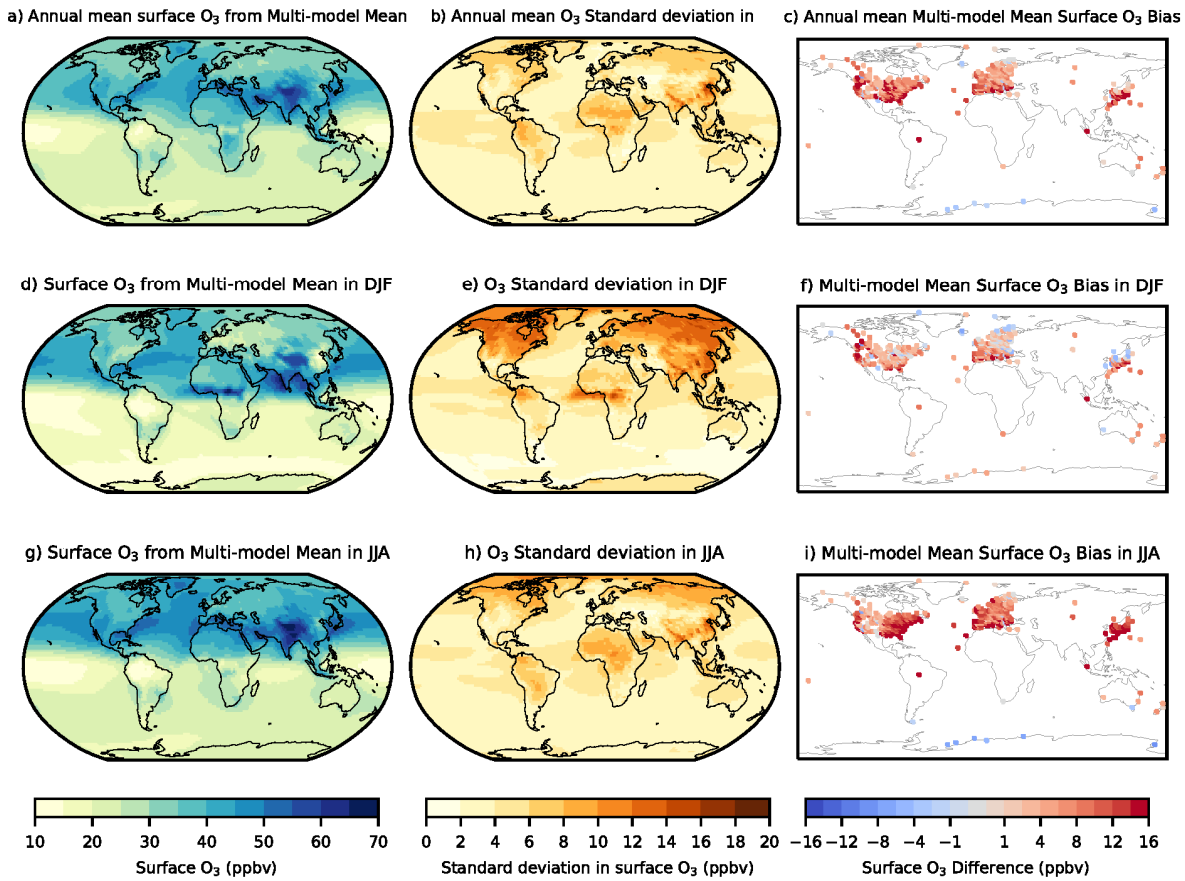

Figure 3 – Multi-model (6 CMIP6 models) annual and seasonal mean surface O_3 concentrations in a) Annual mean, d) December January, February (DJF) and g) June, July, August (JJA) over the 2005-2014 period. The standard deviation in the multi-model mean in b) Annual mean, e) DJF and h) JJA. The difference between the multi-model mean and TOAR observations in c) Annual mean, f) DJF and i) JJA (colour bar saturates).

We have included simulated seasonal mean changes in air pollutants over the historical and future time periods on Figures in the revised manuscript and supplementary material to connect better with the present-day evaluation work. A new Figure S16 (shown below) has been included within the supplementary material showing the annual and seasonal mean change in surface O_3 and $PM_{2.5}$ between 1850 and 2014.

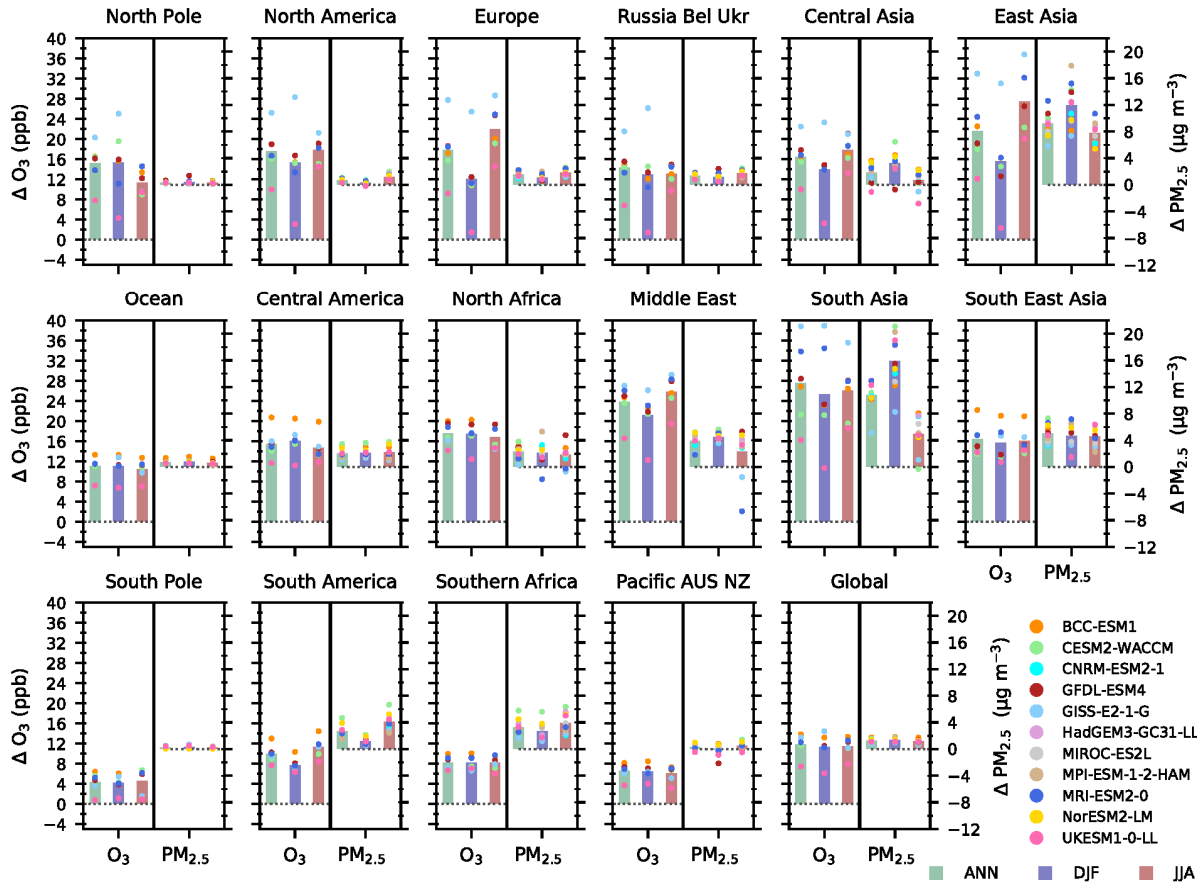

Figure S16 – Annual and seasonal regional mean changes in surface O_3 and $PM_{2.5}$ from pre-industrial (1850-1859 mean) to present day (2005-2014 mean) across 11 CMIP6 models. Individual circles represent each annual and seasonal mean changes from individual CMIP6 models, with the multi-model mean represented by the solid bar.

The following changes to the manuscript have been made in Section 4 to include the seasonal historical changes. The following new sentence has been included on page 17 line 382:

"*Globally and over most regions there has been a larger historical increase in surface O_3 in JJA than in DJF (Figure S16).*"

A new sentence has been included on page 18 line 388

"*Larger differences between CMIP6 models are shown in the DJF mean historical changes over northern hemisphere regions than occurred in JJA (Figure S16), reflecting the differences shown in the model evaluation (Fig. 4) and the strong seasonality of the changes*."

The sentence on page 18, line 390 has been amended to the following:

"*South Asia is the region with the largest diversity in simulated historical changes in surface O_3 of between 16 and 40 ppb, with a larger range in DJF (10-40 ppb) than in JJA (19-36 ppb).*"

The sentence on page 18, line 391 has been amended to the following:

"*Surface O_3 is simulated to have increased by between 10 to 30 ppb on an annual mean basis and by a larger amount in JJA (12 to 37 ppb) over the major northern anthropogenic source regions since 1850, driven mainly by the large increases in anthropogenic precursor emissions of CH_4, NOx, CO, and NMVOCs over this period.*"

The sentence on page 19 line 408 has been amended to the following:

"*Larger regional increases in surface annual mean $PM_{2.5}$ of up to 12 μg m^{-3} are simulated across South and East Asia, with changes in DJF (up to 21 μg m^{-3}) larger than those in JJA (up to 12 μg m^{-3}) (Fig. S16), reflecting the strong seasonality of $PM_{2.5}$ concentrations in these regions.*"

The sentence on Page 19, line 410-412 has been amended as follows:

"The largest model diversity is also exhibited over the Asian regions with variations in the response between models of up to 50%, ~~potentially simulation dust emissions and simulation of organic aerosols~~ with larger differences between models in DJF than JJA (Figure S16), reflecting the differences shown in the present day model evaluation (Fig. 6)."

In addition, we have also included simulated seasonal mean changes in air pollutants over the future time periods on Figures 12 and 14 (now Fig. 15) in the revised manuscript to try to better link the future predictions with the present-day evaluation work. An example of a revised Figure 12 (shown below) has been included within the revised manuscript, now showing both the annual and seasonal mean change in surface O_3 in 2050 and 2095 in the ssp370 future scenario for four CMIP6 models. A similar revised Figure has also been included within the manuscript for future surface $PM_{2.5}$ changes in ssp370.

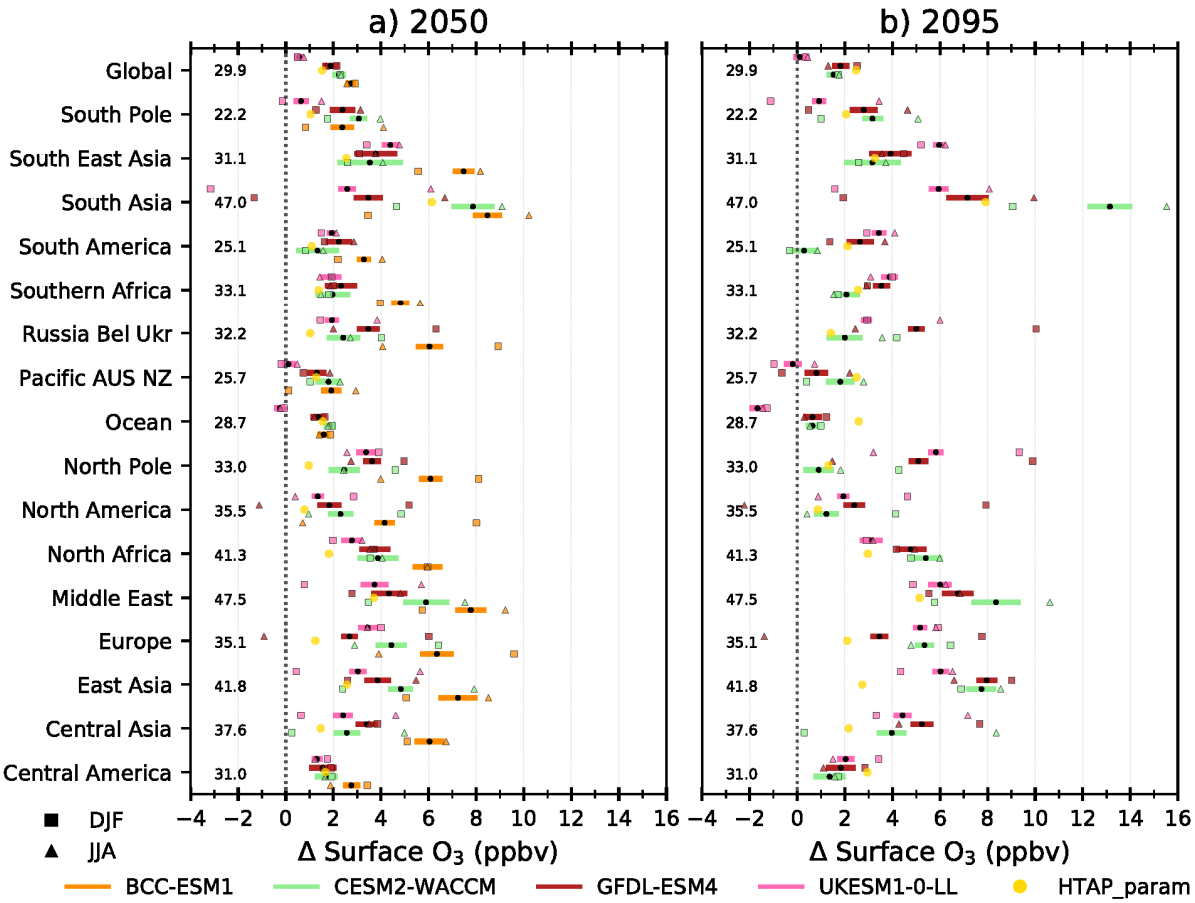

Figure 12 – Future global and regional changes in the decadal annual and seasonal mean surface O_3, relative to the 2005-2014 mean, for the ssp370 pathway used in CMIP6. Each black circle represents the decadal annual mean response for an individual model in a) 2045-2055 and b) 2090-2100, with the coloured bars showing the standard deviation across the decadal annual mean. The DJF and JJA seasonal mean response averaged over the relevant 10 year period is shown by squares and triangles respectively. The multi-model regional mean over the

period 2005- 2014 is given towards the left of each panel. The response from the HTAP_param in each time period is shown by the separate gold circle.

The following changes to the manuscript have been made in Section 5 to include mention to the seasonal future changes in air pollutants.

Page 23 lines 491-492 have been amended to the following:

"*Over the North Pole region all models show surface O_3 increases that are larger than the HTAP_param, with a larger increase in DJF than JJA.*"

A new Figure S21 showing the future DJF surface O_3 changes in ssp370 has been included in the supplementary material, as well as a new sentence on Page 24 line 495 and an amended sentence on line 496:

"*The lower annual mean response in UKESM1-0-LL and GFDL-ESM4 is driven by a reduction in DJF in these models (Fig. S21), which results in the DJF change in 2050 being lower than the 2005-2014 annual mean value (Fig. 12). The large increase in NOx emissions in ssp370~~this scenario~~ over South Asia (~80%) has resulted in areas of NOx titration, particularly in DJF, near the Indo-Gangetic plain in both UKESM1-0-LL and GFDL-ESM4, reducing surface O_3 concentrations (Fig. S~~14~~19 and S~~14~~21). This strong feature of NOx titration of O_3 in DJF is absent in both CESM2-WACCM and BCC-ESM1, resulting in larger O_3 production over South Asia.*"

The following new sentence is included on Page 24 line 502:

"*These changes over South America are larger in JJA in all models, with small seasonal differences over Southern Africa.*"

A new sentence is included on Page 24 line 512:

"*There are differences in simulated seasonal response across these regions, with all models showing a smaller increase in JJA than DJF across North America and Europe, whilst across East Asia there tends to a be a larger future surface O_3 increase in JJA than DJF*."

The sentence on page 27, lines 566-567 has been amended as follows:

"*In a similar analysis to that for surface O_3, a more detailed comparison has been undertaken of four CMIP6 models predicting changes in annual and seasonal surface $PM_{2.5}$ in 2050 and 2095 under ssp370 (Figure 14).*"

The sentence on page 27, line 568-569 has been amended to:

"*Small reductions in annual mean surface $PM_{2.5}$ concentrations (<2 µg m^{-3}) are simulated consistently by all CMIP6 models across North America and Europe in ssp370, ~~mainly attributed to decreases in the BC and SO_4 components~~ with larger reductions simulated in DJF than JJA.*"

A new sentence has been included on page 27, line 571.

"*Across South Asia, all models simulate a larger increase in DJF mean surface $PM_{2.5}$ concentrations, of up to 18 µg m^{-3} by 2050, than occurs in JJA, and reflects the seasonality shown in the model evaluation.*"

The sentence on page 28, line 576-577 has been amended to:

"*Small regional annual mean increases are predicted in 2050 due to $PM_{2.5}$ increases in JJA from all models apart from GFDL-ESM4. A larger reduction in the SO_4 component is simulated over East Asia by GFDL-ESM4 than in other models (Fig S~~17~~25), resulting in an overall decrease in $PM_{2.5}$. In 2095 most models simulate a reduction in $PM_{2.5}$ concentrations in both seasons across East Asia, apart from CESM2-WACCM due to the increase in JJA."*

The sentence on page 28, line 591-594 has been amended to:

"*The decadal annual and seasonal mean $PM_{2.5}$ response is variable across individual CMIP6 models over regions close to natural sources of particulate matter (North Africa, Central Asia and Pacific, Australia and New Zealand). Over these regions there is a large range in both the sign and magnitude of the annual and seasonal $PM_{2.5}$ response, which can be mainly attributed to the dust fraction (Fig. S26) and the fact that this aerosol source has a large inter-annual variability in its emission strength."*

The sentence on page 30, line 641-642 has been amended to:

"*Across the historical period (1850-2014), the CMIP6 models simulated a global annual increase in surface O_3 of between 7 and 14 ppb, with a larger increase in JJA than DJF.*"

The sentence on page 30, line 646-648 has been amended to:

"*Small global increases in surface $PM_{2.5}$ are simulated over the historical period by CMIP6 models, with larger regional changes of up to 12 μg m^{-3} on annual mean basis and up to 18 μg m^{-3} in DJF across East and South Asia.*"

Second, the authors could better demonstrate the new contributions here, perhaps by looking a bit more closely at some aspect of the inter-model differences rather than ending with qualitative and in some cases speculative statements. For example, are there clear relationships between the inter-model spread in the global or regional temperature or precipitation changes and the air pollution changes projected over time?

Could previously identified general conclusions regarding relationships between global ozone, NOx and methane (see Figure 6 of Stevenson et al. 2006, Figure 13 of Young et al., 2013) be extended to surface ozone, and regionally? Can any conclusions be made as to whether future changes in particulate matter depend most on a particular component? There is a lot of useful information in the supplement regarding aerosol components and temperature changes that could be connected more closely to the changes reported in the main text. I find Figures 12 and 14 particularly interesting and the results presented there would be even more useful if they were connected more directly to changes in regional or global temperature, precipitation, humidity, air pollutant emissions, precursor surface concentrations, or whichever quantities are available across the set of models.

We thank the reviewer for this useful comment on trying to connect the changes in air pollutants better with other variables such as aerosol components, temperature, precipitation and emissions. We have conducted additional analysis by comparing regional future changes in air pollutants from individual models in ssp370 over the period 2015 to 2100 with selected variables. However, there are additional experiments being performed within AerChemMIP that will enable further quantification of the emission and climate change effect on air quality. A summary figure for both O_3 and $PM_{2.5}$ showing the correlation coefficients for these comparisons has now been included as a new Figure 13 and 16 within the manuscript (and shown below). Changes to the manuscript listed below have been made to reflect this new analysis.

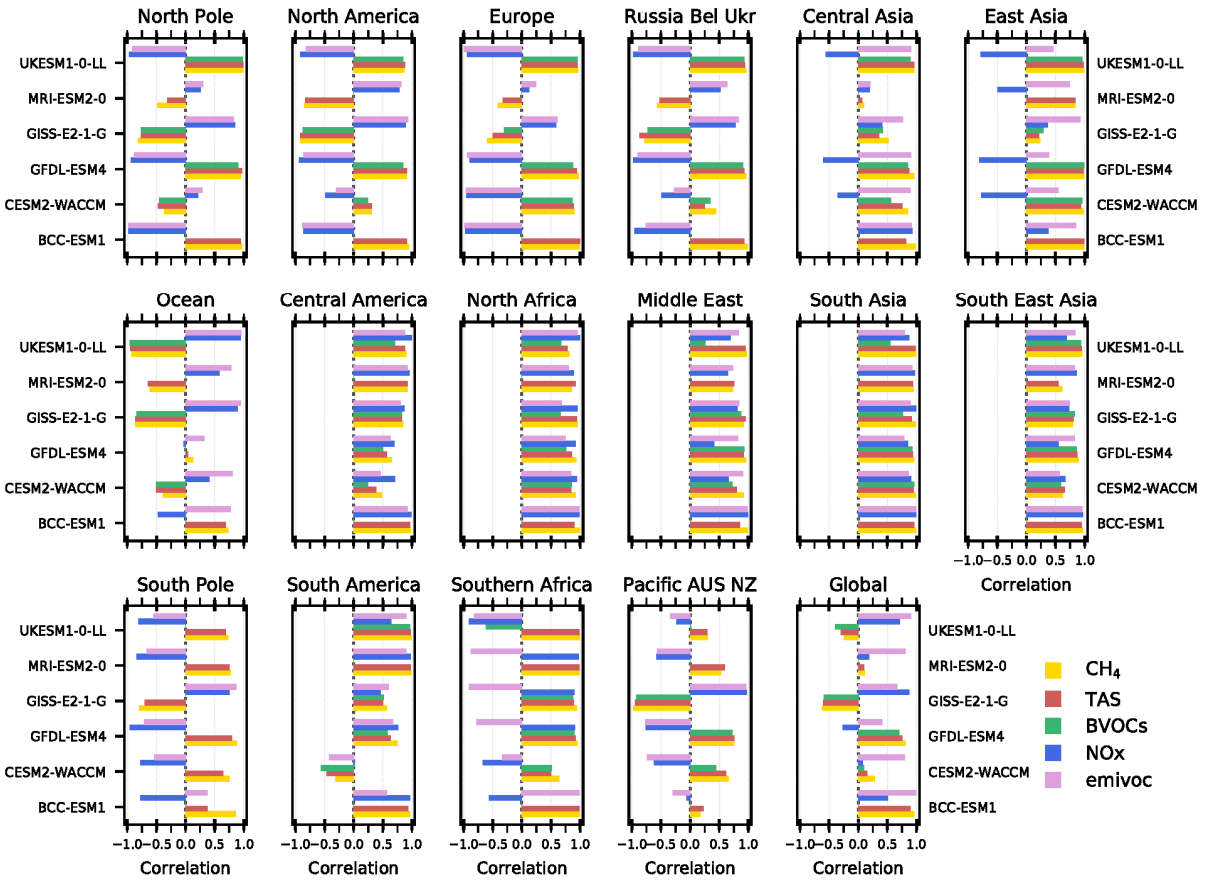

Figure 13 - Correlation coefficients calculated when comparing future annual mean surface O_3 concentrations against individual variables of CH_4 concentrations, surface air temperature (TAS), emissions of biogenic volatile organic compounds (BVOCs), NOx (NO + NO_2) concentrations and anthropogenic emissions of non-methane volatile organic compounds (NMVOCs) from individual CMIP6 models over the period 2015 to 2100 in the ssp370 scenario.

A new sentence has been included at Page 23 line 486:

"*An analysis of the relationships, in terms of correlation coefficients, between future annual mean surface O_3 concentrations and other variables (CH_4 concentrations, surface air temperature, NOx concentrations, emissions of BVOCs and anthropogenic emissions of NMVOCs) is undertaken for CMIP6 models in the ssp370 scenario (Figure 13).*"

A new sentence has been included at Page 23 line 489:

"*The future surface O_3 response in UKESM1-0-LL over the ocean region exhibits a large negative correlation with surface temperature changes (Figure 13), indicating the importance of future climate change in this model over remote regions.*"

Page 24 lines 492-493 have been amended to the following:

"The large future temperature response over the Arctic, as well as changes to NOx concentrations and emissions of NMVOCs are particularly important drivers of surface O_3 changes across CMIP6 models in this region with comparatively low local emissions (Figure 13)."

Page 24 line 498-499 have been amended to the following:

"The comparison in Fig. 12 shows how the O_3 chemistry within models responds differently across a particular area in a future scenario with a large climate change signal and over a region with large increases in local precursor emissions, but that all drivers related to regional O_3 change in South Asia are similarly important across all models (Figure 13)."

Page 24 line 507-509 have been amended to the following:

"*Figure 13 shows that there are differing relationships between future surface O_3 concentrations, BVOC emissions and NOx concentrations across CMIP6 models over South America and Southern Africa. Over Southern Africa, UKESM1-0-LL shows a different relationship between BVOC emissions and surface O_3 concentrations than other CMIP6 models, indicating that this could be leading to the different future O_3 response in this model over this region. Similarly, Figure 13 shows that over South America, CESM2-WACCM has a different relationship between surface O_3 and the variables considered here than in other CMIP6 models, particularly for BVOCs, leading to the different future responses in this model over this region.* ~~*The BVOC emission changes appear to have affected the future O3 formation differently in the individual models over these regions*~~ *Figure 13 shows that there are differences between models in the surface O_3 response over regions such as South America and Southern Africa,* ~~*and represents an*~~ *which are potentially linked to the land-surface response and are important* ~~*process*~~ *to understand more in* ~~*further*~~ *future work.*"

Page 24 line 513-515 have been changed to the following:

"*Figure 13 shows that there is a negative correlation between surface O_3 and NOx concentrations, as well as between O_3 and NMVOCs emissions, for most CMIP6 models across these regions, reflecting that as most anthropogenic precursor emissions (including NOx) decrease in this scenario* ~~*across all these regions*~~ *(Fig. 2) then surface O_3 is simulated to increase. An exception to this is across East Asia, where the increase in NMVOC emissions in ssp370 (Fig. 2) are positively correlated with surface O_3, indicating different chemical drivers of future O_3 across this region. In addition, there are positive correlations between the other variables (temperature, CH_4 and BVOCs) for most CMIP6 models indicating that changes in climate and global CH_4 abundances* ~~*seem to be the major*~~ *are also important drivers of surface O_3 increases over these regions.*"

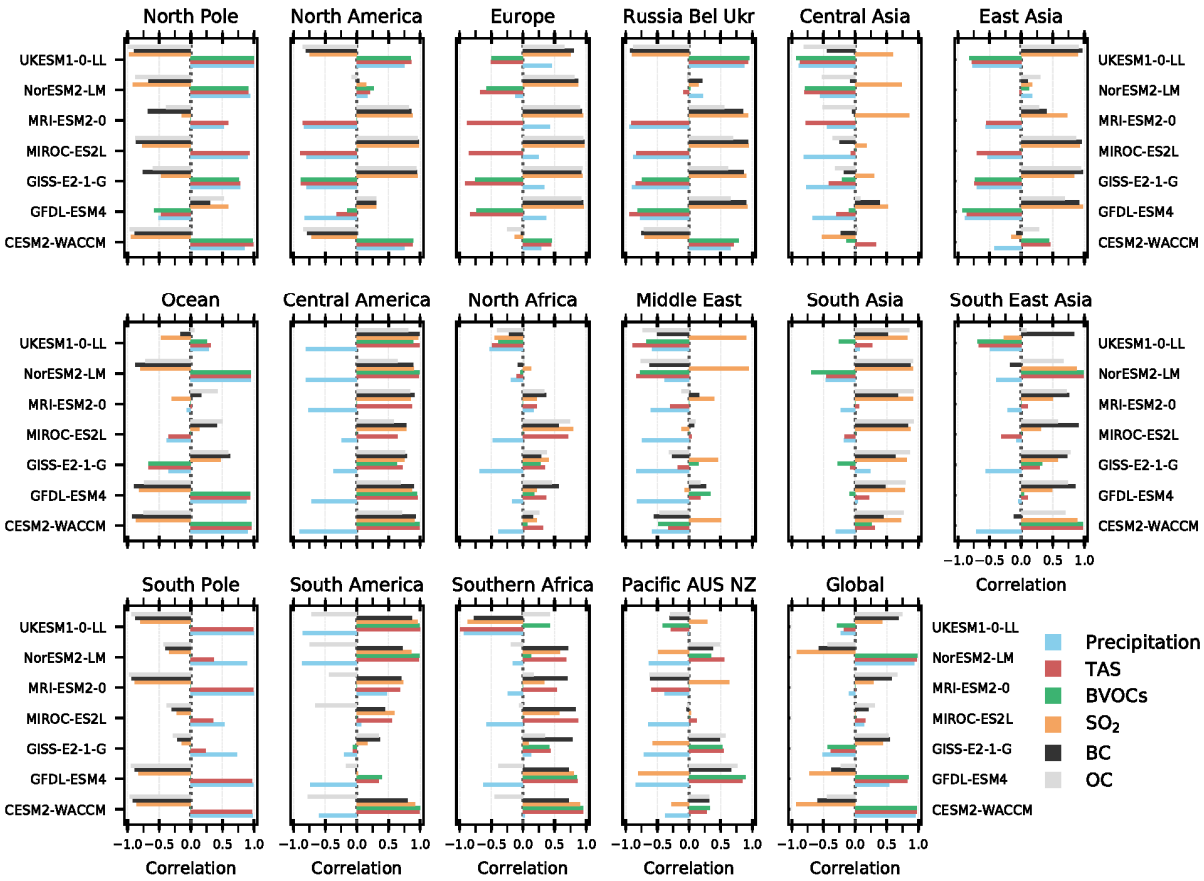

Figure 16 – Correlation coefficients calculated when comparing future annual mean surface $PM_{2.5}$ concentrations against individual variables of precipitation, surface air temperature (TAS), emissions of biogenic volatile organic compounds (BVOCs) and emissions of SO_2, black carbon (BC) and organic carbon (OC) from individual CMIP6 models (that had data out to 2100) over the period 2015 to 2100 in the ssp370 scenario.

Page 26 lines 533 to 534 have been amended as follows:

"*The increases in $PM_{2.5}$ are driven mainly by the increase in aerosol and aerosol precursor emissions in this scenario (Fig. 2), shown by the positive correlations between emissions and surface $PM_{2.5}$ in CMIP6 models across these regions (Figure 16).*"

A new sentence has been included at Page 27 line 567:

"*In addition, an analysis of the relationships, in terms of correlation coefficients, between future annual mean surface $PM_{2.5}$ and other variables (total surface precipitation, surface air temperature and emissions of BVOCs, SO_2, BC and organic aerosol) has been undertaken for CMIP6 models in the ssp370 scenario (Figure 16).*"

A new sentence has been added on page 27, line 568-569:

"*The reductions in annual mean $PM_{2.5}$ over Europe and North America are mainly attributed to decreases in the BC and SO_4 components (Fig. S24 and S25), as indicated by the strong positive correlations with BC and SO_2 emissions across most CMIP6 models (Figure 16). However, by 2095 a small increase (up to 2 µg m^{-3}) is simulated in JJA by UKESM1-0-LL and CESM2-WACCM over North America, which could be attributed to changes in climate due to the strong positive correlations in both models for temperature, precipitation and BVOCs (Figure 16).*"

A new sentence has been added on page 27, line 571:

"*The future increases in annual mean surface $PM_{2.5}$ appear to be strongly driven by emission changes as there are strong positive correlations between these variables across South Asia in all models (Figure 16).*"

Page 28 Lines 581-586 have been amended as follows:

"*CESM2-WACCM includes a more complex treatment of SOA formation, showing a strong response to climate and historical trends in OA (Tilmes et al., 2019). Positive correlations are shown for CESM2-WACCM between surface $PM_{2.5}$ and emissions of BVOC and temperature (Fig. 16), which are not present in other models and could explain the ~~multi-model~~ differences between this model and others across East Asia. The discrepancies in CMIP6 models are not as obvious over South Asia as the effect of the increase in OA over South Asia in CESM2-WACCM is masked by coincident increases in other components across other models, as indicated by the strong correlations with emissions here. CESM2-WACCM also shows larger simulated increases in $PM_{2.5}$ over South America, Central America, Southern Africa and South East Asia than other models, which can be attributed to the larger increase in the OA fraction (Fig. S26) and the strong correlations in this model with changes in temperature and emissions (BVOCs and SO_2).*"

Page 28 Lines 586-590 have been amended as follows:

"*~~However, o~~Over Southern Africa UKESM1-0-LL shows a reduction in future $PM_{2.5}$, in contrast to the other models, ~~This can again be attributed~~ due to a reduction in the BC, OA and dust aerosol components (Fig. S24, S26 and S27). UKESM1-0-LL exhibits particularly strong negative correlations for surface $PM_{2.5}$ when compared with temperature and precipitation. These relationships over Southern Africa are quite different to other CMIP6 models, which is also highlighted in the model evaluation over this region (Fig. 8) and indicates that climate change influences aerosol concentrations differently over this region in this model (Figure 16). In addition, there is a slight positive correlation of $PM_{2.5}$ with BVOC emissions in UKESM1-0-LL over Southern Africa. Future biogenic emissions (including monoterpenes) reduce here in ssp370 (Fig. S22), potentially due to land-use vegetation change as UKESM1-0-LL has dynamic vegetation coupled to BVOC emissions (Table S1). This could also reduce $PM_{2.5}$ concentrations over this region because monoterpene emissions are the main precursor to SOA formation in UKESM1-0-LL (Mulcahy et al., 2019).*"

A new sentence has been included on Page 28 Lines 594

"*There is also a lack of consistency across CMIP6 models in the correlations of $PM_{2.5}$ with any individual driver, indicating the variability of the aerosol sources in these regions within models.*"

Page 28 Lines 597-601 have been amended as follows:

"*A strong increase in sea salt concentrations is simulated in all models across the Southern Ocean (and other oceans), potentially driven by changes to meteorological conditions (reflected by the positive correlations of $PM_{2.5}$ with the climate variables temperatures and precipitation in Fig. 16), which increase wind speed and sea salt emissions. As ssp370 is a scenario with a large climate change signal, the increases in $PM_{2.5}$ across the North Pole, particularly in 2100, can be attributed to the melting of sea ice increasing sea salt emissions, which again is reflected in the positive correlations of $PM_{2.5}$ with climate variables over this region.*"

Detailed comments

One of the more interesting aspects of the paper is the comparison with the parameterisation based on HTAP models to separately attribute changes to emissions versus the combined emissions and climate changes simulated by the AerChemMIP models. However, it would help to have a better summary of how the parameterisation was developed and applied. Is it one parameterisation, or an ensemble of parameterisations that were developed separately for each model? Is there any overlap in the models used in developing the parameterisation and the AerChemMIP models? If so, can that subset of models be analyzed to attribute with greater confidence the role of climate change? Would this study support future work to extend this parameterisation to include the effects of temperature, humidity, or some other changes in climate variables?

The O_3 parameterisation is built upon models and emission perturbation experiments contributing to phase 1 and 2 of the Hemispheric Transport of Air Pollutants (HTAP) project. The models used to construct the O_3 parameterisation are independent of those used in CMIP6 and in the analysis presented in this manuscript. The parameterisation is based solely on emission perturbation experiments and does not account for any changes in O_3 due to climate or meteorology. Therefore, comparison of the results from the parameterisation with CMIP6 models provides an indication of the impact on surface O_3 from non-emission driven changes. Further development of the parameterisation is planned in the future to include some representation of the impact of climate change on surface O_3.

Based on the reviewers comment we have included more details on the development and application of the O_3 parameterisation in the manuscript. The following has been included on Page 6, line 206:

"*The HTAP_param was previously developed based upon the source-receptor relationships of O_3 derived from perturbation experiments of regional precursor emissions and global CH_4 abundances (Wild et al., 2012; Turnock et al., 2018). The HTAP_param applies the fractional change in global CH_4 abundance and regional emission precursors (NOx, CO and NMVOCs) for a particular scenario to the ozone response from each individual model used in the parameterisation. The total O_3 response is obtained by summing up the response from each of the individual models to all precursor changes across all source regions. The surface O_3 response previously calculated from the HTAP_param in both the historical and future CMIP6 scenarios is compared to that from the CMIP6 models (Turnock et al., 2019).*"

The referencing throughout the text seems to focus on more recent work rather than early papers that first identified important relationships. For example, the role of increasing water vapor in increasing ozone loss was first pointed out by Johnson et al., 1999 (text around line 65, and especially 450); the role of methane for surface ozone by Fiore et al. 2002 and Shindell et al. 2012 (text around line 65); the increase in ozone under climate change scenarios by Wu et al. 2009 and Weaver et al. 2009 (text around line 645).

Following the recommendations of the reviewer we have updated the text in the manuscript at the appropriate places to include reference to these papers.

Try to quantify wherever possible in the text, such as line 29 "consistent overestimate", line 31 "consistently underestimated", by how much? Is there any improvement in biases, or worsening, relative to prior studies? Line 40 "important differences", can anything be said as to which is most important or handled most realistically? Line 44-45 should include at least one example to support this statement.

We thank the reviewer for the suggestions and tried to make improvements throughout the text to provide more quantitative statements.

In response to the specific comments above Page 1, line 29-33 has been amended to:

"*CMIP6 models consistently overestimate observed surface O_3 concentrations across most regions and in most seasons by up to 16 ppb, with a large diversity in simulated values over northern hemisphere continental regions. Conversely, observed surface $PM_{2.5}$ concentrations are consistently underestimated in CMIP6 models by up to 10 µg m^{-3}, particularly for the northern hemisphere winter months, with the largest model diversity near natural emission source regions. The biases in CMIP6 models when compared to observations of O_3 and $PM_{2.5}$ are similar to those found in previous studies.*"

Page 1 Line 40 has been slightly amended to reflect that differences between models vary on a regional basis.

"*A comparison of simulated regional changes in both surface O_3 and $PM_{2.5}$ from individual CMIP6 models highlights important regional differences due to the simulated interaction of aerosols, chemistry, climate and natural emission sources within models*."

Line 44 -45

"*Differences between individual models emphasises the importance of understanding how future Earth system feedbacks influence natural emission sources e.g. response of biogenic emissions under climate change.*"

Lines 113-114. Why do this for a future scenario rather than the historical period where there might be some opportunity to evaluate with observations?

The inter-model comparison of CMIP6 models for ssp370 was undertaken to explore the differences in their simulated response of air pollutants to future changes in emissions and climate. The model evaluation of simulated surface O_3 and $PM_{2.5}$ against observations in the present day (2004-2014) was conducted to benchmark each of the CMIP6 models, as well as identify biases and differences between CMIP6 models. The evaluation highlights particular discrepancies between CMIP6 models such as the higher present day concentrations of surface O_3 simulated by BCC-ESM1 and GISS-E2-1-G and the large seasonal cycle in surface O_3 simulated by UKESM1. In addition, higher concentrations of surface $PM_{2.5}$ are simulated by CESM2-WACCM and UKESM1 over Asia, whereas lower values are simulated by MIROC-ES2L over remote regions. We have made amendments to the text in the model evaluation section of the manuscript to try and bring out some of the inter-model differences in addition to biases against observations.

Figure 2 is difficult to digest. Why does this need to be in the main text? This is an example where more could be gleaned from the analysis if these changes in emissions could be shown to be related to the projected changes in ozone and/or PM2.5, perhaps through scatterplots.

We included Figure 2 to highlight the regional disparity in emission trajectories of air pollutants compared to the global changes presented in Figure 1. In addition, we wanted to highlight the importance of different short-term or long-term trajectories in future scenario e.g. increases in NOx emissions across East Asia in ssp370 by 2050 but then reductions out to 2100. Figure 2 has been revised based on the comments from reviewer 1 to make it easier to understand (see response to reviewer 1 above). We have also made comparisons of changes in air pollutants to emissions in the future ssp370 scenario (see above) as suggested in the initial comments by reviewer 2.

Line 271. This can be checked and stated more confidently by examining NO2+O3 rather than just O3.

The sensitivity of O_3 formation to NOx concentrations in each individual CMIP6 model is discussed further in the response to point 4 of reviewer 1, which highlights that UKESM1 has some of the largest regional NOx concentrations and lower surface O_3 concentrations. Page 9 , line 271 has been amended to include reference to the new figure. In addition, comparisons of O_3 and NOx concentrations are made for each model and presented in response to the initial comments by reviewer 2.

Lines 444-445 is not new as this was a major result from CMIP5 era RCP8.5. Some of that work probably deserves a citation, such as Gao et al. 2013.

This section has been amended to include references as per the response to point 5 of reviewer 1 above.

The biases in Figure 3 are very hard to read. It should be stated if the color bar saturates.

The colour bar on Figure 3 does saturate, which has now been stated in the figure caption. Figure 3 has also been amended to try and make the biases clearer, along with the inclusion of the annual comparisons in response to an earlier point by reviewer 2.

Lines 494-500. These seemingly different responses may occur because of different responses in winter versus summer across the models being mixed together in the annual mean.

The reviewer is correct in that this response in amplified on a seasonal mean basis. This section has been amended as stated in the initial response to reviewer 2 above.

Lines 503-514. Can these points about sources of inter-model differences be illustrated and based on evidence rather than surmised? Same goes for lines 580-590 & 600-602, where it might be worth moving some of the supplemental information into the main text to support more strongly these points.

Two new figures have been included in the manuscript to show correlations between future changes in air pollutants and different variables. The text of the manuscript has been edited as shown in the initial response to reviewer 2 to reflect the additional information on the reasons between differences in models.

Lines 648-650 should be supported with observations for this conclusion to be made here.

The following amendment to the text has been made to reference other studies that observe the same temporal changes in $PM_{2.5}$ concentrations.

"CMIP6 models simulate the peak in $PM_{2.5}$ concentrations in the 1980s across Europe and North America, prior to the simulating the observed decline in concentrations to present day (Leibensperger et al., 2012; Tørseth et al., 2012; Turnock et al., 2015), ~~resulting from~~ attributed to the implementation of air pollutant emission controls over these regions."

Stronger evidence should also be included to support conclusions on lines 665-666 & 677-678.

Further evidence has been provided as to the reasons for the differences between CMIP6 models in the initial response to reviewer 2, along with changes to the text of the manuscript. We have slightly amended the text in the conclusion to reflect these changes.

Page 31 lines 665-66 have been amended to the following:

"*Disagreements in the prediction of future changes to regional surface $PM_{2.5}$ concentrations between individual CMIP6 models can ~~mainly~~ be attributed to differences in the complexity of the aerosol schemes implemented within models, in particular the formation mechanisms of organic aerosols and emission of BOVCs over certain regions ~~Additionally~~, along with the strength of the climate change signal (temperature and precipitation) ~~within~~ simulated by models and ~~how this can have important~~ the impact this has on natural aerosol emissions via Earth system couplings ~~leading to discrepancies between models~~.*"

Page 31 lines 677-678 have been amended to the following:

"*Important differences between individual CMIP6 models have been identified in terms of how they ~~treat the~~ simulate air pollutants from the interaction of chemistry (O_3 and NOx), climate (temperature and precipitation) and natural precursor emissions (BVOCs) in the future.*"

References

Aas, W., Mortier, A., Bowersox, V., Cherian, R., Faluvegi, G., Fagerli, H., Hand, J., Klimont, Z., Galy-Lacaux, C., Lehmann, C. M. B., Myhre, C. L., Myhre, G., Olivié, D., Sato, K., Quaas, J., Rao, P. S. P., Schulz, M., Shindell, D., Skeie, R. B., Stein, A., Takemura, T., Tsyro, S., Vet, R. and Xu, X.: Global and regional trends of atmospheric sulfur, Sci. Rep., 9(1), 953, doi:10.1038/s41598-018-37304-0, 2019.

Archibald, A., O'Connor, F., Abraham, N. L., Archer-Nicholls, S., Chipperfield, M., Dalvi, M., Folberth, G., Dennison, F., Dhomse, S., Griffiths, P., Hardacre, C., Hewitt, A., Hill, R., Johnson, C., Keeble, J., Köhler, M., Morgenstern, O., Mulchay, J., Ordóñez, C., Pope, R., Rumbold, S., Russo, M., Savage, N., Sellar, A., Stringer, M., Turnock, S., Wild, O. and Zeng, G.: Description and evaluation of the UKCA stratosphere-troposphere chemistry scheme (StratTrop vn 1.0) implemented in UKESM1, Geosci. Model Dev., 13, 1223–1266, doi:10.5194/gmd-2019-246, 2020.

Bauer, S. E., Tsigaridis, K. and Miller, R.: Significant atmospheric aerosol pollution caused by world food cultivation, Geophys. Res. Lett., 43(10), 5394–5400, doi:10.1002/2016GL068354, 2016.

Bauer, S. E., Im, U., Mezuman, K. and Gao, C. Y.: Desert Dust, Industrialization, and Agricultural Fires: Health Impacts of Outdoor Air Pollution in Africa, J. Geophys. Res. Atmos., 124(7), 4104–4120, doi:10.1029/2018JD029336, 2019.

Bauer, S. E., Tsigaridis, K., Faluvegi, G., Kelley, M., Lo, K. K., Miller, R. L., Nazarenko, L., Schmidt, G. A. and Wu, J.: Historical (1850-2014) aerosol evolution and role on climate forcing using the GISS ModelE2.1 contribution to CMIP6, J. Adv. Model. Earth Syst., doi:10.1029/2019ms001978, 2020.

Brauer, M., Freedman, G., Frostad, J., van Donkelaar, Aaron Martin, R. V, Dentener, F., Dingenen, R. van, Estep, K., Amini, H., Apte, J. S., Balakrishnan, K., Barregard, L., Broday, D., Feigin, V., Ghosh, S., Hopke, P. K., Knibbs, L. D., Kokubo, Y., Liu, Y., Ma, S., Morawska, L., Sangrador, J. L. T., Shaddick, G., Anderson, H. R., Vos, T., Forouzanfar, M. H., Burnett, R. T. and Cohen, A.: Ambient Air Pollution Exposure Estimation for the Global Burden of Disease 2013, Environ. Sci. Technol., 50(1), 79–88, doi:DOI: 10.1021/acs.est.5b03709, 2016.

Burnett, R. T., Arden Pope, C., Ezzati, M., Olives, C., Lim, S. S., Mehta, S., Shin, H. H., Singh, G., Hubbell, B., Brauer, M., Ross Anderson, H., Smith, K. R., Balmes, J. R., Bruce, N. G., Kan, H., Laden, F., Prüss-Ustün, A., Turner, M. C., Gapstur, S. M., Diver, W. R. and Cohen, A.: An integrated risk function for estimating the global burden of disease attributable to ambient fine particulate matter exposure, Environ. Health Perspect., 122, 397–403, doi:10.1289/ehp.1307049, 2014.

Butt, E. W., Turnock, S. T., Rigby, R., Reddington, C. L., Yoshioka, M., Johnson, J. S., Regayre, L. A., Pringle, K. J., Mann, G. W. and Spracklen, D. V.: Global and regional trends in particulate air pollution and attributable health burden over the past 50 years, Environ. Res. Lett., 12(10), doi:10.1088/1748-9326/aa87be, 2017.

Chin, M., Diehl, T., Tan, Q., Prospero, J. M., Kahn, R. A., Remer, L. A., Yu, H., Sayer, A. M., Bian, H., Geogdzhayev, I. V., Holben, B. N., Howell, S. G., Huebert, B. J., Hsu, N. C., Kim, D., Kucsera, T. L., Levy, R. C., Mishchenko, M. I., Pan, X., Quinn, P. K., Schuster, G. L., Streets, D. G., Strode, S. A., Torres, O. and Zhao, X.-P.: Multi-decadal aerosol variations from 1980 to 2009: a perspective from observations and a global model, Atmos. Chem. Phys., 14(7), 3657–3690, doi:10.5194/acp-14-3657-2014, 2014.

Chowdhury, S., Dey, S. and Smith, K. R.: Ambient PM2.5 exposure and expected premature mortality to 2100 in India under

climate change scenarios, Nat. Commun., 9(1), doi:10.1038/s41467-017-02755-y, 2018.

Colette, A., Andersson, C., Baklanov, A., Bessagnet, B., Brandt, J., Christensen, J. H., Doherty, R., Engardt, M., Geels, C., Giannakopoulos, C., Hedegaard, G. B., Katragkou, E., Langner, J., Lei, H., Manders, A., Melas, D., Meleux, F., Rouïl, L., Sofiev, M., Soares, J., Stevenson, D. S., Tombrou-Tzella, M., Varotsos, K. V and Young, P.: Is the ozone climate penalty robust in Europe?, Environ. Res. Lett., 10(8), 084015, doi:10.1088/1748-9326/10/8/084015, 2015.

Deushi, M. and Shibata, K.: Development of a Meteorological Research Institute chemistry-climate model version 2 for the study of tropospheric and stratospheric chemistry, Pap. Meteorol. Geophys., 62(May), 1–46, doi:10.2467/mripapers.62.1, 2011.

van Donkelaar, A., Martin, R. V., Brauer, M., Kahn, R., Levy, R., Verduzco, C. and Villeneuve, P. J.: Global estimates of ambient fine particulate matter concentrations from satellite-based aerosol optical depth: Development and application, Environ. Health Perspect., 118(6), 847–855, doi:10.1289/ehp.0901623, 2010.

Dunne, J. P., Horowitz, L. W., Adcroft, A. J., Ginoux, P., Held, I. M., John, J. G., Malyshev, S., Naik, V., Paulot, F., Shevliakova, E., AStock, C., Zadeh, N., Blanton, C., Dunne, K. A., Dupuis, C., Durachta, J., Dussin, R., G Gauthier, P. P., Griffies, M., Guo, H., Hallberg, R. W., Harrison, M., He, J., Hurlin, W., McHugh, C., D Milly, P. C., Nikonov, S., Paynter, D. J., Ploshay, J., Radhakrishnan, A., Rand, K., Reichl, B. G., Robinson, T., Schwarzkopf, D. M., Sentman, L. T., Underwood, S., Winton, M., Wittenberg, A. T., Wyman, B., Zeng, Y. and Zhao, M.: The GFDL Earth System Model version 4.1 (GFDL-ESM4.1): Model 1 description and simulation characteristics, J. Adv. Model. Earth Syst., Submitted, 2020.

Emmons, L. K., Schwantes, R. H., Orlando, J. J., Tyndall, G., Kinnison, D., Lamarque, J., Marsh, D., Mills, M. J., Tilmes, S., Bardeen, C., Buchholz, R. R., Conley, A., Gettelman, A., Garcia, R., Simpson, I., Blake, D. R., Meinardi, S. and Pétron, G.: The Chemistry Mechanism in the Community Earth System Model Version 2 (CESM2), J. Adv. Model. Earth Syst., 12(4), 1–21, doi:10.1029/2019ms001882, 2020.

Fiore, A. M., Dentener, F. J., Wild, O., Cuvelier, C., Schultz, M. G., Hess, P., Textor, C., Schulz, M., Doherty, R. M., Horowitz, L. W., MacKenzie, I. A., Sanderson, M. G., Shindell, D. T., Stevenson, D. S., Szopa, S., Van Dingenen, R., Zeng, G., Atherton, C., Bergmann, D., Bey, I., Carmichael, G., Collins, W. J., Duncan, B. N., Faluvegi, G., Folberth, G., Gauss, M., Gong, S., Hauglustaine, D., Holloway, T., Isaksen, I. S. A., Jacob, D. J., Jonson, J. E., Kaminski, J. W., Keating, T. J., Lupu, A., Manner, E., Montanaro, V., Park, R. J., Pitari, G., Pringle, K. J., Pyle, J. A., Schroeder, S., Vivanco, M. G., Wind, P., Wojcik, G., Wu, S. and Zuber, A.: Multimodel estimates of intercontinental source-receptor relationships for ozone pollution, J. Geophys. Res. Atmos., 114(4), 1–21, doi:10.1029/2008JD010816, 2009.

Fortems-Cheiney, A., Foret, G., Siour, G., Vautard, R., Szopa, S., Dufour, G., Colette, A., Lacressonniere, G. and Beekmann, M.: A 3 °C global RCP8.5 emission trajectory cancels benefits of European emission reductions on air quality, Nat. Commun., 8(89), 1–5, doi:10.1038/s41467-017-00075-9, 2017.

Gao, M., Han, Z., Liu, Z., Li, M., Xin, J., Tao, Z., Li, J., Kang, J.-E., Huang, K., Dong, X., Zhuang, B., Li, S., Ge, B., Wu, Q., Cheng, Y., Wang, Y., Lee, H.-J., Kim, C.-H., Fu, J. S., Wang, T., Chin, M., Woo, J.-H., Zhang, Q., Wang, Z. and Carmichael, G. R.: Air quality and climate change, Topic 3 of the Model Inter-Comparison Study for Asia Phase III (MICS-Asia III)-Part 1: Overview and model evaluation, Atmos. Chem. Phys, 18, 4859–4884, doi:10.5194/acp-18-4859-2018, 2018.

Gao, Y., Fu, J. S., Drake, J. B., Lamarque, J.-F. and Liu, Y.: The impact of emission and climate change on ozone in the United States under representative concentration pathways (RCPs), Atmos. Chem. Phys., 13(18), 9607–9621, doi:10.5194/acp-13-9607-2013, 2013.

Gettelman, A., Mills, M. J., Kinnison, D. E., Garcia, R. R., Smith, A. K., Marsh, D. R., Tilmes, S., Vitt, F., Bardeen, C. G., McInerny, J., Liu, H. L., Solomon, S. C., Polvani, L. M., Emmons, L. K., Lamarque, J. F., Richter, J. H., Glanville, A. S., Bacmeister, J. T., Phillips, A. S., Neale, R. B., Simpson, I. R., DuVivier, A. K., Hodzic, A. and Randel, W. J.: The Whole Atmosphere Community Climate Model Version 6 (WACCM6), J. Geophys. Res. Atmos., 124(23), 12380–12403, doi:10.1029/2019JD030943, 2019.

Glotfelty, T., He, J. and Zhang, Y.: Impact of future climate policy scenarios on air quality and aerosol-cloud interactions using an advanced version of CESM/CAM5: Part I. model evaluation for the current decadal simulations, Atmos. Environ., 152, 222–239, doi:10.1016/J.ATMOSENV.2016.12.035, 2017.

Griffiths, P., Archibald, A. T., Zeng, G., Zanis, P., Hassler, B., O'Connor, F. M., Turnock, S. T., Naik, V., Young, P., Wild, O., Keeble, J., Shin, Y., Ziemke, J. R., Galbally, I., Tarasick, D., Jingxian., L., Omid, M. and Murray, L. T.: Tropospheric Ozone in CMIP6 Simulations, Submitted, 2019.

Guenther, A., Hewitt, C. N., Erickson, D., Fall, R., Geron, C., Graedel, T., Harley, P., Klinger, L., Lerdau, M., Mckay, W. A., Pierce, T., Scholes, B., Steinbrecher, R., Tallamraju, R., Taylor, J. and Zimmerman, P.: A global model of natural volatile organic compound emissions, J. Geophys. Res., 100(D5), 8873, doi:10.1029/94JD02950, 1995.

Hajima, T., Watanabe, M., Yamamoto, A., Tatebe, H., Noguchi, M. A., Abe, M., Ohgaito, R., Ito, A., Yamazaki, D., Okajima,

H., Ito, A., Takata, K., Ogochi, K., Watanabe, S. and Kawamiya, M.: Development of the MIROC-ES2L Earth system model and the evaluation of biogeochemical processes and feedbacks, Geosci. Model Dev., 13, 2197–2244, doi:https://doi.org/10.5194/gmd-13-2197-2020, 2020.

Horowitz, L. W., Naik, V., Paulot, F., Ginoux, P. A., Dunne, J. P., Mao, J., Schnell, J., Chen, X., He, J., John, J. G., Lin, M., Lin, P., Malyshev, S., Paynter, D., Shevliakova, E. and Zhao, M.: The GFDL Global Atmospheric Chemistry-Climate Model AM4.1: Model Description and Simulation Characteristics, J. Adv. Model. Earth Syst., Submitted, 2019.

Im, U., Christensen, J. H., Geels, C., Hansen, K. M., Brandt, J., Solazzo, E., Alyuz, U., Balzarini, A., Baro, R., Bellasio, R., Bianconi, R., Bieser, J., Colette, A., Curci, G., Farrow, A., Flemming, J., Fraser, A., Jimenez-Guerrero, P., Kitwiroon, N., Liu, P., Nopmongcol, U., Palacios-Peña, L., Pirovano, G., Pozzoli, L., Prank, M., Rose, R., Sokhi, R., Tuccella, P., Unal, A., Vivanco, M. G., Yarwood, G., Hogrefe, C. and Galmarini, S.: Influence of anthropogenic emissions and boundary conditions on multi-model simulations of major air pollutants over Europe and North America in the framework of AQMEII3, Atmos. Chem. Phys., 18(12), 8929–8952, doi:10.5194/acp-18-8929-2018, 2018.

Jerrett, M., Burnett, R. T., Pope, C. A., Ito, K., Thurston, G., Krewski, D., Shi, Y., Calle, E. and Thun, M.: Long-Term Ozone Exposure and Mortality, N. Engl. J. Med., 360(11), 1085–1095, doi:10.1056/NEJMoa0803894, 2009.

Jerrett, M., Turner, M. C., Beckerman, B. S., Pope, C. A., van Donkelaar, A., Martin, R. V., Serre, M., Crouse, D., Gapstur, S. M., Krewski, D., Diver, W. R., Coogan, P. F., Thurston, G. D. and Burnett, R. T.: Comparing the health effects of ambient particulate matter estimated using ground-based versus remote sensing exposure estimates, Environ. Health Perspect., 125(4), 552–559, doi:10.1289/EHP575, 2017.

Johnson, J., Regayre, L., Yoshioka, M., Pringle, K., Turnock, S., Browse, J., Sexton, D. M., Rostron, J., Schutgens, N. A., Partridge, D., Liu, D., Allan, J., Coe, H., Ding, A., Cohen, D., Atanacio, A., Vakkari, V., Asmi, E. and Carslaw, K.: Robust observational constraint of uncertain aerosol processes and emissions in a climate model and the effect on aerosol radiative forcing, Atmos. Chem. Phys. Discuss., (November), 1–51, doi:10.5194/acp-2019-834, 2019.

Kirkevåg, A., Grini, A., Olivié, D., Seland, Ø., Alterskjær, K., Hummel, M., Karset, I. H. H., Lewinschal, A., Liu, X., Makkonen, R., Bethke, I., Griesfeller, J., Schulz, M. and Iversen, T.: A production-tagged aerosol module for Earth system models, OsloAero5.3 – extensions and updates for CAM5.3-Oslo, Geosci. Model Dev., 11(10), 3945–3982, doi:10.5194/gmd-11-3945-2018, 2018.

Lamarque, J.-F., Bond, T. C., Eyring, V., Granier, C., Heil, a., Klimont, Z., Lee, D., Liousse, C., Mieville, a., Owen, B., Schultz, M. G., Shindell, D. T., Smith, S. J., Stehfest, E., Van Aardenne, J., Cooper, O. R., Kainuma, M., Mahowald, N., McConnell, J. R., Naik, V., Riahi, K. and van Vuuren, D. P.: Historical (1850–2000) gridded anthropogenic and biomass burning emissions of reactive gases and aerosols: methodology and application, Atmos. Chem. Phys., 10(15), 7017–7039, doi:10.5194/acp-10-7017-2010, 2010.

Leibensperger, E. M., Mickley, L. J., Jacob, D. J., Chen, W.-T., Seinfeld, J. H., Nenes, a., Adams, P. J., Streets, D. G., Kumar, N. and Rind, D.: Climatic effects of 1950–2050 changes in US anthropogenic aerosols – Part 1: Aerosol trends and radiative forcing, Atmos. Chem. Phys., 12(7), 3333–3348, doi:10.5194/acp-12-3333-2012, 2012.

Li, J., Wang, X., Chen, J., Zhu, C., Li, W., Li, C., Liu, L., Xu, C., Wen, L., Xue, L., Wang, W., Ding, A. and Herrmann, H.: Chemical composition and droplet size distribution of cloud at the summit of Mount Tai, China, Atmos. Chem. Phys., 17(16), 9885–9896, doi:10.5194/acp-17-9885-2017, 2017.

Li, K., Jacob, D. J., Liao, H., Shen, L., Zhang, Q. and Bates, K. H.: Anthropogenic drivers of 2013–2017 trends in summer surface ozone in China, Proc. Natl. Acad. Sci. U. S. A., 116(2), 422–427, doi:10.1073/pnas.1812168116, 2019.

Li, Y., Henze, D. K., Jack, D. and Kinney, P. L.: The influence of air quality model resolution on health impact assessment for fine particulate matter and its components, Air Qual. Atmos. Heal., 9(1), 51–68, doi:10.1007/s11869-015-0321-z, 2016.

Michou, M., Nabat, P., Saint-Martin, D., Bock, J., Decharme, B., Mallet, M., Roehrig, R., Séférian, R., Sénési, S. and Voldoire, A.: Present-day and historical aerosol and ozone characteristics in CNRM CMIP6 simulations, J. Adv. Model. Earth Syst., 2019MS001816, doi:10.1029/2019MS001816, 2019.

Mortier, A., Gliss, J., Schulz, M., Aas, W., Andrews, E., Bian, H., Chin, M., Ginoux, P., Hand, J., Holben, B., Hua, Z., Kipling, Z., Kirkevåg, A., Laj, P., Lurton, T., Myhre, G., Neubauer, D., Olivié, D., von Salzen, K., Takemura, T. and Tilmes, S.: Evaluation of climate model aerosol trends with ground-based observations over the last two decades – an AeroCom and CMIP6 analysis, Atmos. Chem. Phys., 1–36, doi:10.5194/acp-2019-1203, 2020.

Mulcahy, J., Johnson, C., Jones, C., Povey, A., Scott, C., Sellar, A., Turnock, S., Woodhouse, M., Andrews, M., Bellouin, N., Browse, J., Carslaw, K., Dalvi, M., Folberth, G., Glover, M., Grosvenor, D., Hardacre, C., Hill, R., Johnson, B., Jones, A., Kipling, Z., Mann, G., Mollard, J., O'Connor, F., Palmieri, J., Reddington, C., Rumbold, S., Richardson, M., Schutgens, N. A., Stier, P., Stringer, M., Tang, Y., Walton, J., Woodward, S. and Yool, A.: Description and evaluation of aerosol in UKESM1 and HadGEM3-GC3.1 CMIP6 historical simulations, Geosci. Model Dev. Discuss., (March), 1–59, doi:10.5194/gmd-2019-357,

2020.

Mulcahy, J. P., Johnson, C., Jones, C. G., Povey, A. C., Scott, C. E., Sellar, A., Turnock, S. T., Woodhouse, M. T., Abraham, N. L., Andrews M., Bellouin, N., Browse, J., Carslaw, K. S., Dalvi, M., Folberth, G., Grosvenor, D., Hardacre, C., Johnson, B., Jones, A., Kipling, Z., Mann, G., Mollard, J., Schutgens, N., O'Connor, F., Palmieri, J., Reddington, C., Richardson, M., Stier, P., Woodward, S. and Yool, A.: Description and evaluation of aerosol in UKESM1 and HadGEM3-GC3.1 CMIP6 historical simulations, Geosci. Model Dev., submited(March), 2019.

Neal, L. S., Dalvi, M., Folberth, G., Mcinnes, R. N., Agnew, P., O 'connor, F. M., Savage, N. H. and Tilbee, M.: A description and evaluation of an air quality model nested within global and regional composition-climate models using MetUM, Geosci. Model Dev, 10, 3941–3962, doi:10.5194/gmd-10-3941-2017, 2017.

Pan, X., Chin, M., Gautam, R., Bian, H., Kim, D., Colarco, P. R., Diehl, T. L., Takemura, T., Pozzoli, L., Tsigaridis, K., Bauer, S. and Bellouin, N.: A multi-model evaluation of aerosols over South Asia: common problems and possible causes, Atmos. Chem. Phys., 15(10), 5903–5928, doi:10.5194/acp-15-5903-2015, 2015.

Parrish, D. D., Lamarque, J. F., Naik, V., Horowitz, L., Shindell, D. T., Staehelin, J., Derwent, R., Cooper, O. R., Tanimoto, H., Volz-Thomas, A., Gilge, S., Scheel, H. E., Steinbacher, M. and Fröhlich, M.: Long-term changes in lower tropospheric baseline ozone concentrations: Comparing chemistry-climate models and observations at northern midlatitudes, J. Geophys. Res., 119(9), 5719–5736, doi:10.1002/2013JD021435, 2014.

Pozzoli, L., Janssens-Maenhout, G., Diehl, T., Bey, I., Schultz, M. G., Feichter, J., Vignati, E. and Dentener, F.: Re-analysis of tropospheric sulfate aerosol and ozone for the period 1980–2005 using the aerosol-chemistry-climate model ECHAM5-HAMMOZ, Atmos. Chem. Phys., 11(18), 9563–9594, doi:10.5194/acp-11-9563-2011, 2011.

Punger, E. M. and West, J. J.: The effect of grid resolution on estimates of the burden of ozone and fine particulate matter on premature mortality in the USA, Air Qual. Atmos. Heal., 6(3), 563–573, doi:10.1007/s11869-013-0197-8, 2013.

Rasmussen, D. J., Hu, J., Mahmud, A. and Kleeman, J. M.: The Ozone Climate Penalty: past, present and future, Environ. Sci. Technol., 47(24), 14258–14266, doi:10.1109/TMI.2012.2196707.Separate, 2013.

Séférian, R., Nabat, P., Michou, M., Saint-Martin, D., Voldoire, A., Colin, J., Decharme, B., Delire, C., Berthet, S., Chevallier, M., Sénési, S., Franchisteguy, L., Vial, J., Mallet, M., Joetzjer, E., Geoffroy, O., Guérémy, J., Moine, M., Msadek, R., Ribes, A., Rocher, M., Roehrig, R., Salas-y-Mélia, D., Sanchez, E., Terray, L., Valcke, S., Waldman, R., Aumont, O., Bopp, L., Deshayes, J., Éthé, C. and Madec, G.: Evaluation of CNRM Earth System Model, CNRM-ESM2-1: Role of Earth System Processes in Present-Day and Future Climate, J. Adv. Model. Earth Syst., 2019MS001791, doi:10.1029/2019MS001791, 2019.

Seland, Ø., Bentsen, M., Seland Graff, L., Olivié, D., Toniazzo, T., Gjermundsen, A., Debernard, J. B., Gupta, A. K., He, Y., Kirkevåg, A., Schwinger, J., Tjiputra, J., Schancke Aas, K., Bethke, I., Fan, Y., Griesfeller, J., Grini, A., Guo, C., Ilicak, M., Hafsahl Karset, I. H., Landgren, O., Liakka, J., Onsum Moseid, K., Nummelin, A., Spensberger, C., Tang, H., Zhang, Z., Heinze, C., Iverson, T. and Schulz, M.: The Norwegian Earth System Model, NorESM2 - Evaluation of theCMIP6 DECK and historical simulations, Geosci. Model Dev. Discuss., (February), 1–68, doi:10.5194/gmd-2019-378, 2020.

Shindell, D. T., Lamarque, J.-F., Schulz, M., Flanner, M., Jiao, C., Chin, M., Young, P. J., Lee, Y. H., Rotstayn, D., Mahowald, N., Milly, G., Faluvegi, G., Collins, W. J., Conley, A. J., Dalsoren, S., Easter, R., Ghan, S., Horowitz, L., Liu, X., Myhre, G., Nagashima, T., Naik, V., Rumbold, S. T., Skeie, R., Sudo, K., Szopa, S., Takemura, T., Voulgarakis, A., Yoon, J.-H. and Lo, F.: Radiative forcing in the ACCMIP historical and future climate simulations, Atmos. Chem. Phys., 13, 2939–2974, doi:10.5194/acp-13-2939-2013, 2013.

Silva, R. A., Adelman, Z., Fry, M. M. and West, J. J.: Impact of emissions sectors on global mortality, , 1776(11), 1776–1784 [online] Available from: https://ehp.niehs.nih.gov/wp-content/uploads/124/11/EHP177.alt.pdf, 2016a.

Silva, R. A., West, J. J., Lamarque, J. F., Shindell, D. T., Collins, W. J., Dalsoren, S., Faluvegi, G., Folberth, G., Horowitz, L. W., Nagashima, T., Naik, V., Rumbold, S. T., Sudo, K., Takemura, T., Bergmann, D., Cameron-Smith, P., Cionni, I., Doherty, R. M., Eyring, V., Josse, B., MacKenzie, I. A., Plummer, D., Righi, M., Stevenson, D. S., Strode, S., Szopa, S. and Zengast, G.: The effect of future ambient air pollution on human premature mortality to 2100 using output from the ACCMIP model ensemble, Atmos. Chem. Phys., 16(15), 9847–9862, doi:10.5194/acp-16-9847-2016, 2016b.

Solazzo, E., Bianconi, R., Hogrefe, C., Curci, G., Tuccella, P., Alyuz, U., Balzarini, A., Baró, R., Bellasio, R., Bieser, J., Brandt, J., Christensen, J. H., Colette, A., Francis, X., Fraser, A., Vivanco, M. G., Jiménez-Guerrero, P., Im, U., Manders, A., Nopmongcol, U., Kitwiroon, N., Pirovano, G., Pozzoli, L., Prank, M., Sokhi, R. S., Unal, A., Yarwood, G. and Galmarini, S.: Evaluation and error apportionment of an ensemble of atmospheric chemistry transport modeling systems: multivariable temporal and spatial breakdown, Atmos. Chem. Phys., 17(4), 3001–3054, doi:10.5194/acp-17-3001-2017, 2017.

Stevenson, D. S., Young, P. J., Naik, V., Lamarque, J.-F., Shindell, D. T., Voulgarakis, A., Skeie, R. B., Dalsoren, S. B., Myhre, G., Berntsen, T. K., Folberth, G. A., Rumbold, S. T., Collins, W. J., MacKenzie, I. A., Doherty, R. M., Zeng, G., van Noije, T. P. C., Strunk, A., Bergmann, D., Cameron-Smith, P., Plummer, D. A., Strode, S. A., Horowitz, L., Lee, Y. H., Szopa, S., Sudo, K.,

Nagashima, T., Josse, B., Cionni, I., Righi, M., Eyring, V., Conley, A., Bowman, K. W., Wild, O. and Archibald, A.: Tropospheric ozone changes, radiative forcing and attribution to emissions in the Atmospheric Chemistry and Climate Model Intercomparison Project (ACCMIP), Atmos. Chem. Phys., 13(6), 3063–3085, doi:10.5194/acp-13-3063-2013, 2013.

Takemura, T.: Distributions and Climate Effects of Atmospheric Aerosols from the preindustrial era to 2100 along Representative Concentration Pathways (RCPs) simulated using the GLobal Aerosol Model SPRINTARS, Atmos. Chem. Phys., 12, 11555–11572 [online] Available from: http://www.atmos-chem-phys.net/12/11555/2012/acp-12-11555-2012.pdf, 2012.

Tegen, I., Neubauer, D., Ferrachat, S., Siegenthaler-Le Drian, C., Bey, I., Schutgens, N., Stier, P., Watson-Parris, D., Stanelle, T., Schmidt, H., Rast, S., Kokkola, H., Schultz, M., Schroeder, S., Daskalakis, N., Barthel, S., Heinold, B. and Lohmann, U.: The global aerosol–climate model ECHAM6.3–HAM2.3 – Part 1: Aerosol evaluation, Geosci. Model Dev., 12(4), 1643–1677, doi:10.5194/gmd-12-1643-2019, 2019.

Tilmes, S., Hodzic, A., Emmons, L. K., Mills, M. J., Gettelman, A., Kinnison, D. E., Park, M., Lamarque, J. -F., Vitt, F., Shrivastava, M., Campuzano Jost, P., Jimenez, J. and Liu, X.: Climate forcing and trends of organic aerosols in the Community Earth System Model (CESM2), J. Adv. Model. Earth Syst., 2019MS001827, doi:10.1029/2019MS001827, 2019.

Tørseth, K., Aas, W., Breivik, K., Fjæraa, a. M., Fiebig, M., Hjellbrekke, a. G., Lund Myhre, C., Solberg, S. and Yttri, K. E.: Introduction to the European Monitoring and Evaluation Programme (EMEP) and observed atmospheric composition change during 1972–2009, Atmos. Chem. Phys., 12(12), 5447–5481, doi:10.5194/acp-12-5447-2012, 2012.

Tsigaridis, K., Daskalakis, N., Kanakidou, M., Adams, P. J., Artaxo, P., Bahadur, R., Balkanski, Y., Bauer, S. E., Bellouin, N., Benedetti, A., Bergman, T., Berntsen, T. K., Beukes, J. P., Bian, H., Carslaw, K. S., Chin, M., Curci, G., Diehl, T., Easter, R. C., Ghan, S. J., Gong, S. L., Hodzic, A., Hoyle, C. R., Iversen, T., Jathar, S., Jimenez, J. L., Kaiser, J. W., Kirkevåg, A., Koch, D., Kokkola, H., Lee, Y. H., Lin, G., Liu, X., Luo, G., Ma, X., Mann, G. W., Mihalopoulos, N., Morcrette, J.-J., Müller, J.-F., Myhre, G., Myriokefalitakis, S., Ng, N. L., O'Donnell, D., Penner, J. E., Pozzoli, L., Pringle, K. J., Russell, L. M., Schulz, M., Sciare, J., Seland, Ø., Shindell, D. T., Sillman, S., Skeie, R. B., Spracklen, D., Stavrakou, T., Steenrod, S. D., Takemura, T., Tiitta, P., Tilmes, S., Tost, H., van Noije, T., van Zyl, P. G., von Salzen, K., Yu, F., Wang, Z., Zaveri, R. A., Zhang, H., Zhang, K., Zhang, Q. and Zhang, X.: The AeroCom evaluation and intercomparison of organic aerosol in global models, Atmos. Chem. Phys., 14(19), 10845–10895, doi:10.5194/acp-14-10845-2014, 2014.

Turnock, S. T., Spracklen, D. V., Carslaw, K. S., Mann, G. W., Woodhouse, M. T., Forster, P. M., Haywood, J., Johnson, C. E., Dalvi, M., Bellouin, N. and Sanchez-Lorenzo, a.: Modelled and observed changes in aerosols and surface solar radiation over Europe between 1960 and 2009, Atmos. Chem. Phys., 15, 9477–9500, doi:10.5194/acp-15-9477-2015, 2015.

Turnock, S. T., Wild, O., Dentener, F. J., Davila, Y., Emmons, L. K., Flemming, J., Folberth, G. A., Henze, D. K., Jonson, J. E., Keating, T. J., Kengo, S., Lin, M., Lund, M., Tilmes, S. and O'Connor, F. M.: The impact of future emission policies on tropospheric ozone using a parameterised approach, Atmos. Chem. Phys., 18(12), 8953–8978, doi:10.5194/acp-18-8953-2018, 2018.

Turnock, S. T., Wild, O., Sellar, A. and O'Connor, F. M.: 300 years of tropospheric ozone changes using CMIP6 scenarios with a parameterised approach, Atmos. Environ., 213, 686–698, doi:10.1016/J.ATMOSENV.2019.07.001, 2019.

Wild, O. and Prather, M. J.: Global tropospheric ozone modeling: Quantifying errors due to grid resolution, J. Geophys. Res. Atmos., 111(11), 1–14, doi:10.1029/2005JD006605, 2006.

Wild, O., Fiore, A. M., Shindell, D. T., Doherty, R. M., Collins, W. J., Dentener, F. J., Schultz, M. G., Gong, S., Mackenzie, I. A., Zeng, G., Hess, P., Duncan, B. N., Bergmann, D. J., Szopa, S., Jonson, J. E., Keating, T. J. and Zuber, A.: Modelling future changes in surface ozone: A parameterized approach, Atmos. Chem. Phys., 12(4), 2037–2054, doi:10.5194/acp-12-2037-2012, 2012.

Wild, O., Voulgarakis, A., O'Connor, F., Lamarque, J. F., Ryan, E. M. and Lee, L.: Global sensitivity analysis of chemistry-climate model budgets of tropospheric ozone and OH: Exploring model diversity, Atmos. Chem. Phys., 20(7), 4047–4058, doi:10.5194/acp-20-4047-2020, 2020.

Wu, T., Zhang, F., Zhang, J., Jie, W., Zhang, Y., Wu, F., Li, L., Yan, J., Liu, X., Lu, X., Tan, H., Zhang, L., Wang, J. and Hu, A.: Beijing Climate Center Earth System Model version 1 (BCC-ESM1): Model description and evaluation of aerosol simulations, Geosci. Model Dev., 13(3), 977–1005, doi:10.5194/gmd-13-977-2020, 2020.

Young, P. J., Archibald, A. T., Bowman, K. W., Lamarque, J.-F., Naik, V., Stevenson, D. S., Tilmes, S., Voulgarakis, A., Wild, O., Bergmann, D., Cameron-Smith, P., Cionni, I., Collins, W. J., Dalsøren, S. B., Doherty, R. M., Eyring, V., Faluvegi, G., Horowitz, L. W., Josse, B., Lee, Y. H., MacKenzie, I. A., Nagashima, T., Plummer, D. A., Righi, M., Rumbold, S. T., Skeie, R. B., Shindell, D. T., Strode, S. A., Sudo, K., Szopa, S. and Zeng, G.: Pre-industrial to end 21st century projections of tropospheric ozone from the Atmospheric Chemistry and Climate Model Intercomparison Project (ACCMIP), Atmos. Chem. Phys., 13(4), 2063–2090, doi:10.5194/acp-13-2063-2013, 2013.

Young, P. J., Naik, V., Fiore, A. M., Gaudel, A., Guo, J., Lin, M. Y., Neu, J. L., Parrish, D. D., Rieder, H. E., Schnell, J. L., Tilmes, S., Wild, O., Zhang, L., Ziemke, J. R., Brandt, J., Delcloo, A., Doherty, R. M., Geels, C., Hegglin, M. I., Hu, L., Im, U., Kumar, R., Luhar, A., Murray, L., Plummer, D., Rodriguez, J., Saiz-Lopez, A., Schultz, M. G., Woodhouse, M. T. and Zeng, G.: Tropospheric Ozone Assessment Report: Assessment of global-scale model performance for global and regional ozone distributions, variability, and trends, Elem Sci Anth, 6(1), 10, doi:10.1525/elementa.265, 2018.

Yukimoto, S., Kawai, H., Koshiro, T., Oshima, N., Yoshida, K., Urakawa, S., Tsujino, H., Deushi, M., Tanaka, T., Hosaka, M., Yabu, S., Yoshimura, H., Shindo, E., Mizuta, R., Obata, A., Adachi, Y. and Ishii, M.: The meteorological research institute Earth system model version 2.0, MRI-ESM2.0: Description and basic evaluation of the physical component, J. Meteorol. Soc. Japan, 97(5), 931–965, doi:10.2151/jmsj.2019-051, 2019.

Historical and future changes in air pollutants from CMIP6 models

Steven T. Turnock[1], Robert J. Allen[2], Martin Andrews[1], Susanne E. Bauer[3,4], Makoto Deushi[5], Louisa Emmons[5,6], Peter Good[1], Larry Horowitz[6,7], Jasmin G. John[7], Martine Michou[7,8], Pierre Nabat[7,8], Vaishali Naik[6,7], David Neubauer[8,9], Fiona M. O'Connor[1], Dirk Olivié[9,10], Naga Oshima[5], Michael Schulz[9,10], Alistair Sellar[1], Sungbo Shim[11], Toshihiko Takemura[10,12], Simone Tilmes[5,6], Kostas Tsigaridis[3,4], Tongwen Wu[11,13], Jie Zhang[11,13]

[1]Met Office Hadley Centre, Exeter, UK
[2]Department of Earth and Planetary Sciences, University of California Riverside, Riverside, California, USA
[3]Center for Climate Systems Research, Columbia University, New York, NY, USA
[4]NASA Goddard Institute for Space Studies, New York, NY, USA
[5] Meteorological Research Institute, Tsukuba, Japan
[6,5]Atmospheric Chemistry Observations and Modelling Lab, National Center for Atmospheric Research, Boulder, CO, USA
[7,6]DOC/NOAA/OAR/ Geophysical Fluid Dynamics Laboratory. Biogeochemistry, Atmospheric Chemistry, and Ecology Division, Princeton, USA
[8,7]Centre National de Recherches Météorologiques (CNRM), Université de Toulouse, Météo-France, CNRS, Toulouse, France
[9,8]Institute of Atmospheric and Climate Science, ETH Zurich, Zurich, Switzerland
[10,9]Division for Climate Modelling and Air Pollution, Norwegian Meteorological Institute, Oslo, Norway
[11] National Institute of Meteorological Sciences, Seogwipo-si, Jeju-do, Korea
[12,10]Research Institute for Applied Mechanics, Kyushu University, Fukuoka, Japan
[13,11]Beijing Climate Center, China Meteorological Administration, Beijing, China

Correspondence to: Steven Turnock (steven.turnock@metoffice.gov.uk)

Abstract.

Poor air quality is currently responsible for large impacts on human health across the world. In addition, the air pollutants, ozone (O_3) and particulate matter less than 2.5 microns in diameter ($PM_{2.5}$), are also radiatively active in the atmosphere and can influence Earth's climate. It is important to understand the effect of air quality and climate mitigation measures over the historical period and in different future scenarios to ascertain any impacts from air pollutants on both climate and human health. The 6th Coupled Model Intercomparison Project (CMIP6) presents an opportunity to analyse the change in air pollutants simulated by the current generation of climate and Earth system models that include a representation of chemistry and aerosols (particulate matter). The shared socio-economic pathways (SSPs) used within CMIP6 encompass a wide range of trajectories in precursor emissions and climate change, allowing for an improved analysis of future changes to air pollutants. Firstly, we conduct an evaluation of the available CMIP6 models against surface observations of O_3 and $PM_{2.5}$. CMIP6 models show a consistently overestimateion of observed surface O_3 concentrations across most regions and in most seasons by up to 16 ppb, with a large diversity in simulated values over northern hemisphere continental regions. Conversely, observed surface $PM_{2.5}$ concentrations are consistently underestimated inby CMIP6 models by up to 10 µg m^{-3}, particularly for the northern hemisphere winter months, with the largest model diversity near natural emission source regions. The biases in CMIP6 models when compared to observations of O_3 and $PM_{2.5}$ are similar to those found in previous studies. Over the historical period (1850-2014) large increases in both surface O_3 and $PM_{2.5}$ are simulated by the CMIP6 models across all regions, particularly over the mid to late 20th Century when anthropogenic emissions increase markedly. Large regional historical changes are simulated for both pollutants, across East and South Asia, with an annual mean increase of up to 40 ppb for O_3 and 12 µg m^{-3} for $PM_{2.5}$. In future scenarios containing strong air quality and climate mitigation measures (ssp126), annual mean concentrations of air pollutants are substantially reduced across all regions by up to 15 ppb for O_3 and 12 µg m^{-3} for $PM_{2.5}$. However, for scenarios that encompass weak action on mitigating climate and reducing air pollutant emissions (ssp370), annual mean increases of both surface O_3 (up 10 ppb) and $PM_{2.5}$ (up to 8 µg m^{-3}) are simulated across most regions,. aAlthough, for regions like North America and Europe small reductions in $PM_{2.5}$ are simulated in this scenario. A comparison of simulated regional changes in both surface O_3 and $PM_{2.5}$ from individual CMIP6 models highlights important regional differences due to the simulated interaction of aerosols, chemistry, climate and natural emission sources within models. The prediction of regional air pollutant

concentrations from the latest climate and Earth system models used within CMIP6 shows that the particular future trajectory of climate and air quality mitigation measures could have important consequences for regional air quality, human health and near-term climate. Differences between individual models emphasises the importance of understanding how future Earth system feedbacks influence natural emission sources e.g. response of biogenic emissions under climate change.

1 Introduction

Air pollutants are important atmospheric constituents as they have large impacts on human health (Lelieveld et al., 2015), damage ecosystems (Fowler et al., 2009) and can also influence climate through changes in the Earth's radiative balance (Boucher et al., 2013; Myhre et al., 2013). Two major components of air pollution at the surface are ozone (O_3) and particulate matter less than 2.5 microns in diameter ($PM_{2.5}$). Exposure to present day ambient concentrations of these two air pollutants was estimated as causing up to 4 million premature deaths per year (Apte et al., 2015; Malley et al., 2017). Over recent decades, the impact on human health from exposure to air pollutants has been increasing (Butt et al., 2017; Cohen et al., 2017). Additionally, elevated levels of air pollutants over recent decades have also been responsible for ecosystem damage to crops and vegetation, although there have been recent improvements in environmental health (de Wit et al., 2015).

In terms of climate impact, tropospheric O_3 has a positive radiative forcing on climate over the industrial period and is the third most important greenhouse gas in terms of radiative forcing (Myhre et al., 2013). However, depletion of O_3 in the stratosphere has resulted in a net negative top of atmosphere radiative forcing over recent decades (Checa-Garcia et al., 2018). Particulate matter (PM), also referred to as aerosols, has an overall negative radiative forcing on climate, both directly and indirectly through the modification of cloud properties (Boucher et al., 2013). Both O_3 and PM are relatively short lived in the troposphere, with a typical lifetime of less than 2 weeks in the lower atmosphere, and are commonly referred to as ~~Near Term~~ Short-lived Climate Forcers (~~NT~~SLCFs). Future air pollutant concentrations and distributions are driven by changes to both precursor emissions and climate. Emission control measures on a national and international level can both influence future changes to air pollutants, with global increases in CH_4 abundance potentially offsetting benefits to surface O_3 from local emission reductions (Fiore et al., 2002; Shindell et al., 2012; Wild et al., 2012). For $PM_{2.5}$, changes in concentrations are dependent on both emission rates and levels of atmospheric oxidants, although changes in specific aerosol components can be more directly related to emissions, e.g. black carbon. In a warming world, background O_3 concentrations over remote locations are likely to decrease (Johnson et al., 1999; Isaksen et al., 2009; Fiore et al., 2012; Doherty et al., 2013), whereas over anthropogenic source regions, which have higher ~~baseline~~average surface O_3 concentrations, an increase is anticipated (Rasmussen et al., 2013; Colette et al., 2015). The climate impact on $PM_{2.5}$ is much more uncertain and variable across regions, with both increases and decreases predicted due to the uncertainty of future meteorological effects (Jacob and Winner, 2009; Allen et al., 2016; Shen et al., 2017). However, any such climate change impacts on $PM_{2.5}$ are considered to be smaller than the effect from implementing emission mitigation measures (Westervelt et al., 2016).

Experiments conducted as part of the 5th Coupled Model Intercomparison Project (CMIP5; Taylor et al., 2012) and the Atmospheric Chemistry and Climate Model Intercomparison Project (ACCMIP, Lamarque et al., 2013) contributed to a multi-model assessment of future trends in air pollutants. Global annual mean surface O_3 concentrations were predicted to increase by up to 5 ppb in 2100 using RCP8.5 (Representative Concentration Pathway with an anthropogenic radiative forcing of 8.5 W m^{-2} in 2100); the RCP with largest increases in methane (CH_4) abundances and the largest climate change signal used in CMIP5 (Kirtman et al., 2013). The other RCPs used in CMIP5 had a lower climate forcing and smaller changes in CH_4 abundance with models predicting global annual mean surface O_3 concentrations that showed little change in the short term (up to 2050) but decreased by around 5 ppb in 2100. The scenario differences in the global mean response for surface O_3 were generally reflected across other regions, although with a larger magnitude of change over the northern hemisphere continental regions. The predicted range of future surface O_3 concentrations was previously found to be dominated by changes in precursor

emissions (Fiore et al., 2012). However, in regions remote from pollution sources (low-NOx) future climate change was shown to result in a small reduction in surface O_3 concentrations. For $PM_{2.5}$, results from CMIP5 and ACCMIP models showed annual mean concentrations declining in most regions and across all scenarios due to the reduction in aerosol emissions. Globally, $PM_{2.5}$ concentrations reduced by ~1 μg m^{-3} by 2100, whereas larger regional reductions of up to 6 μg m^{-3} were predicted by 2100. Exceptions to this occurred over South and East Asia where $PM_{2.5}$ concentrations increased by up to 3 μg m^{-3} in the near-term (up to 2050), after which concentrations reduced by 2100. The largest difference in the response of $PM_{2.5}$ across the scenarios was also shown across East and South Asia due to differences in the carbonaceous and sulphur dioxide (SO_2) emission trajectories (Fiore et al., 2012). Future $PM_{2.5}$ concentrations over Africa and the Middle East were shown to be quite noisy due to the large meteorological variability that influences dust emissions over these regions.

The current set of experiments conducted for the 6th Coupled Model Intercomparison Project (CMIP6; Eyring et al., 2016) represent an opportunity to update the assessment of current and future levels of air pollutants using the latest generation of Earth system and climate models. A new set of future scenarios have been generated for CMIP6, the Shared Socio-economic Pathways (SSPs), which combine different trends in social, economic and environmental developments (O'Neill et al., 2014). Varying amounts of emission mitigation to ~~NT~~SLCFs are applied on top of the baseline social and economic developments to meet predefined climate and air quality targets in the future, allowing for a wider range of future air pollutant trajectories to be assessed than occurred in CMIP5 (Rao et al., 2017; Riahi et al., 2017). Initial assessments have been made of future changes to air pollutants in the SSPs using simplified models (Reis et al., 2018; Turnock et al., 2018, 2019). The sustainability pathway (SSP1) leads to improvements in both air quality and climate, whereas SSP3 (regional rivalry) is not compatible with achieving air quality and climate goals, and the conventional fuels (SSP5) pathway improves air quality at the expenses of climate (Reis et al., 2018). Strong climate and air pollutant mitigation measures in SSP1 were shown to reduce global annual mean surface O_3 concentrations by more than 3.5 ppb, whereas for SSP3 O_3 concentrations over Asia were predicted to increase by 6 ppb (Turnock et al., 2019). These studies highlighted the potential large regional variability in the response of air pollutants to the different assumptions in the future pathways and also the need for a full model assessment using the current generation of Earth System Models (ESMs) that take into account both changes in emissions and climate.

In this study, we use results from experiments conducted as part of CMIP6 to make a first assessment of historical and future changes in air pollutants. First, we assess the performance of CMIP6 models in simulating present day air pollutants by conducting an evaluation against observations of O_3 and $PM_{2.5}$. Regional changes in surface O_3 and $PM_{2.5}$ are computed over the historical period (1850-2014) to provide context with future changes. We are then able to show future projections of air pollutants over different world regions under different Shared Socio-economic Pathways ~~(SSPs)~~ used in the CMIP6 experiments. Finally, a comparison is made of individual CMIP6 models for a single future scenario (ssp370) to identify potential reasons for model discrepancies.

2 Methods

2.1 Air Pollutant Emissions

A new set of historical and future anthropogenic air pollutant emissions has been developed and used as part of CMIP6. The historical anthropogenic emissions are from the Community Emissions Data System (CEDS) and a new dataset was developed for biomass burning emissions, both of which provides information on emissions from 1750 to 2014 (van Marle et al., 2017; Hoesly et al., 2018). The SSPs used in future CMIP6 experiments represent an update from the RCPs used in CMIP5, as they combine pathways of socio-economic development with targets to achieve a certain level of climate mitigation (O'Neill et al., 2014; van Vuuren et al., 2014; Riahi et al., 2017). The SSPs are divided into the following 5 different pathways depending on their social, economic and environmental development: SSP1 – sustainability, SSP2 - middle-of-the-road, SSP3 – regional rivalry, SSP4 - inequality, SSP5 – fossil fuel development. An assumption about the degree of air pollution control (strong,

medium or weak) is included on top of the baseline pathway, with stricter air pollution controls assumed to be tied to economic development (Rao et al., 2016). Weak air pollution controls occur in SSP3 and SSP4, with medium controls in SSP2 and strong air pollution controls in SSP1 and SSP5 (Gidden et al., 2019). A particular climate mitigation target, in terms of an anthropogenic radiative forcing by 2100, and the range of emission mitigation measures associated with achieving it ~~is~~are included ~~on top of~~in addition to the existing policy measures within each baseline SSP scenario~~and is achieved using a range of emissions mitigation measures appropriate to each SSP~~. Climate mitigation targets vary from a weak mitigation scenario with an anthropogenic radiative forcing of 8.5 W m^{-2} by 2100, comparable with a 5 °C temperature change (Riahi et al., 2017), to a strong mitigation scenario with a radiative forcing of 1.9 W m^{-2} by 2100, in accordance with the Paris agreement for keeping temperatures below 2 °C (United Nations, 2016). Some climate mitigation targets are comparable with those of the RCPs used in CMIP5 (2.6, 4.5 and 6.0), whilst others are new, e.g. ssp534-over is included as a delayed mitigation scenario. A scenario specific to the Aerosol and Chemistry Model Intercomparison Project (AerChemMIP), ssp370-lowNTCF, is also included to study the impact of mitigation measures to specifically control ~~NT~~SLCFs on top of ssp370. Future biomass burning emissions vary in each scenario, depending on the particular land-use assumptions (Rao et al., 2017). Whilst future anthropogenic and biomass burning emissions are prescribed in each CMIP6 model from the same dataset, other natural emissions, e.g. dust, biogenic volatile organic compounds (BVOCs) etc., will be different and depend on the individual model configuration.

Figure 1 shows the future changes in global total (anthropogenic and biomass) emissions of the major air pollutant precursors across all of the CMIP6 scenarios, provided as input to the CMIP6 models. The overlying feature is that global air pollutant emissions are predicted to reduce across the majority of scenarios by 2100. The exception to this is that global and regional emissions increase or remain at present day levels for ssp370 (Figs. 1 and ~~Fig.~~ 2). Some air pollutant emissions increase in the near-term in other scenarios e.g. nitrogen oxides (NOx) in ssp585 (by up to 15%), but by 2100 these have been reduced. Future CH_4 abundances show the largest diversity amongst the SSPs. Large increases in global CH_4 abundances of more than 50% are predicted for the fossil fuel dominated pathways of ssp370 and ssp585, whereas large reductions of ~50% are predicted to occur in the strong mitigation scenarios of SSP1.

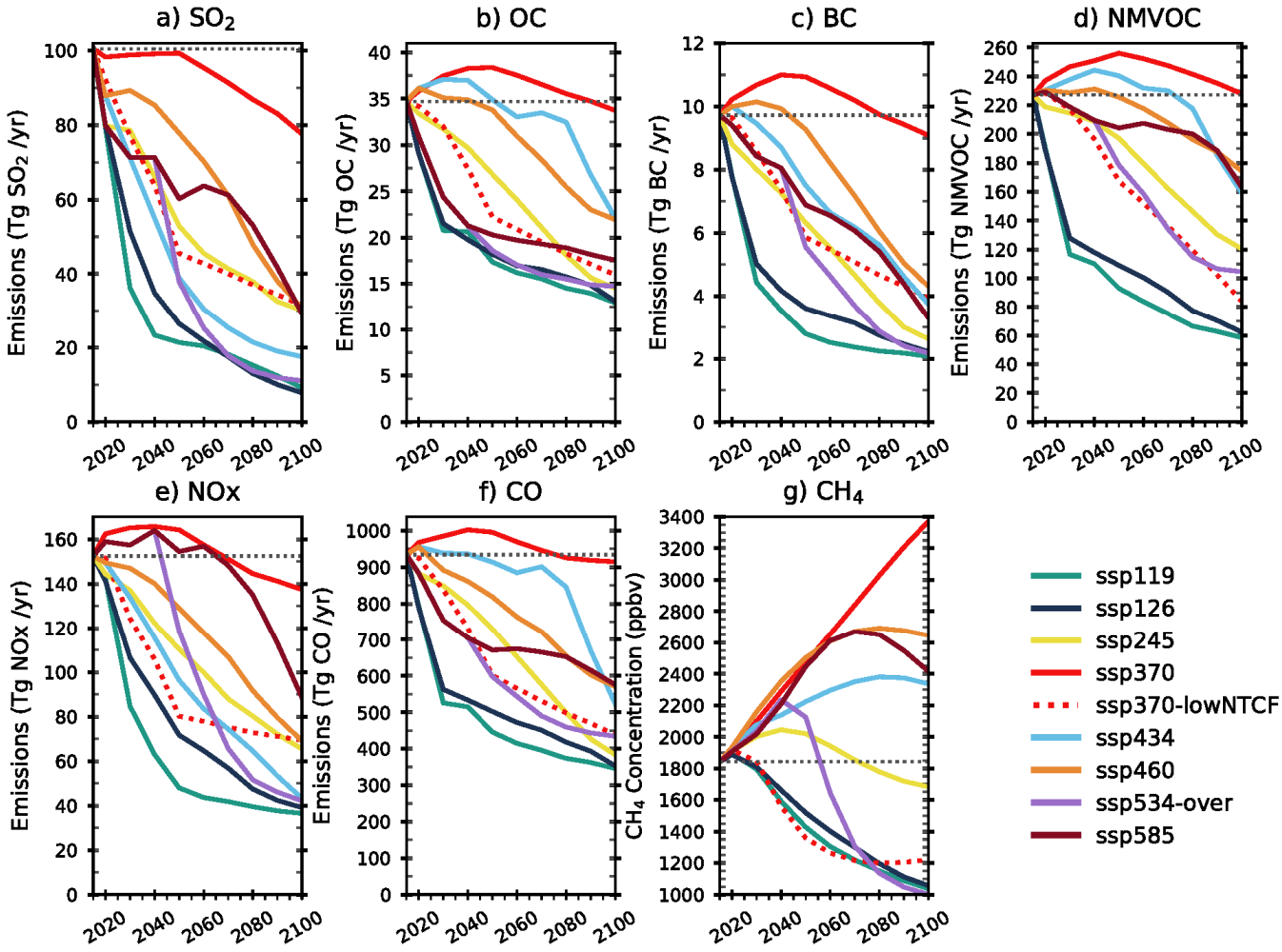

Figure 1: Changes in annual total (anthropogenic and biomass) global air pollutant emissions (relative to 2015) of sulphur dioxide (SO_2), organic carbon (OC), black carbon (BC), non-methane volatile organic compounds (NMVOCs), nitrogen oxides (NOx), carbon monoxide (CO) and global methane (CH_4) abundances in the future CMIP6 scenarios used as input to CMIP6 models. The dashed black line represents the 2015 value. Global CH_4 abundances are not reduced in the AerChemMIP ssp370-lowNTCF simulations used here.

For SO_2, large reductions of more than 50% are shown for most scenarios and across most regions (Figure 2), apart from Africa and Asia in ssp370. Near-term (2050) increases in SO_2 occur over South Asia and other developing regions, which are then reduced in the latter half of the 21st Century. Over Europe and North America consistent decreases are predicted across all scenarios. The other major aerosol emissions, OC and BC, show similar reductions to SO_2 across all scenarios and regions. For all aerosol and aerosol precursors, a reduction of 80-100% (relative to 2015) in regional emissions is predicted by 2100 in the strong mitigation scenarios. Changes in the emissions of the O_3 precursors, NOx, CO and non-methane volatile organic compounds (NMVOCs), show a similar increase across most regions for ssp370 but a general decrease in other scenarios. The change in these emissions are particularly diverse across all the scenarios in South Asia with large relative increases in ssp370 (of up to 50%), in contrast to the large decreases in ssp126 (up to 40%). Across East Asia there is an 20% increase in NOx emissions for ssp370 in 2050 but a long term reduction across all scenarios.

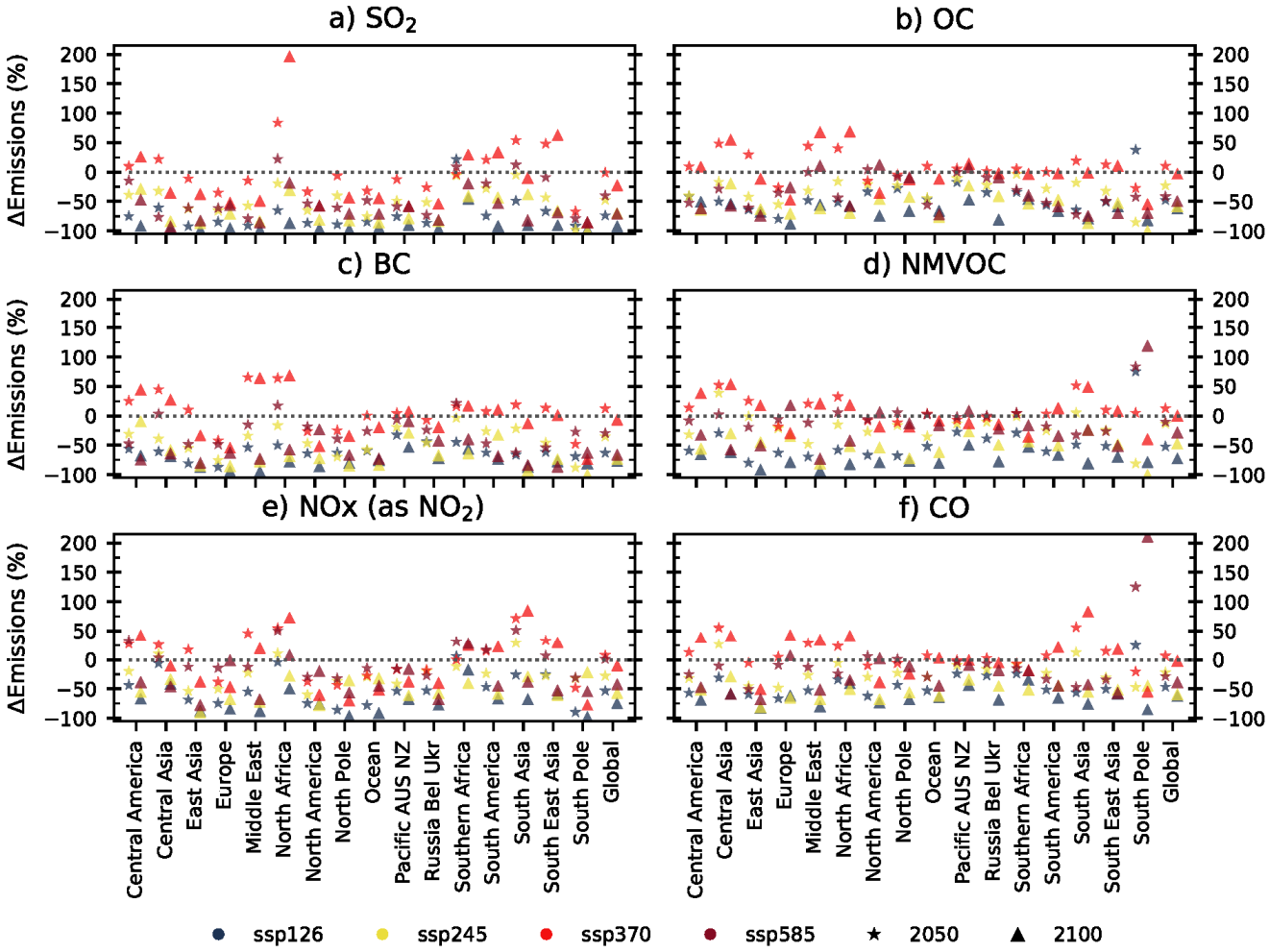

170

~~**Figure 2: Percent change in 2050 (stars) and 2100 (triangles), relative to 2015, for annual mean total (anthropogenic and biomass) air pollutant emissions of SO_2, OC, BC, NMVOCs, NOx and CO across different world regions in the 4 Tier 1 future CMIP6 scenarios. Regions are defined in Figure S1.**~~

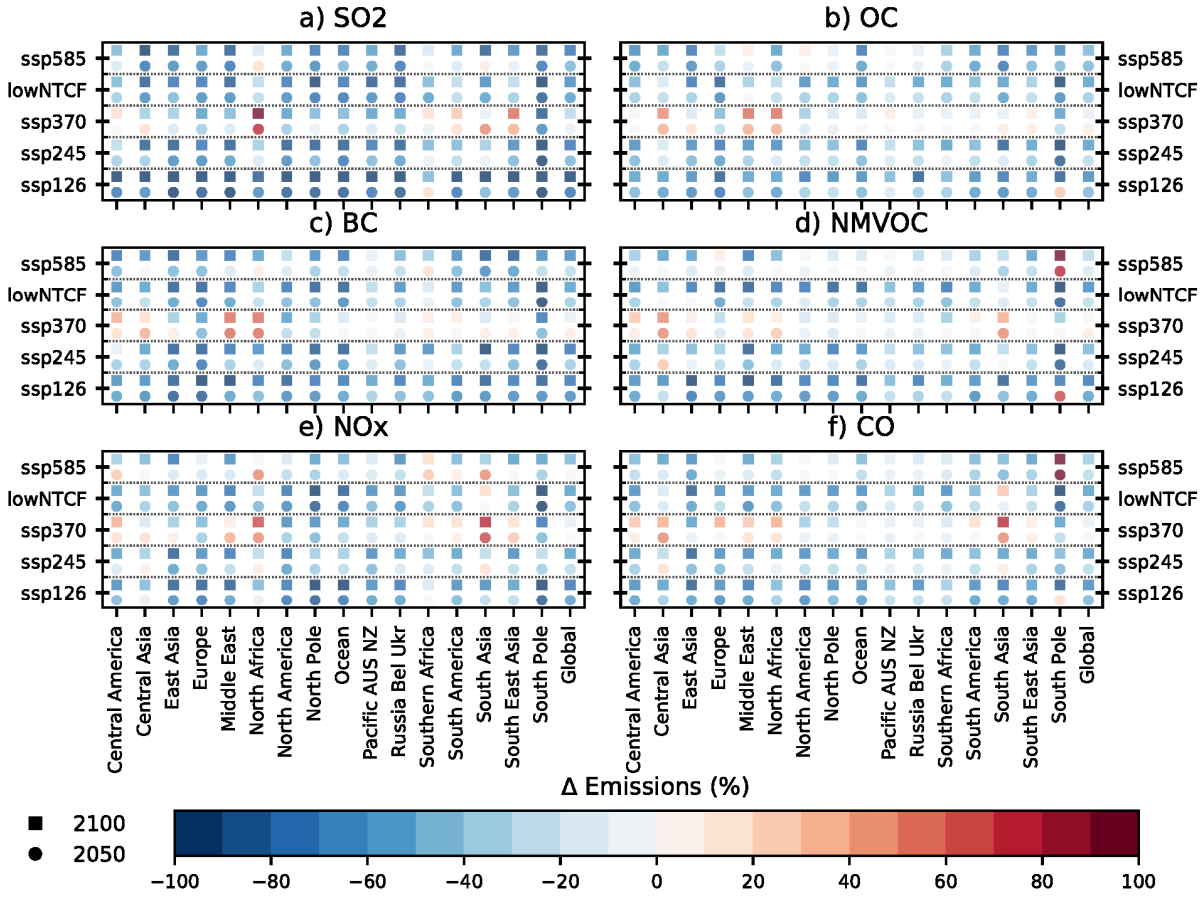

Figure 2: Percent change in 2050 (circles) and 2100 (squares), relative to 2015, for annual mean total (anthropogenic and biomass) air pollutant emissions of a) SO_2, b) OC, c) BC, d) NMVOCs, e) NOx and f) CO across different world regions in the 4 Tier 1 future CMIP6 scenarios and the ssp370-lowNTCF scenario (identified as lowNTCF). Regions are defined in Figure S1.

2.2 CMIP6 Simulations

Surface concentrations of O_3 and $PM_{2.5}$ have been obtained from all the CMIP6 models that made appropriate data available on the Earth System Grid Federation (ESGF) at the time of writing. To study changes in surface air pollutants over the industrial period data has been obtained from the coupled historical simulations (Eyring et al., 2016) over the period 1850 to 2014 from all of the available ensemble members of each available CMIP6 model. For each model, a mean is taken using all available ensemble members prior to the calculation of multi-model mean. For model evaluation purposes, 10 years of data from historical simulations has been used over the period that is relevant to the particular observational dataset (2000-2010 for ground-based $PM_{2.5}$, 2004-2014 for $PM_{2.5}$ reanalysis product and 2005-2014 for ground-based O_3). To investigate future changes in air pollutants, all available data has been obtained over the period 2015 to 2100 for each of the different future coupled atmosphere-ocean model experiments, conducted as part of ScenarioMIP (O'Neill et al., 2016). CMIP6 model data has also been obtained for the AerChemMIP specific ssp370-lowNTCF scenario, which was only required to be conducted over the period 2015-2055 (Collins et al., 2017).

Concentrations of both pollutants at the surface have been obtained by extracting the lowest vertical level of the full 3D field output on the ~~native~~ horizontal and vertical grid of each model (the "AERmon" CMIP6 table ID). For O_3, this is supplied as a separate diagnostic which can be used directly. However, models contributing to CMIP6 will not all directly output $PM_{2.5}$ and the calculation of $PM_{2.5}$ will not be consistent across individual models due to the different treatment of aerosols and their components. For example only a few CMIP6 models include the simulation of ammonium nitrate in their aerosol scheme (currently, only GISS-E2-1-G~~H~~ and GFDL-ESM4 have provided nitrate mass mixing ratios on the ESGF database). Therefore ~~it has been necessary~~ to use a consistent definition ~~of $PM_{2.5}$, which is consistent~~ across all models, ~~and is~~we calculated $PM_{2.5}$ offline. In this study surface $PM_{2.5}$ is defined as the sum of the individual dry aerosol mass mixing ratios of black carbon (BC),

total organic aerosol (OA – both primary and secondary sources), sulphate (SO_4), sea salt (SS) and dust (DU) from the lowest model level extracted ~~of~~ from the full 3D model fields. All BC, OA and SO_4 aerosol mass is assumed to be present in the fine size fraction (< 2.5 µm), whereas a factor of 0.25 for SS and 0.1 for DU has been used to calculate the approximate contribution from these components to the fine aerosol size fraction (Eq. 1).

$$PM_{2.5} = BC + OA + SO_4 + (0.25 \times SS) + (0.1 \times DU) \quad (1)$$

The factors used to calculate the contribution of SS and DU concentrations to the $PM_{2.5}$ size fraction are likely to depend on the individual aerosol scheme and the simulated aerosol size distribution within a particular model. The calculation of an approximate $PM_{2.5}$ concentration using Eq. (1) is therefore likely to introduce some errors but it does provide an estimate that is consistent across models and also with that previously used in CMIP5 and ACCMIP (Fiore et al., 2012; Silva et al., 2013, 2017). For the CNRM-ESM2-1 model, anomalously large concentrations were obtained from the sea salt mass mixing ratios. Sensitivity tests with this model suggested that a much smaller factor of 0.01 was more appropriate to use for SS, which takes into account the non-dry nature of the sea salt aerosols and the large possible size range, up to 20 µm in diameter, of sea salt particles within the CNRM-ESM2-1 model (P Nabat 2019, personal communication, 27th November).

Details of the data used in this study from different CMIP6 models, in both the historical and future scenarios, is presented below in Table 1. For the historical period, data was available from 5 different CMIP6 models for O_3 and 10 models for $PM_{2.5}$. The future scenario with the most data available was ssp370, with 4 models suppling data for O_3 and 7 models for $PM_{2.5}$. For the other Tier 1 CMIP6 scenarios (ssp126, ssp245 and ssp585), data was only available for 2 models for O_3 and 4 for $PM_{2.5}$ (all components). It was decided to focus the analysis on ssp370 and other Tier 1 scenarios due to the limited availability of model data for Tier 2 scenarios (ssp119, ssp434, ssp460 and ssp534-over). The results from an O_3 parameterisation (Turnock et al., 2018, 2019), referred to in this study as HTAP_param, haves also been included in the analysis of surface O_3 from CMIP6 models for both the historical and future scenarios ~~and is referred to in this study as HTAP_param~~. The HTAP_param was previously developed based upon the source-receptor relationships of O_3 derived from perturbation experiments of regional precursor emissions and global CH_4 abundances (Wild et al., 2012; Turnock et al., 2018). The HTAP_param applies the fractional change in global CH_4 abundance and regional emission precursors (NOx, CO and NMVOCs) for a particular scenario to the ozone response from each individual model used in the parameterisation. The total O_3 response is obtained by summing up the response from each of the individual models to all precursor changes across all source regions. The surface O_3 response previously calculated from the HTAP_param in both the historical and future CMIP6 scenarios is compared to that from the CMIP6 models (Turnock et al., 2019). The O_3 parameterisation does not take into account the effects of climate change on surface O_3 concentrations and therefore provides an estimate of the emission-only driven changes to surface O_3~~–~~, ~~with~~ which ~~to~~we compare to the climate and Earth System models.

Table 1 –Number of ensemble members used for the historical and future scenarios experiments from each model in the analysis of surface O_3 and $PM_{2.5}$ in this study

Model	Pollutant	historical	ssp126	ssp245	ssp370	ssp370-lowNTCF	ssp585	Model Refs	Data Citation
BCC-ESM1	O_3, $PM_{2.5}$	3			3	3		(Wu et al., 2019, 2020)	(Zhang et al., 2018, 2019)
CESM2-WACCM	O_3, $PM_{2.5}$	3			1	1		(Gettelman et al., 2019; Tilmes et al., 2019; Emmons et al., 2020)	(Danabasoglu, 2019b, 2019c, 2019a)
CNRM-ESM2-1	$PM_{2.5}$	3			3	3		(Michou et al., 2019; Séférian et al., 2019)	(Seferian, 2018, 2019; Voldoire, 2019)
GFDL-ESM4	O_3, $PM_{2.5}$	1	1	1	1	1	1	(Horowitz et al., 2019; Dunne et al., 2020)	(Horowitz et al., 2018; John et al., 2018; Krasting et al., 2018)
HadGEM3-GC31-LL	$PM_{2.5}$	4	1	1			1	(Kuhlbrodt et al., 2018)	(Ridley et al., 2018; Good, 2019)
MIROC6 - ES2L	$PM_{2.5}$	3	1	1	1		1	(Takemura, 2012; Hajima et al., 2019)	(Hajima and Kawamiya, 2019; Tachiiri and Kawamiya, 2019)
MPI-ESM1.2-HAM	$PM_{2.5}$	1			1	1		(Tegen et al., 2019)	(Neubauer et al., 2019)
MRI-ESM2-0	O_3, $PM_{2.5}$	5 5	1 1	1 1	3 3	1 1	1 1	(Yukimoto et al., 2019d; Oshima et al., 2020)	(Yukimoto et al., 2019b, 2019c, 2019a)
GISS-E2-1-GH	O_3, $PM_{2.5}$	5 42	1 1	5 5	1 1		1 1	(Bauer et al., 2020)	(NASA Goddard Institute For Space Studies (NASA/GISS), 2018)
NorESM2-LM	$PM_{2.5}$	1	3	3	3	3	3	(Karset et al., 2018; Kirkevåg et al., 2018)	(Norwegian Climate Center (NCC), 2018)
UKESM1-0-LL	O_3, $PM_{2.5}$	5	5	5	5	3	5	(Sellar et al., 2019)	(Good et al., 2019; Tang et al., 2019)
Total Number of models	O_3	65	24	24	46	35	24		
	$PM_{2.5}$	110	47	47	710	48	47		

2.3 Surface Observations

Present day surface O_3 and $PM_{2.5}$ simulated by all of the CMIP6 models is evaluated against surface observations to ascertain model biases and inter-model discrepancies. Surface O_3 observations are obtained from the database of the Tropospheric Ozone Assessment Report (TOAR) (Schultz et al., 2017). The TOAR database provides a gridded product of surface O_3 observations over the period 1970 to 2015. The majority of measurement sites are located in North America and Europe, with a smaller number of other sites in East Asia, Australia, New Zealand, South America, Southern Africa, Antarctica and remote ocean locations. Here we compile a monthly mean climatology of all available O_3 observations over the period 2005-2014 from measurement locations that are classified as rural in the TOAR database (Schultz et al., 2017). The rural locations were selected to be representative of background (i.e. non-urban) O_3 concentrations and are considered to be more appropriate in evaluating the simulated values obtained at the relatively coarse horizontal resolution of the global ESMs. Simulated surface O_3 concentrations from the CMIP6 models are re-gridded onto the same resolution of the observational product (2° x 2°) for evaluation purposes.

Surface $PM_{2.5}$ observations have been obtained from all of the locations compiled in the database of the Global Aerosol Synthesis and Science Project (GASSP: http://gassp.org.uk/data/, Reddington et al., 2017) to evaluate CMIP6 models. Background, non-urban, $PM_{2.5}$ data is compiled in the GASSP database from three major networks: the Interagency Monitoring of Protected Visual Environments (IMPROVE) network in North America, the European Monitoring and Evaluation Programme (EMEP) and Asia-Pacific Aerosol Database (A-PAD). Again, like for O_3, the networks/observations for $PM_{2.5}$ were selected to be representative of non-urban environments, which are more appropriate for the evaluation of global ESMs. With the exception of the IMPROVE network, most measurements of $PM_{2.5}$ began after the year 2000. Like for O_3, we compile a monthly mean climatology of $PM_{2.5}$ but now over the period of 2000 to 2010, selected as the GASSP database contained the most observations within this period. Simulated surface $PM_{2.5}$ was computed from CMIP6 models over the same time period as the observations and linearly interpolated to each measurement location. Whilst the surface observations measure total $PM_{2.5}$ mass, the computed $PM_{2.5}$ from CMIP6 models use Eq. 1 and does not include all observable $PM_{2.5}$ aerosol components (e.g. nitrate aerosol). Therefore it is anticipated that the CMIP6 models will underrepresent the $PM_{2.5}$ observations in this comparison.

To address the anticipated disparity between the observed ground based $PM_{2.5}$ and the approximate $PM_{2.5}$ from CMIP6 models, a further comparison has been made between the CMIP6 models and the Modern-Era Retrospective Analysis for Research and Applications, version 2 (MERRA-2), aerosol reanalysis product (Buchard et al., 2017; Randles et al., 2017). The MERRA-2 aerosol product assimilates observations of Aerosol Optical Depth (AOD) from ground based and satellite remote sensing platforms into model simulations that use the GEOS-5 atmospheric model coupled to the GOCART aerosol module. The data assimilation used in MERRA-2 generally improves comparisons of $PM_{2.5}$ with observations but there are still overestimations due to dust and sea salt and underestimations over East Asia (Buchard et al., 2017; Provençal et al., 2017). Separate mass mixing ratios for BC, OA, SO_4, SS and DU aerosol components are provided from MERRA-2, which are then combined using the formula in Eq. 1 to make an approximate $PM_{2.5}$. Monthly mean approximate $PM_{2.5}$ concentrations are then computed over the period 2005-2014 from the MERRA-2 reanalysis product to provide a more direct comparison and enhanced spatial coverage against the approximate $PM_{2.5}$ concentrations calculated from the CMIP6 models calculated over the same time period.

3 Present-day Model Evaluation of Air Pollutants

3.1 Surface Ozone

The ~~5~~6 CMIP6 models with data available for the historical experiments are evaluated against surface O_3 observations from the TOAR database over the period 2005-2014. A long-term evaluation of surface O_3 concentrations from CMIP6 models using observations compiled over the 20th Century is presented separately in Griffiths et al., (2020). Figure 3 shows the annual and seasonal multi-model mean in surface O_3 over the period 2005-2014 and the standard deviation across the 6~~5~~ CMIP6 models. The annual and seasonal mean surface O_3 concentrations and evaluation against observations for individual CMIP6 models are shown in Figures S2–S~~6~~7. Higher surface O_3 concentrations are simulated in the northern hemisphere summer (June, July, August- JJA) when O_3 formation is enhanced by increased photolytic activity and levels of oxidants, as well as larger biogenic emissions. The hemispheric difference in surface O_3 is smaller in December, January and February (DJF) when O_3 production is less in the northern hemisphere but higher in the southern hemisphere. However, model diversity is larger in DJF (Fig. 3b) due to individual models simulating different seasonal cycles of O_3, particularly UKESM1-0-LL which has the most pronounced seasonal cycle of all 6~~5~~ models (Fig. S2).

The multi-model mean of CMIP6 models overestimates surface O_3 concentrations by up to 16 ppb annually and in both seasons when compared to observations from the TOAR database, although they do capture the broad hemispheric gradient in O_3 concentrations (Fig. 3c, 3f and 3i~~f~~). The model observational comparison of CMIP6 models to the TOAR observations ~~These results~~ are consistent across all models and with the previous evaluation of ACCMIP models (Young et al., 2018). This indicates a common source of error within models for example uncertainties in emission inventories, deposition processes or vertical mixing (Wild et al., 2020). In addition, the coarse resolution of the ESMs could lead to an overproduction of O_3 across polluted regions, with finer resolutions exhibiting improvements in the simulation of surface O_3 (Wild and Prather, 2006; Neal et al., 2017). ~~The overestimation in the CMIP6 models analysed here could be due to the coarse resolution of the ESMs, an excess of O_3 chemical production (potentially due to an overabundance of NOx and/or VOCs) and weak O_3 deposition~~. Smaller model biases exist in DJF (<5 ppb) than in JJA (5-15 ppb), mostly attributed to the strong seasonal cycle simulated by UKESM1-0-LL. In contrast to other models (Fig. S2 – S~~6~~7), UKESM1-0-LL underpredicts surface O_3 in DJF over most continental northern hemisphere locations, potentially indicating there is excessive NOx titration of O_3 in this model, which is also shown by the large sensitivity of O_3 formation to NOx concentrations over the historical period (Fig. S17).

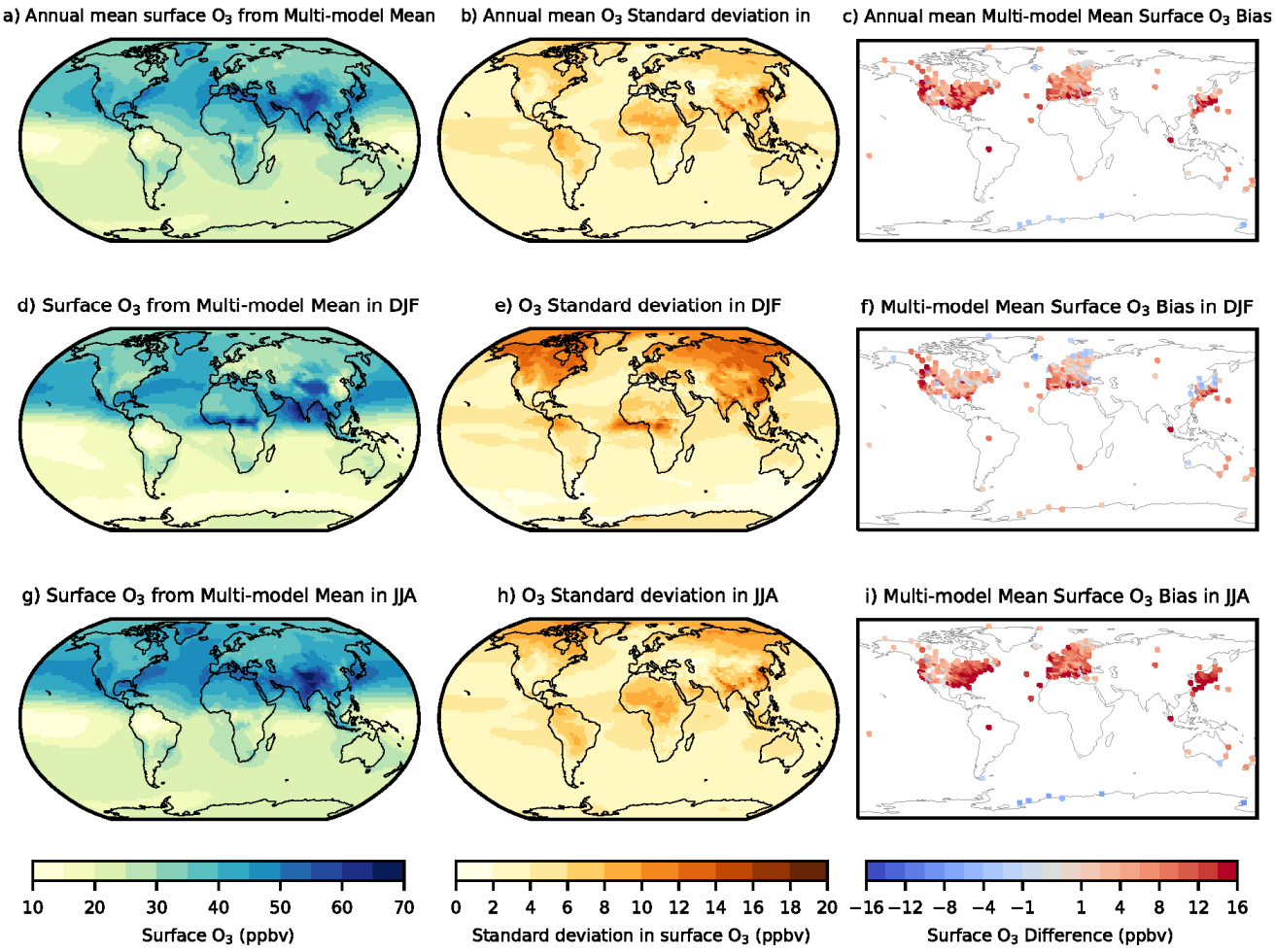

Figure 3 – Multi-model (~~5~~6 CMIP6 models) annual and seasonal mean surface O_3 concentrations in a) Annual mean, d) December January, February (DJF) and ~~d~~g) June, July, August (JJA) over the 2005-2014 period. The standard deviation in the multi-model mean in b) Annual mean, e) DJF and ~~e~~h) JJA. The difference between the multi-model mean and TOAR observations in c) Annual mean, f) DJF and ~~f~~i) JJA (colour bar saturates).

The observed annual cycle in surface O_3 averaged across measurement locations within different regions is compared to that simulated by CMIP6 models (Figure 4). Across most regions, the mean annual cycle from CMIP6 models compares relatively well to that observed. The overprediction of surface O_3 values in JJA is evident across most regions, as is the large concentrations in BCC-ESM1 and GISS-E2-1-G and the strong seasonal cycle in UKESM1-0-LL across~~for~~ northern hemisphere continental regions. Additionally, the timing of peak O_3 over continental northern hemisphere locations occurs earlier in the observations (springtime) than in the CMIP6 models (spring and summer), which is consistent with that from ACCMIP models (Young et al., 2018). At oceanic observation locations, ~~there is also a consistent overestimate of~~ surface O_3 is overestimated ~~by~~in CMIP6 models by up to 20 ppb across all seasons, indicating that O_3 deposition rate could be underestimated here. There is also a large overestimation (~20 ppb) in all models at the one observation location in South East Asia, potentially due to difficulty in simulating O_3 in the maritime continental boundary layer using lower resolution global ESMs. In contrast to this, CMIP6 models, particularly UKESM1-0-LL and GISS-E2-1-G, tend to underpredict the observed surface O_3 concentrations at locations in the South Pole region in JJA by ~5 ppb. This could be due to lack of long range transport of O_3 to these sites, inaccuracies in southern hemisphere precursor emissions, or because of the difficulty in simulating O_3 concentrations at the appropriate elevation of measurement sites located on the Antarctic ice sheet.

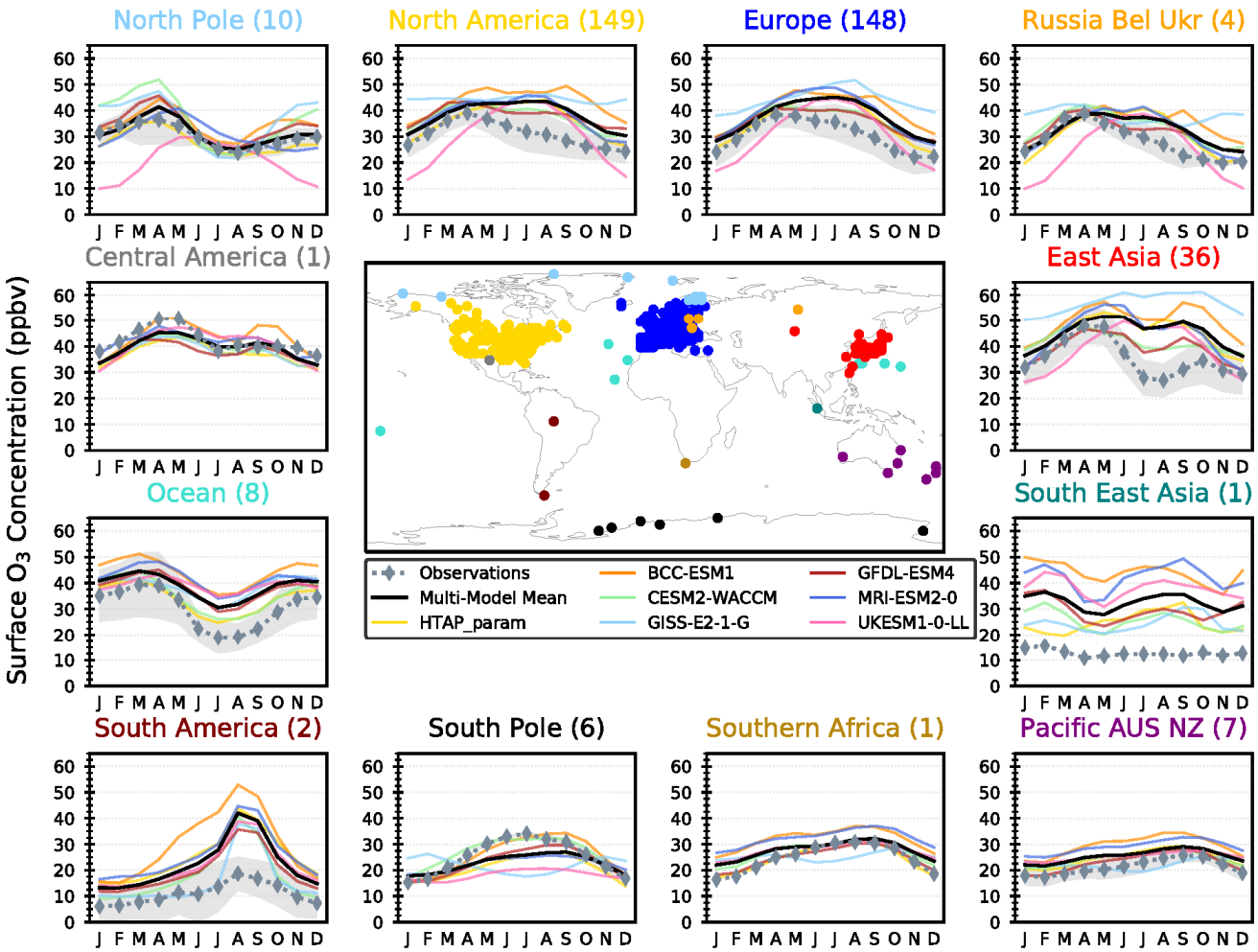

Figure 4 – Individual and multi-model (~~6~~5 CMIP6 models and HTAP_param) monthly mean surface O_3 concentrations across different world regions compared with the regional monthly values from all the TOAR observations within the region for the period 2005-2014. The number of observations within a region is shown in parenthesis. The shading shows variability in observations across all sites within the region.

3.2 Surface $PM_{2.5}$

3.2.1 Ground Based Observations

A similar comparison is made for annual and seasonal mean surface $PM_{2.5}$ concentrations from CMIP6 models against ground based surface observations (Figure 5). The annual and seasonal multi-model mean from CMIP6 models shows that elevated $PM_{2.5}$ concentrations (>50 µg m^{-3}) occur close to the large dust emission source regions of the Sahara and Middle East in both DJF and JJA over 2000-2010. These natural source regions are also one of the largest areas of diversity in $PM_{2.5}$ concentrations (up to 20 µg m^{-3}) between the different CMIP6 models (Fig. 5b, 5e, 5h and S~~7~~8). High concentrations of $PM_{2.5}$ (>40 µg m^{-3}) are also simulated over the large anthropogenic source regions of South and East Asia, particularly in DJF when there is enhanced variability across CMIP6 models due to the different contribution from anthropogenic $PM_{2.5}$ components (Fig. S~~8~~9-S11~~0~~). The diversity in CMIP6 model is particularly evident in the organic aerosol concentrations across Asia, with higher present day values simulated by CESM2-WACCM and UKESM1-0-LL and lower values in CNRM-ESM2-1 and MIROC-ES2L (Fig. S11). Lower $PM_{2.5}$ concentrations (<10 µg m^{-3}) are predicted across both North America and Europe, with more agreement between CMIP6 models. Across the biomass burning regions of South America and Southern Africa, $PM_{2.5}$ concentrations are elevated in JJA with larger diversity in the CMIP6 models due to the differing contributions of the BC and OA components, particularly shown in NorESM2-LM, GISS-E2-1-G and GFDL-ESM4 (Fig. S~~9~~10 and S11~~0~~). Relatively consistent $PM_{2.5}$ concentrations of <10 µg m^{-3}, with small model diversity (<5 µg m^{-3}), are shown across oceanic regions,

mainly from emissions of sea salt (Fig. S12~~1~~). Apart from the natural sources of aerosol, which are subject to meteorological variability, the CMIP6 models are relatively consistent when simulating $PM_{2.5}$ concentrations across most regions.

Compared to the ground based observations from the GASSP database, the CMIP6 multi-model mean underpredicts the observed $PM_{2.5}$ values by up to 10 µg m^{-3} in both seasons, with a slightly larger underestimation in DJF than JJA. As discussed in section 2.3, an underestimation was anticipated from comparing approximate $PM_{2.5}$ concentrations, derived from CMIP6 models, to observed values. Nevertheless, the evaluation highlights that fine particulate matter ($PM_{2.5}$) is generally underrepresented in the CMIP6 models across North America, Europe and parts of Asia for which observations are available; a similar result to other studies evaluating global and regional models (Tsigaridis et al., 2014; Pan et al., 2015; Glotfelty et al., 2017; Solazzo et al., 2017; Im et al., 2018). Numerous reasons potentially exist for the model observation discrepancy shown here and in other studies including ~~This could be potentially due to~~ uncertainties in emission~~s~~ inventories (e.g. local dust sources), ~~or~~errors in the wet/dry deposition schemes ~~(dry or wet)~~, ~~the coarse resolution of global models and~~ the absence/underrepresentation of aerosol formation processes (e.g. ~~nitrate aerosols or~~ secondary organic aerosols) and the coarse resolution of global models leading to errors in emissions and simulated meteorology. Understanding the causes of model observational discrepancies is an area of active research and should be explored in further research, for example in a global multi-model sensitivity study that examines model uncertainties.

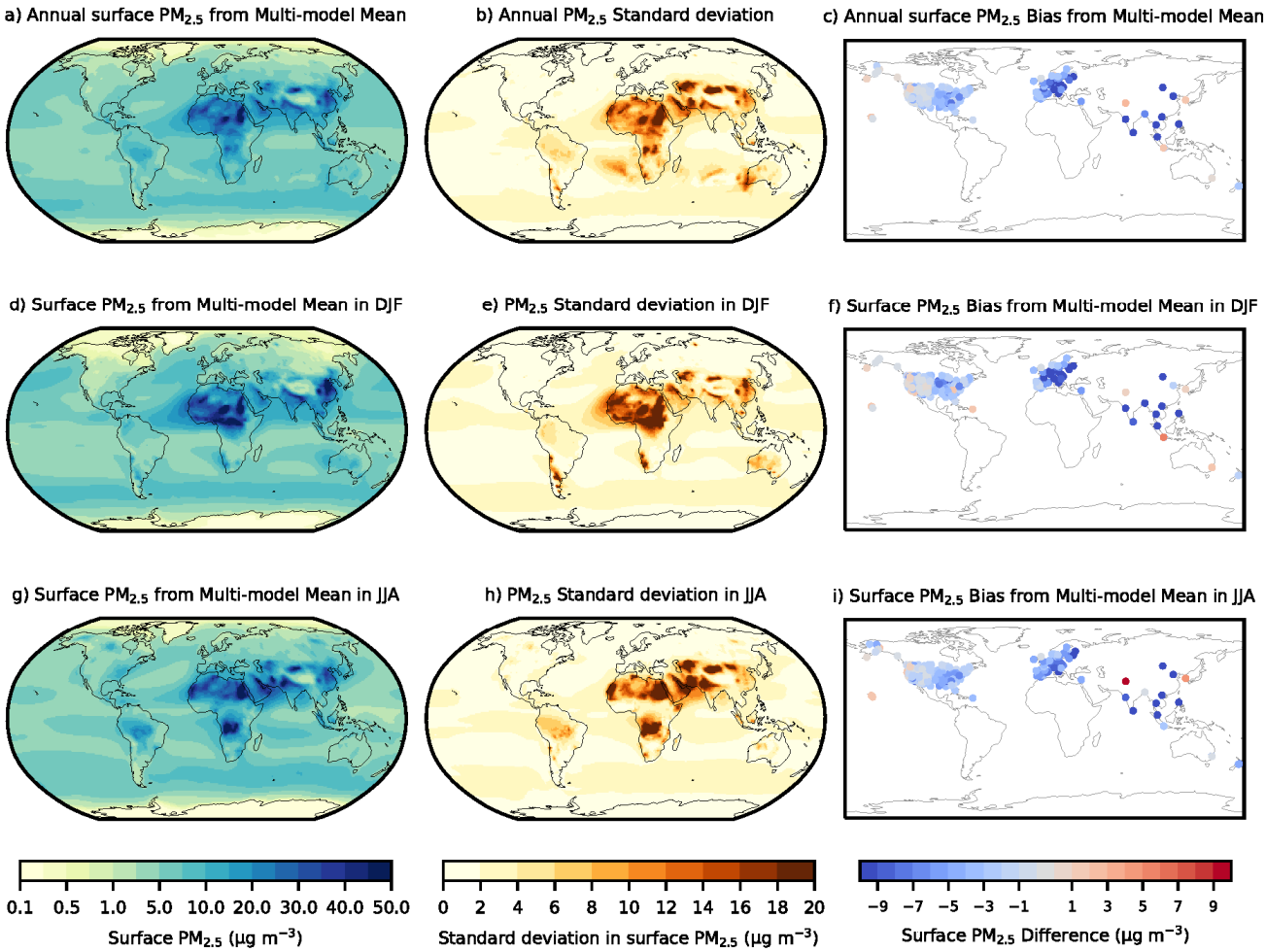

Figure 5 – Multi-model (11~~0~~ CMIP6 models) annual and seasonal mean surface $PM_{2.5}$ concentrations in a) annual mean, d) December January, February (DJF) and ~~d~~g) June, July, August (JJA) over the 2000-2010 period. The standard deviation in the multi-model mean in b) annual mean, e) DJF and ~~e~~h) JJA. The difference between the multi-model mean and $PM_{2.5}$ observations in c) annual mean, f) DJF and ~~i~~f) JJA (colour bar saturates).

The simulated regional mean annual cycle in surface $PM_{2.5}$ from different CMIP6 models against observations is shown in Figure 6. The low model bias in $PM_{2.5}$ concentrations is highlighted across all regions, except for the ocean region where there is a relatively large diversity in model simulations, particularly MIROC-ES2L and NorESM2-LM, at these observation

locations. Across North America, the region with most observations, the annual cycle is simulated relatively well with a peak in concentrations in JJA and a lower model bias, although a larger model bias (factor of ~1.5 to 2) occurs in winter and spring. Across Europe, there is a larger underestimation of observed $PM_{2.5}$ concentrations by CMIP6 models in DJF (factor > 2) than JJA. Nitrate aerosols are observed and modelled (from two CMIP6 models in Fig. S132) to contribute between 1 and 5 µg m^{-3} of the total aerosol mass over Europe (Fagerli and Aas, 2008; Pozzer et al., 2012), explaining part, but not all, of the model observational discrepancy here. Additionally, on Fig. 6 the CMIP6 models also underestimate the MERRA-2 reanalysis product (which does not include nitrate aerosols), indicating that other aerosol sources/processes are underrepresented across Europe and other regions in the models. The limited number of observations across other regions makes it difficult to infer particular model/observational biases. However, over Asia CMIP6 $PM_{2.5}$ concentrations tend to be within a factor of 2 of the observations and represent the seasonal cycle relatively well at these locations. Over Asia, larger $PM_{2.5}$ concentrations are simulated in the CMIP6 models CESM2-WACCM, HadGEM3-GC31-LL and UKESM1-0-LL, mainly due to the larger OA component (Fig. S11). Across South Asia, concentrations are relatively well simulated in JJA but a larger discrepancy (15 µg m^{-3}) exists in DJF between the model and observations.

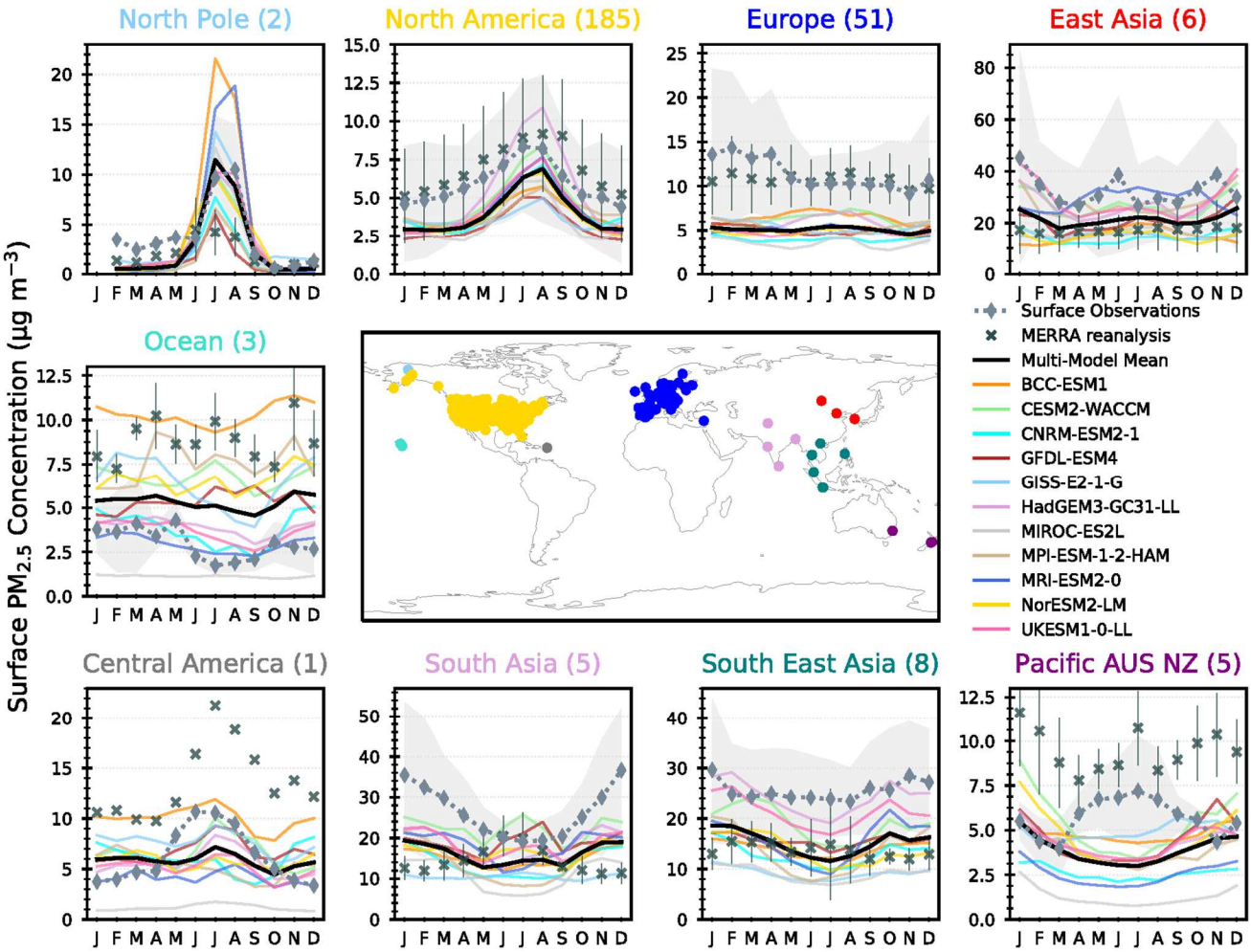

Figure 6 – Individual and multi-model (110 CMIP6 models) monthly mean surface $PM_{2.5}$ concentrations across different world regions compared with the regional monthly values from all the $PM_{2.5}$ observations (◊) and the MERRA-2 reanalysis product (x) within the region for the period 2000-2010. The number of observations within the region is shown in parenthesis. The shading and errors bars show variability in observations and the reanalysis product across all sites within the region.

3.2.2 MERRA Reanalysis Product

An additional comparison of surface $PM_{2.5}$ concentrations from the MERRA-2 aerosol reanalysis product is made with that simulated by the CMIP6 models to improve the spatial coverage and provide a more consistent evaluation of the approximate $PM_{2.5}$ concentrations. Figure 7 shows the same comparison as in Fig. 5 but now using the approximate $PM_{2.5}$ obtained from

the MERRA-2 reanalysis product over the period 2005-2014. In comparison to MERRA-2, the CMIP6 models are shown to underpredict $PM_{2.5}$ concentrations across North America, Europe and Eurasia, but by a smaller amount than in comparison to ground-based observations. A similar seasonal cycle comparison is shown for Europe and North America (regions with most ground based observations) in both Fig. 6 and 8, providing confidence that the underestimation of $PM_{2.5}$ by CMIP6 models is robust over these regions. Across all other regions, the MERRA-2 reanalysis product provides much greater spatial coverage for each region and therefore the features shown in the site-level comparison (Fig. 6) will not necessarily apply here. A large overestimation of the MERRA-2 reanalysis product by the CMIP6 multi-model mean is shown across East and South Asia. Figure 8 shows that on a regional mean basis most CMIP6 models are within the spread of the MERRA-2 concentrations for East Asia, although MERRA-2 was previously shown to underestimate $PM_{2.5}$ concentrations across East Asia (Buchard et al., 2017; Provençal et al., 2017) and also on Fig. 6. CESM2-WACCM and MRI-ESM2-0 ~~is~~are the exceptions to this with distinctly higher $PM_{2.5}$ concentrations over East Asia, potentially due to larger OA concentrations and more dust aerosols within the western side of this region (Fig. S8~~7~~ and S1~~0~~). Across the South Asian region, CMIP6 models ~~show a more~~ consistently overestimate~~ion of~~ MERRA-2 by more than 10 µg m^{-3}~~,~~ in certain months. ~~with~~ UKESM1-0-LL, MRI-ESM2-0 and CESM2-WACCM ~~showing~~simulate particularly high monthly $PM_{2.5}$ concentrations of 20-40 µg m^{-3} over South Asia, ~~again~~ due to large contributions from SO_4, dust and OA. Across North Africa there is considerable~~a lot of inter regional~~ variability in $PM_{2.5}$ within this region, as ~~with~~ CMIP6 models both under and over-estimate~~ing~~ the MERRA-2 $PM_{2.5}$ concentrations, although this results in a relatively good regional mean representation (Fig. 7 and 8). The annual mean cycle in MERRA-2 $PM_{2.5}$ concentrations across South America is well represented by the CMIP6 models, although the peak in the biomass burning season is underestimated by 5-10 µg m^{-3} ~~-~~in some models. A more pronounced annual cycle is exhibited by UKESM1-0-LL across Southern Africa, ~~potentially~~ due to the larger contributions from the OA fraction (Fig. S1~~0~~), ~~that~~potentially ~~result~~ from enhanced biogenic emissions that~~leading to~~ result in secondary OA formation (SOA). Across oceanic locations all of the CMIP6 models underestimate the MERRA-2 $PM_{2.5}$ concentrations by 5 µg m^{-3}, although MERRA-2 was previously shown to overestimate sea-salt concentrations (Buchard et al., 2017; Provençal et al., 2017), accounting for some of this discrepancy. Overall, comparisons of CMIP6 models with the MERRA-2 reanalysis product show biases across Europe and North America that are consistent with the comparison to ground-based observations. Additionally, similar comparisons are shown in annual mean cycles across other regions, for which appropriate ground based data is lacking.

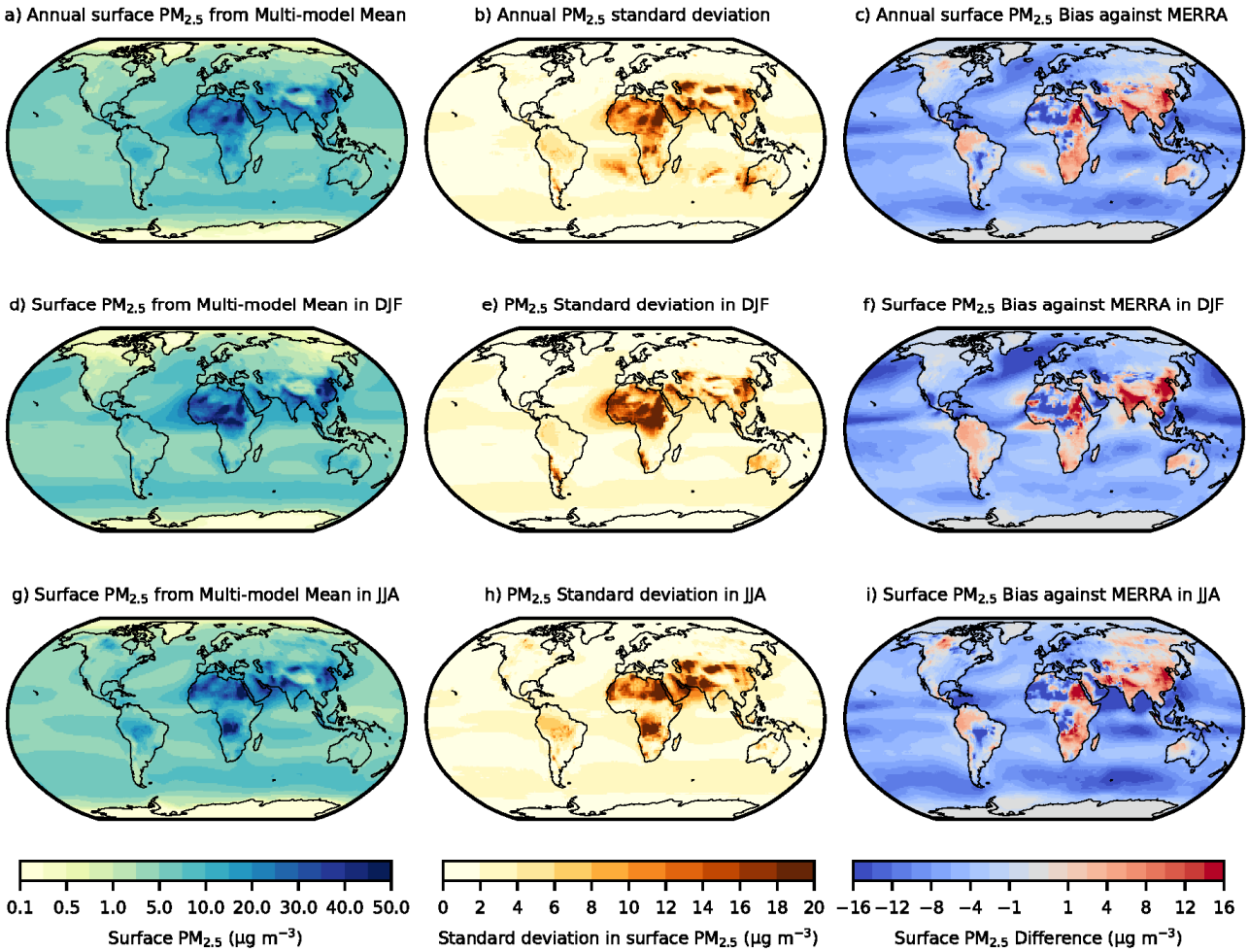

Figure 7 – Multi-model (1~~0~~1 CMIP6 models) annual and seasonal mean surface $PM_{2.5}$ concentrations in a) annual mean, d) December January, February (DJF) and ~~d~~g) June, July, August (JJA) over the 2005-2014 period. The standard deviation in the multi-model mean in b) annual mean, e) DJF and ~~e~~h) JJA. The difference between the multi-model mean and MERRA-2 reanalysis for c) annual mean, f) DJF and ~~i~~f) JJA.

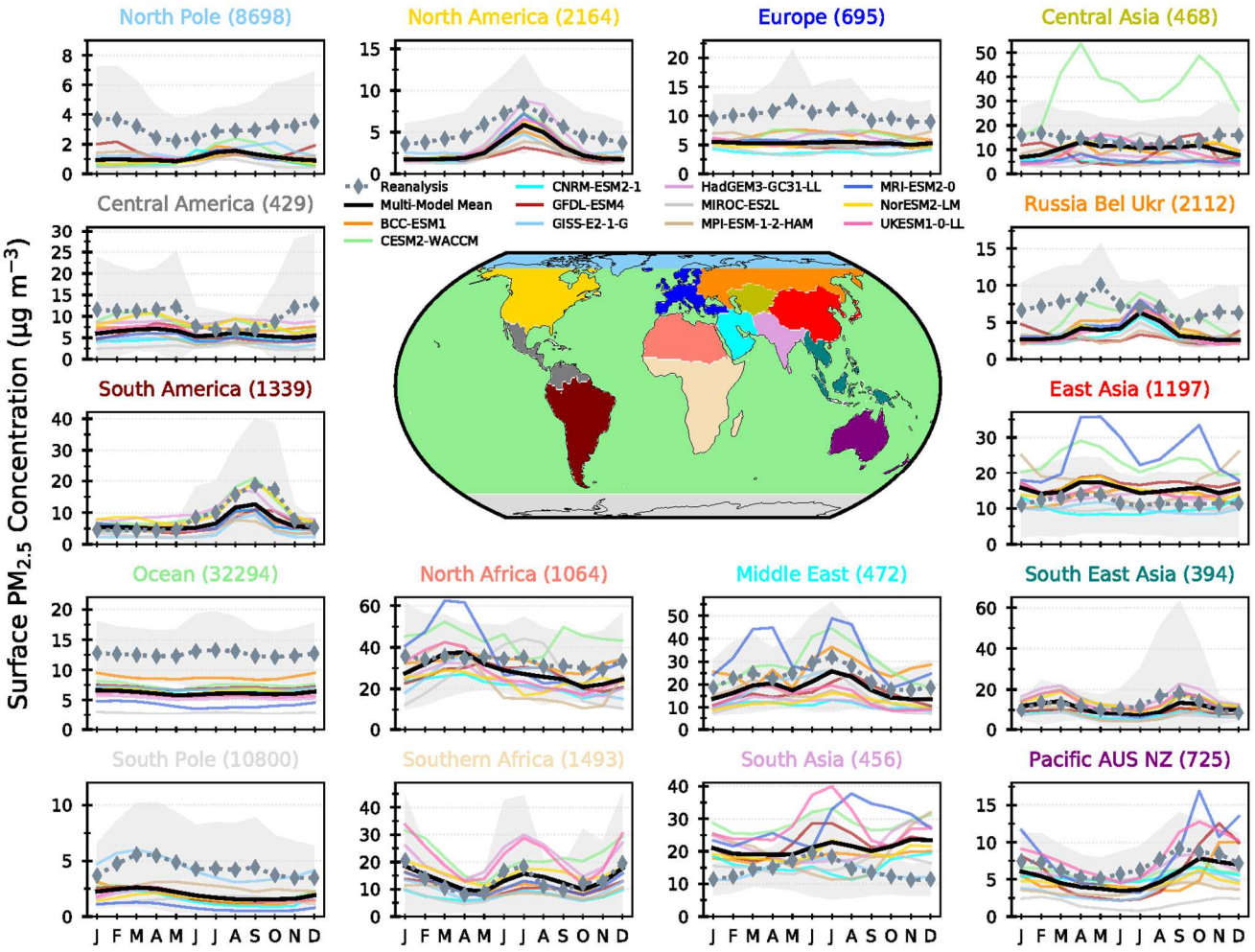

Figure 8 – Individual and multi-model (10~~0~~1 CMIP6 models) monthly mean surface $PM_{2.5}$ concentrations across different world regions compared with the regional monthly values from the $PM_{2.5}$ MERRA-2 reanalysis within the region for the period 2005-2014. The number of reanalysis points within the region is shown in parenthesis. The shading shows variability in the values of the MERRA-2 reanalysis products across the region.

4 Air Pollutants from Pre-Industrial to Present-day

4.1 Surface Ozone

The simulated changes in surface O_3 across 6~~5~~ CMIP6 models and the HTAP_param are shown in Figure 9 and S14-S15 over the historical period of 1850 to 2014. The CMIP6 multi-model mean shows that global annual mean surface O_3 has increased by 11.7~~5~~ +/- 2.3~~2~~ ppb since 1850 (+/- 1 standard deviation), although the change could be as large as 14 ppb (from BCC-ESM1) or as little as 7 ppb (from UKESM1-0-LL). Globally and over most regions there has been a larger historical increase in surface O_3 in JJA than in DJF (Figure S16). The 1850 to 2000 multi-model annual mean change in surface O_3 from the CMIP6 models of 10.6 ppb is in good agreement with the 10 +/- 1.6 ppb simulated by the CMIP5 models used in ACCMIP (Young et al., 2013). An evaluation of the long-term changes in surface O_3 over the historical period simulated by the CMIP6 models at specific measurement locations is presented separately in the tropospheric O_3 CMIP6 companion paper of Griffiths et al., (2020). ~~, which~~This shows that ~~the~~ CMIP6 models ~~are able to~~can reasonably represent long term changes in surface ozone since the 1960s, providing a degree of confidence in the future projections of changes in the CMIP6 scenarios. However, long term changes in simulated surface O_3 from the previous generation of global coupled chemistry-climate models (used in CMIP5) were found to underestimate the observed trend at northern hemisphere monitoring locations (Parrish et al., 2014). Further comparisons of historical surface O_3 simulated by CMIP6 models with long-term historical observations is outside the scope of the current work but will be the subject of future research.

A large diversity in the simulated historical changes is shown across the different regions analysed here, with UKESM1-0-LL tending to simulate the ~~lowe~~smallest historical change and GISS-E2-1-G~~H~~ or BCC-ESM1 the ~~high~~largest. The large diversity across CMIP6 models in the surface O_3 response over the historical period can be attributed to the different magnitude of simulated O_3 concentrations in the 1850 period (Figure S14) and the rate of change in regional mean O_3 concentrations (Figure S15), which is related to the different chemical sensitivity of O_3 formation in each model to changing NOx concentrations (Figure S17). Larger differences between CMIP6 models are shown in the DJF mean historical changes over northern hemisphere regions than occurred in JJA (Figure S16), reflecting the differences shown in the model evaluation (Fig. 4) and the strong seasonality of the changes. Even, though the historical surface O_3 response is small in UKESM1-0-LL, it is shown to have larger tropospheric changes in O_3 over the historical period compared to other CMIP6 models (Griffiths et al., 2020). South Asia is the region with the largest diversity in simulated historical changes in surface O_3 of between 16 and 40 ppb, with a larger range in DJF (10-40 ppb) than in JJA (19-36 ppb). The large diversity in CMIP6 models is attributed to the large differences in simulated NOx concentrations, and hence chemical sensitivities of O_3 formation, occurring across South Asia over the historical period (Figure S17). In addition, the large historical change in $PM_{2.5}$ over this region (Fig. S18) could alter the heterogeneous loss rate of radicals to aerosols and therefore also affect O_3 formation. Surface O_3 is simulated to have increased -by between 10 to 30 ppb on an annual mean basis and by a larger amount in JJA (12 to 37 ppb) over the major northern anthropogenic source regions since 1850, driven mainly by the large increases in anthropogenic precursor emissions of CH_4, NOx, CO, and NMVOCs over this period.

A qualitative estimate of the influence of non-emission driven processes (chemistry and climate change) can be ascertained by comparing results from the HTAP_param, an emission-only driven model, to those of the CMIP6-models. Simulated historical changes in surface O_3 from UKESM1-0-LL are ~~similar~~comparable to those from the HTAP_param, indicating that the magnitude of change~~s~~ simulated by UKESM1-0-LL ~~are~~is ~~strongly determined~~similar to that solely ~~by~~from changes in precursor emissions. However, the global annual mean surface O_3 response of 7.6 +/- 0.7 ppb from HTAP_param over the historical period is ~~3.9~~4.1 ppb lower than the CMIP6 multi-model mean, indicating globally that non-emission driven processes have contributed to approximately 30% of the change in surface O_3, although this contribution varies regionally. The different magnitude of response across models could be due to non-emission driven process, e.g. from different chemistry schemes and climate change signals within models.

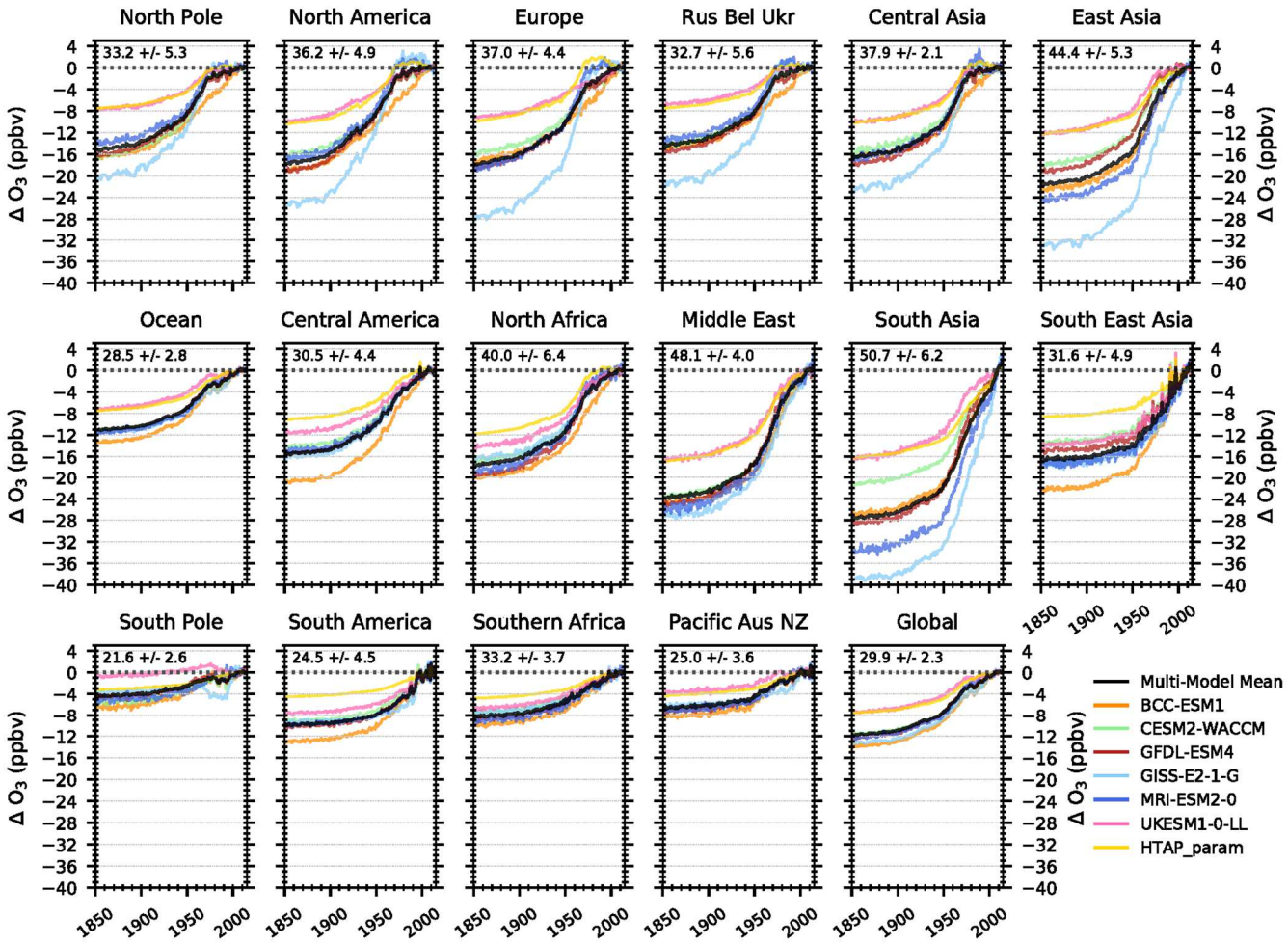

Figure 9 – Changes in the regional and global annual mean surface O_3 concentrations, relative to a 2005-2014 mean value, across ~~5~~6 CMIP6 models and the HTAP_param. The multi-model annual mean year 2005-2014 surface O_3 concentrations (+/- 1 standard deviation) are shown in the top left of each panel. Regions are defined in Figure S1.

4.2 Surface $PM_{2.5}$

The simulated change in annual mean surface $PM_{2.5}$ across 1~~0~~1 CMIP6 models is shown in Figure 10 ~~across~~over the historical period of 1850 to 2014. Since 1850, CMIP6 models simulated an increase in global annual and seasonal mean surface $PM_{2.5}$ concentrations of <2 μg m^{-3} (15-20%). Larger regional increases of surface annual mean $PM_{2.5}$ of up to 12 μg m^{-3} are simulated across South and East Asia, with changes in DJF (up to 21 μg m^{-3}) larger than those in JJA (up to 12 μg m^{-3}) (Fig. S16), reflecting the strong seasonality of $PM_{2.5}$ concentrations in these regions. The historical increase in surface $PM_{2.5}$ is primarily driven by the large increase in anthropogenic aerosol and aerosol precursor emissions over the 1850-2014 period (Hoesly et al., 2018). The largest model diversity is also exhibited over the Asian regions with variations in the response between models of up to 50%, ~~potentially due to differences in~~ with larger differences between models in DJF than JJA (Figure S16), reflecting the differences shown in the present day model evaluation (Fig. 6). The inter-model differences can be attributed to the different simulation of historical changes in the anthropogenic components sulphate, black carbon and organic aerosols (Figure S18) ~~dust emissions and simulation of organic aerosols~~. The largest interannual variability in surface $PM_{2.5}$ concentrations occurs over the North African and Middle East regions as they are located near large sources of dust, whose emissions are highly dependent on meteorological fluctuations (wind speed). Over Europe, and to a lesser extent Russia, Belarus, Ukraine and North America, the increase in surface $PM_{2.5}$ concentrations since 1850 peaked in the 1980s at 4 μg m^{-3} above the 2005-2014 mean value before decreasing over the last 30 years. ~~This change is consistent with both observations and simulated changes in aerosols over this period in response to emission reductions from the implementation of air quality legislation (Leibensperger et al., 2012; Tørseth et al., 2012; Daskalakis et al., 2016; Turnock et al., 2016; Archibald et al., 2017)~~ There is limited long-

term multi-decadal observational data available to assess changes in aerosols simulated by global models. Previous studies using long-term data since the 1980s, mainly over Europe and North America, have found that global models are able to reproduce the observed multi-decadal changes in aerosols relatively well (Pozzoli et al., 2011; Leibensperger et al., 2012; Tørseth et al., 2012; Chin et al., 2014; Turnock et al., 2015; Aas et al., 2019). More recently, global composition models, including some CMIP6 models, were shown to be able to reproduce the observed changes in AOD, sulphate and particulate matter over the last two decades (Mortier et al., 2020). The ability of global composition models to reproduce historical changes in aerosols provides a degree of confidence in the future projections under the CMIP6 scenarios. Further model observational comparisons of multi-decadal changes in aerosols will need to be undertaken to improve the understanding of changing aerosol properties and processes.

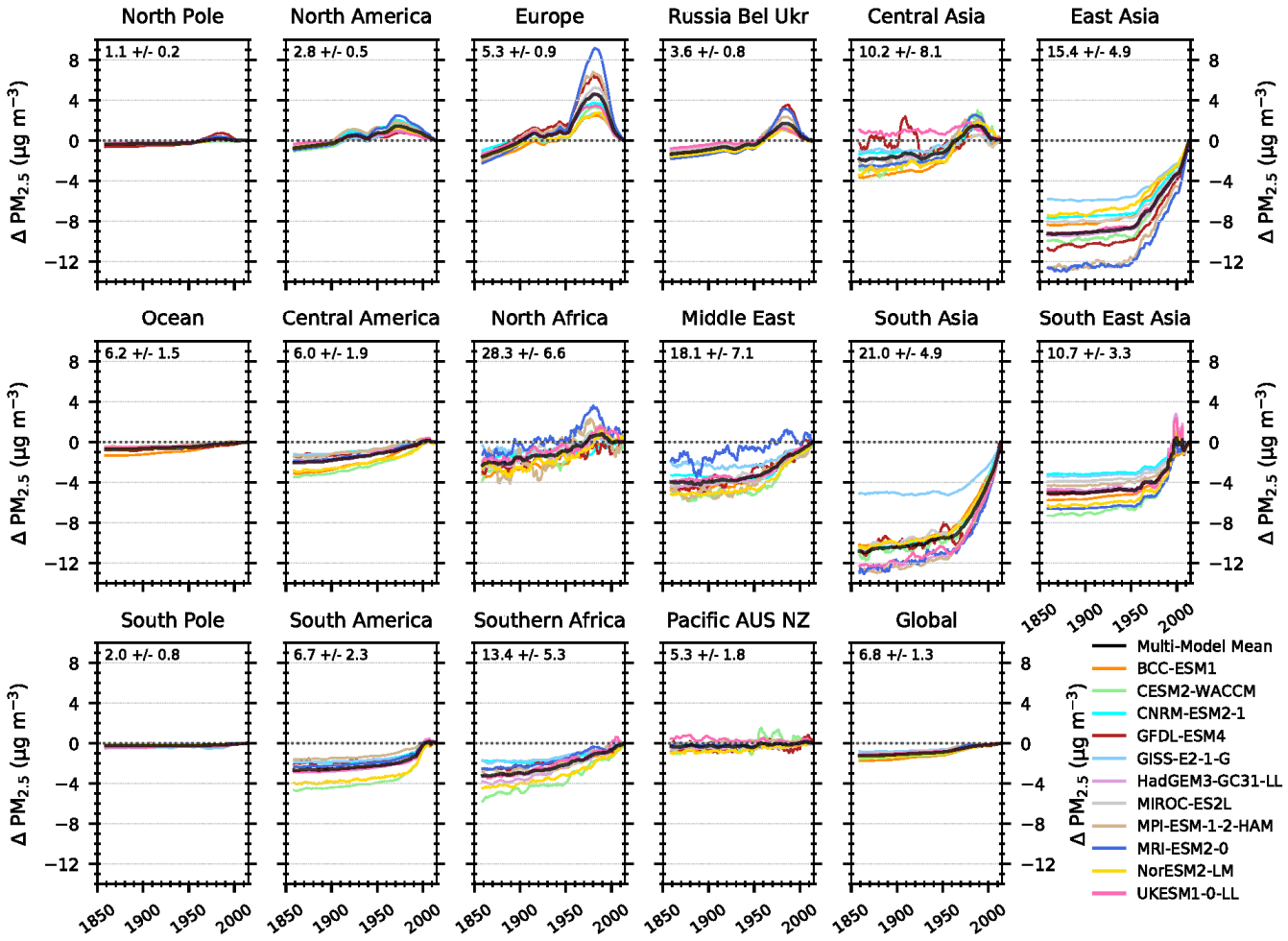

Figure 10 – Changes in the regional and global annual mean surface $PM_{2.5}$ concentrations, relative to a 2005-2014 mean value, across 11~~0~~ CMIP6 models. Changes for each region are computed as 10 year running means over the historical period. The multi-model mean 2005-2014 surface $PM_{2.5}$ concentrations (+/- 1 standard deviation) are shown in the top left of each panel. Regions are defined in Figure S1.

5 Air Pollutants from Present-day to 2100

An analysis is now made of the future projections of air pollutants in the CMIP6 Tier 1 scenarios, including ssp370-lowNTCF. A comparison is made of the projected future changes ~~by~~in 2050 and 2100 ~~in~~from the four CMIP6 models (CESM2-WACCM, GFDL-ESM4 and UKESM1-0-LL for both O_3 and $PM_{2.5}$, along with BCC-ESM1 for O_3 and MIROC-ES2L for $PM_{2.5}$) ~~which~~that had the most data available for the ssp370 scenario.

5.1 Surface Ozone

Global annual mean surface O_3 is reduced by more than 45 +/- 01.25 ppb (+/- 1 standard deviation value of the multi-model mean) in the near-term (2050) and by 98 +/- 1.60 ppb in 2100 in the strong air pollutant and climate mitigation scenario ssp126 (Figure 11). Smaller reductions in global annual mean surface O_3 are predicted for the middle of the road pathway (ssp245) of 34 +/- 0.1.7 ppb by 2100. Whereas for the weak climate and air pollutant mitigation scenario ssp370, a global annual mean increase in surface O_3 of 1.86 +/- 0.98 ppb in 2050 and 10.06 +/- 01.09 ppb is predicted by 2100. However, implementing strong emission controls for NTSLCFs on top of a weak climate mitigation scenario (ssp370-lowNTCF) shows that previous increases in global annual mean surface O_3 can be substantially reduced to values that are 2.5 +/- 0.54 ppb below the 2005-2014 mean value in 2050, with benefits to air quality and climate (Allen et al., 2020). For ssp585, which has weak climate mitigation measures but strong air pollution controls, a near-term increase in global annual mean surface O_3 of 21.4 +/- 0.87 ppb is predicted in 2050 but by 2100 surface O_3 reduces by 42.7 +/- 01.58 ppb, relative to 2005-2014, due to the implementation of air pollutant controls in the latter half of the 21st Century.

The global response in annual mean surface O_3 concentrations to the different scenarios is also repeated across the different world regions, albeit with differing magnitudes. In ssp370 increases in annual mean surface O_3 are predicted to occur across North America (+1.69 ppb), Europe (+5.4.8 ppb) and East Asia (+75.95 ppb), with the largest increase predicted in South Asia of 915.17 +/- 39.67 ppb by 2100. Surface O_3 increases across most world regions in this scenario can be attributed to the large increase in global CH_4 abundances (80%) and the large predicted increase in surface temperatures (Figure S13), dDespite the reductions in O_3 precursor emissions across North America, Europe and East Asia by 2100 (Fig. 2) surface O_3 concentrations have continued to increase up to the end of this period, indicating the importance of future changes in chemistry, global CH_4 abundances and climate on the response of surface O_3 in ssp370 (Wild et al., 2012; Gao et al., 2013; Rasmussen et al., 2013; Young et al., 2013; Colette et al., 2015; Fortems-Cheiney et al., 2017; Li et al., 2019; Turnock et al., 2019). South Asia shows the largest increase in surface O_3 as precursor emissions are anticipated to increase across this region on top of the large climate change signal and growth in CH_4 abundance. Additionally, the largest diversity in predictions between the CMIP6 models is shown over South Asia, indicating that there is some disagreement between the models as to the magnitude and extent of changes over this region. Surface O_3 across oceanic regions (background) are predicted to remain at or near current values in ssp370 due to the increases in water vapour in a warming world leading to more O_3 destruction (Johnson et al., 1999; Doherty et al., 2013). The impact of more aggressive near-term reductions to emissions of NTSLCFs (but not CH_4) on top of the ssp370 pathway is shown by the smaller changes in the ssp370-lowNTCF (Fig. 11 and Figures S19-S20 for individual models). In this pathway surface O_3 concentrations are reduced globally and across most regions to be at or near 2005-2014 values, a substantial benefit to surface O_3 air quality compared to ssp370. Surface O_3 concentrations are predicted to have almost halved by 2050 across South Asia in ssp370-lowNTCF. However, across East Asia the additional precursor emission reductions in ssp370-lowNTCF have resulted in made little differencesmaller benefits to surface O_3 concentrations predictedbeing simulated by the CMIP6 models than in other regions (Figure S20), indicating that other factors are more important over this region (chemistry or climate change) which is attributed to an increase in surface O_3 concentrations over Eastern China (a part of the larger East Asian region shown in Fig. S1). This increase in surface O_3 results from the slight increase in NMVOC emissions (Fig. 2) and a reduction in the NOx titration of O_3 due to the large decreases in NOx emissions in ssp370-lowNTCF. In addition, a reduction in the heterogeneous loss of radicals due to decreases in $PM_{2.5}$ concentrations in ssp370-lowNTCF could also lead to increased surface O_3 concentrations (Li et al., 2019).

Surface O_3 concentrations predicted across northern hemisphere regions in ssp585 are similar to ssp370 due to comparable changes in air pollutant emissions and climate change. However, a notable exception is a reduction in surface O_3 across regions towards the latter half of the 21st Century (post 2080) when there are additional reductions in precursor emissions and global CH_4 abundances by 2100. Surface O_3 is predicted to stay at or near 2005-2014 values shows a slower increase until 2040 over South Asia in ssp585 than occurred in ssp370. This is despite increases in NOx precursor emissions and changes in climate,

indicating that there are potentially some changes in chemical O_3 formation within certain CMIP6 models across this region and in this scenario that constrain any increases in surface O_3.

The future scenario ssp245 (middle-of-the-road) predicts annual mean surface O_3 concentrations that tend to remain at or near the 2005-2014 mean values by 2100 across the major anthropogenic source regions of the Northern Hemisphere, whereas for other tropical and southern hemisphere regions surface O_3 concentrations are reduced by ~~up to~~more than 4 ppb. The changes in ssp245 are driven by larger precursor emission controls, a smaller climate change signal and controlling CH_4 so that global abundances are ~~just~~ below 2015 values by 2100 (Fig. 1g). In ssp245 a near-term (up to 2040) increase in surface O_3 is shown across ~~Europe,~~ East Asia and South Asia, which could be attributed to the peaking of global CH_4 abundances at this point prior to then reducing.

The Tier1 future scenario with the strongest climate and air pollutant mitigation measures, ssp126, shows substantial decreases in surface O_3 concentrations across most regions due to the large reduction in precursor emissions, global CH_4 abundances, and small climate change signal. Reductions in surface O_3 of more than 10~~8~~ ppb are predicted across anthropogenic emission source regions of the northern hemisphere, with smaller reductions across southern hemisphere regions.

Predictions from the CMIP6 models show that to achieve global benefits for regional surface O_3 it is important to control O_3 precursor emissions (including CH_4) in addition to limiting future climate change. However, scenarios with ~~large increases in global CH_4 abundances, a~~ large climate change signals (ssp370 and ssp585) ~~and limited~~ but different post 2050 controls of~~n~~ O_3 precursors ~~emissions~~(most notably CH_4 and NOx), ~~fail to restrict regional increases in~~show different long-term changes in regional surface O_3 concentrations, ~~leading to poor future air quality and~~which could have important consequences for any potential human health impacts ~~(Silva et al., 2017)~~.

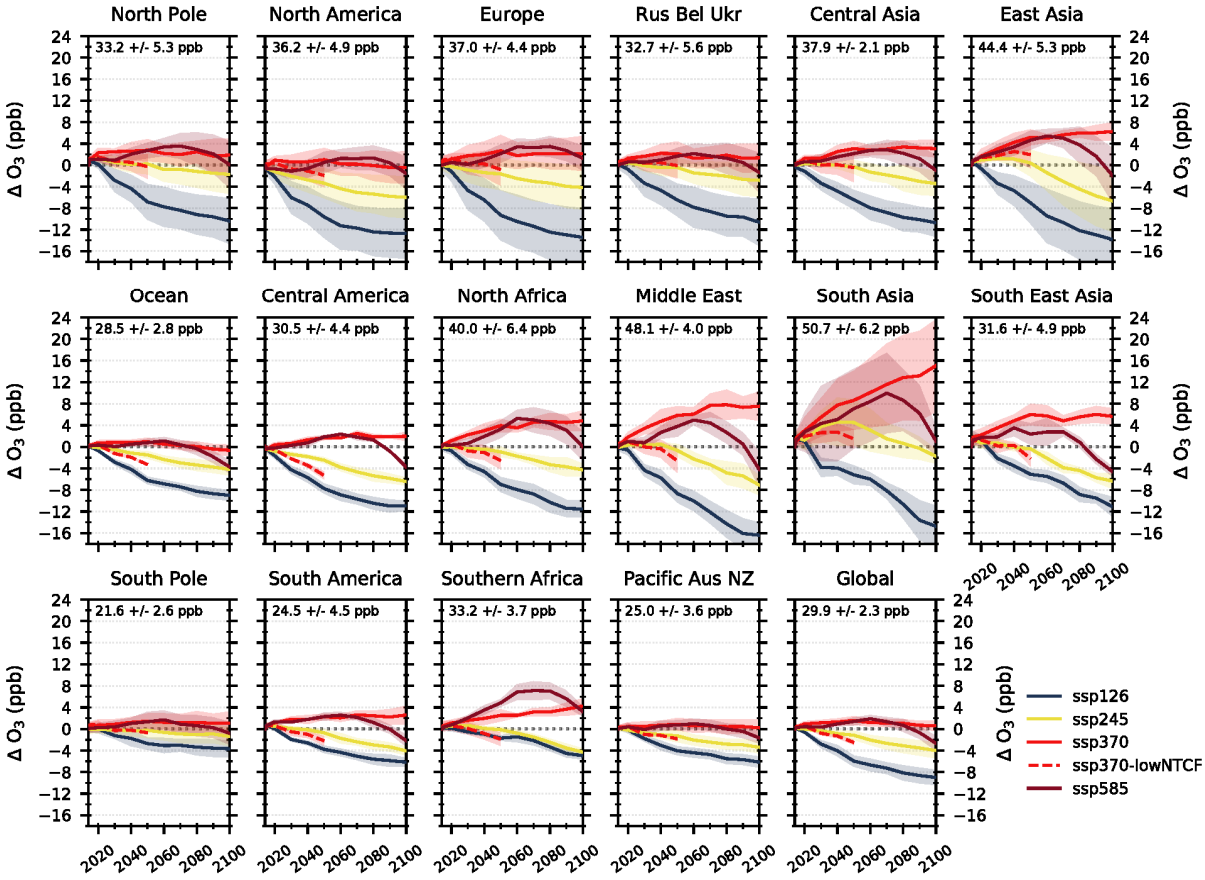

Figure 11 – Future global and regional changes in annual mean surface O_3, relative to 2005-2014 mean, for the different SSPs used in CMIP6. Each line represents a multi-model mean across the region with shading representing the +/- 1 standard deviation in the mean. See Table 1 for details of models contributing to each scenario. The multi-model regional mean value (+/- 1 standard deviation) for the year 2005-2014 is shown in the top left corner of each panel.

A more detailed comparison of future surface O_3 predictions between CMIP6 models has been undertaken for ssp370, as it is the scenario with the largest number of available models (Table 1). The regional change in decadal annual and seasonal mean surface O_3, relative to 2005-2014, in 2050 (2045 - 2055 mean) and 2095 (2090 – 2100 mean) for ssp370 from four CMIP6 models and the HTAP_param is shown in Figure 12. An analysis of the relationships, in terms of correlation coefficients, between future annual mean surface O_3 concentrations and other variables (CH_4 concentrations, surface air temperature, NOx concentrations, emissions of BVOCs and anthropogenic emissions of NMVOCs) is undertaken for CMIP6 models in the ssp370 scenario (Figure 13). Discrepancies in the simulated response of background O_3 across the ocean region (also South Pole and Pacific, Australia and New Zealand) are noticeable between individual models, with UKESM1-0-LL predicting a decrease in surface O_3 compared to the small increase from the HTAP_param and most other models in both 2050 and 2095 (Figure S1914). The future surface O_3 response in UKESM1-0-LL over the ocean region exhibits a large negative correlation with surface temperature changes (Figure 13), indicating the importance of future climate change in this model over remote regions. UKESM1-0-LL is a model with high equilibrium climate sensitivity (ECS, 5.4 K) compared to other CMIP6 models (Forster et al., 2019; Sellar et al., 2019), and therefore will exhibit a larger climate response (surface temperature and water vapour), leading to enhanced background O_3 destruction via water vapour and the hydroxyl radical (OH). Over the North Pole region all models show surface O_3 increases that are larger than the HTAP_param, with a larger increase in DJF than JJA. ~~indicating that t~~The large future temperature response over the Arctic, as well as changes in NOx concentrations and emissions of NMVOCs are particularly ~~or changes to long-range transport could be an~~ important drivers of surface O_3 changes across most CMIP6 models in~~over~~ this region with comparatively low local emissions (Figure 13).

Differences in the predicted surface O_3 between models exist across South Asia where CESM2-WACCM (and BCC-ESM1 in 2050) predict a response that is twice as large as UKESM1-0-LL and GFDL-ESM4. The lower annual mean response over South Asia in UKESM1-0-LL and GFDL-ESM4 is driven by a reduction in DJF in these models (Fig. S21), which results in the DJF change in 2050 being lower than the 2005-2014 annual mean value (Fig. 12). The large increase in NOx emissions in ssp370~~this scenario~~ over South Asia (~80%) has resulted in areas of NOx titration, particularly in DJF, near the Indo-Gangetic plain in both UKESM1-0-LL and GFDL-ESM4, reducing surface O_3 concentrations (Fig. S19 and S2114). This strong feature of NOx titration of O_3 in DJF is absent in both CESM2-WACCM and BCC-ESM1, resulting in larger O_3 production over South Asia. The comparison in Fig. 12 shows how the O_3 chemistry within models responds differently across a particular area in a future scenario with a large climate change signal and over a region with large increases in local precursor emissions, but that all the drivers related to regional O_3 change in South Asia are similarly important across all models (Figure 13).

Over South America and Southern Africa, particularly the tropical areas (Fig. S1914), larger future changes in surface O_3, particularly by 2100, -are predicted by GFDL-ESM4 and ~~/~~UKESM1-0-LL than by CESM2-WACCM. These changes over South America are larger in JJA in all models, with small seasonal differences over Southern Africa. Over this region, biogenic emissions (particularly isoprene) are an important source of O_3 formation. Discrepancies in the ~~magnitude of change in~~future response of these BVOC emissions between models could be occurring due to the differing magnitudes of climate and land-use change and how they are coupled within individual CMIP6 models (Table S1), which could affect ~~lead to the inter-model differences in~~ future surface O_3. Future changes in the ~~T~~total emissions of BVOCs ~~(isoprene and monoterpenes~~) and those solely from isoprene ~~their future change in ssp370~~ obtained from ~~three~~five CMIP6 models (Figure S22 and S2315) show that CESM2-WACCM has larger total BVOC emissions over the period 2005-2014 (due to the inclusion of more BVOCs), which then increase in the future ssp370 scenario, along with isoprene emissions, resulting in a smaller increase (and decreases over some parts of the region) in O_3. Whereas, ~~GFDL-ESM4 and~~ UKESM1-0-LL shows a larger increase in O_3 ~~have smaller increases~~ and a reduction in BVOC emissions, mainly from isoprene (Fig. 23), ~~with some emissions reducing~~ over parts of South America and tropical Africa ~~in UKESM1~~. Figure 13 shows that there are differing relationships between future surface O_3 concentrations, BVOC emissions and NOx concentrations across CMIP6 models over South America and Southern Africa. Over Southern Africa, UKESM1-0-LL shows a different relationship between BVOC emissions and surface O_3 concentrations

than other CMIP6 models, indicating that this could be leading to the different future O_3 response in this model over this region. Similarly, Figure 13 shows that over South America, CESM2-WACCM has a different relationship between surface O_3 and the variables considered here than in other CMIP6 models, particularly for BVOCs, leading to the different future responses in this model over this region. ~~The BVOC emission changes appear to have affected the future O_3 formation differently in the individual models over these regions and represents an~~ Figure 13 shows that there are differences between models in the surface O_3 response over regions such as South America and Southern Africa, which are potentially linked to the land-surface response and are important ~~process~~ to understand ~~further~~more in future work.

Whilst there ~~is~~are disagreements between models over some regions, there is also substantial consistency in the predicted increase to annual mean surface O_3 in ssp370 over North America, Europe and East Asia, which is larger than that from HTAP_param. ~~-~~However, BCC-ESM1 tends to predict a larger increase than the other three models, potentially due to the coarser resolution of this ESM. There are differences in simulated seasonal response across these regions, with all models showing a smaller increase in JJA than DJF across North America and Europe, whilst across East Asia there tends to a be a larger future surface O_3 increase in JJA than DJF. Figure 13 shows that there is a negative correlation between surface O_3 and NOx concentrations, as well as between O_3 and NMVOC emissions, for most CMIP6 models across these regions, reflecting that ~~A~~as most anthropogenic precursor emissions (including NOx) ~~are~~ decrease~~ing~~ in this scenario (Fig. 2)~~across all these regions,~~ then surface O_3 is simulated to increase. An exception to this is across East Asia, where the increase in NMVOC emissions in ssp370 (Fig. 2) are positively correlated with surface O_3, indicating different chemical drivers of future O_3 across this region. In addition, there are positive correlations between the other variables (temperature, CH_4 and BVOCs) for most CMIP6 models indicating that changes in climate and global CH_4 abundances ~~seem to be the major~~ are also important drivers of surface O_3 increases over these regions.

The differences between the individual CMIP6 models highlight the importance of further understanding how future O_3 chemistry is affected by changes to precursor emissions and climate. The predicted differences in models can be quite pronounced over regions like South Asia where changes in one model can be double that of another model, which could have important consequences for future regional air quality.

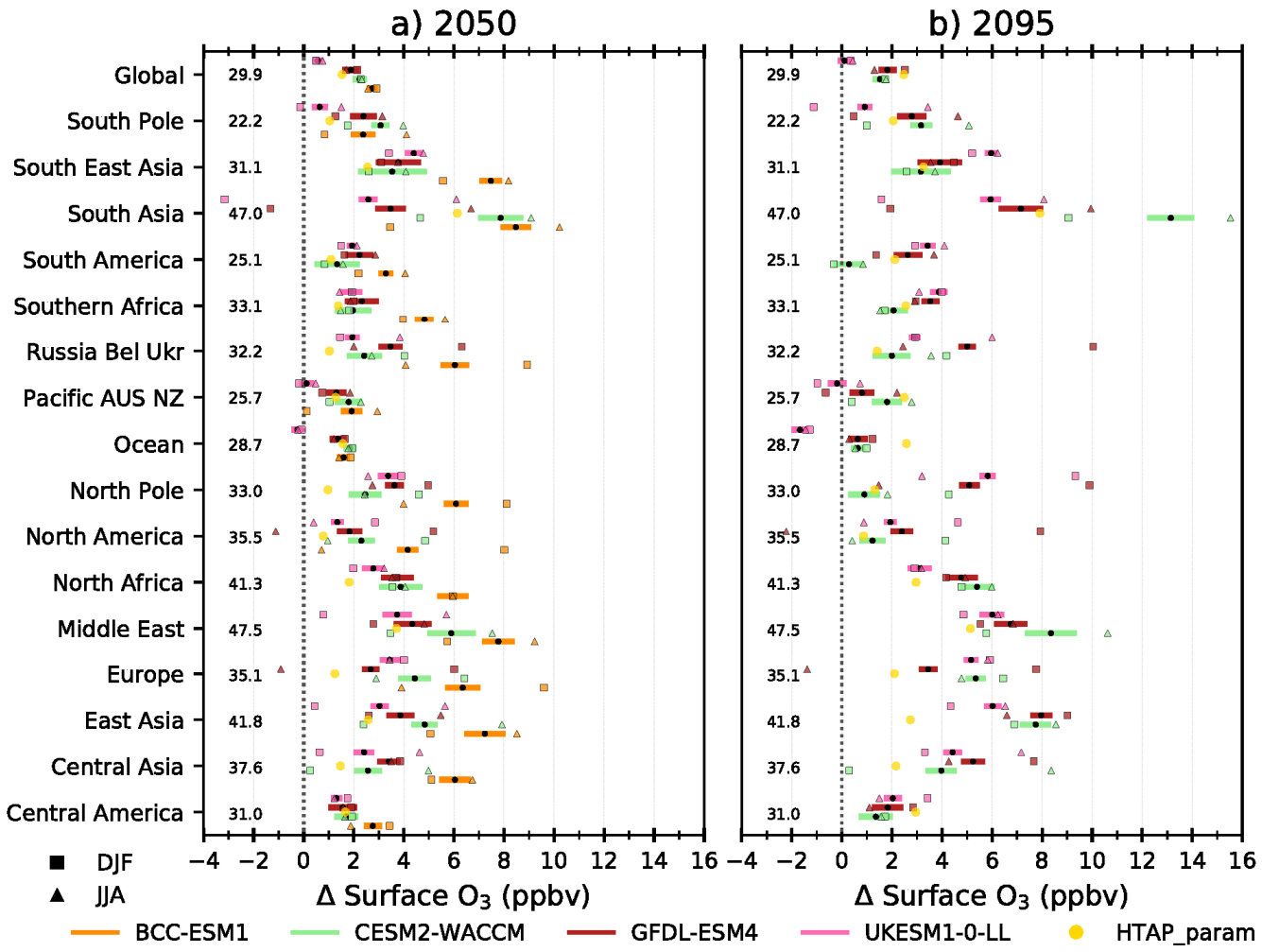

Figure 12 – Future global and regional changes in the decadal annual and seasonal mean surface O_3, relative to the 2005-2014 mean, for the ssp370 pathway used in CMIP6. Each black circle represents the decadal annual mean response for an individual model in a) 2045-2055 and b) 2090-2100, with the coloured bars showing the standard deviation across the decadal annual mean. The DJF and JJA seasonal mean response averaged over the relevant 10 year period is shown by squares and triangles respectively. The multi-model regional mean over the period 2005- 2014 is given towards the left of each panel. The response from the HTAP_param in each time period is shown by the separate gold circle.

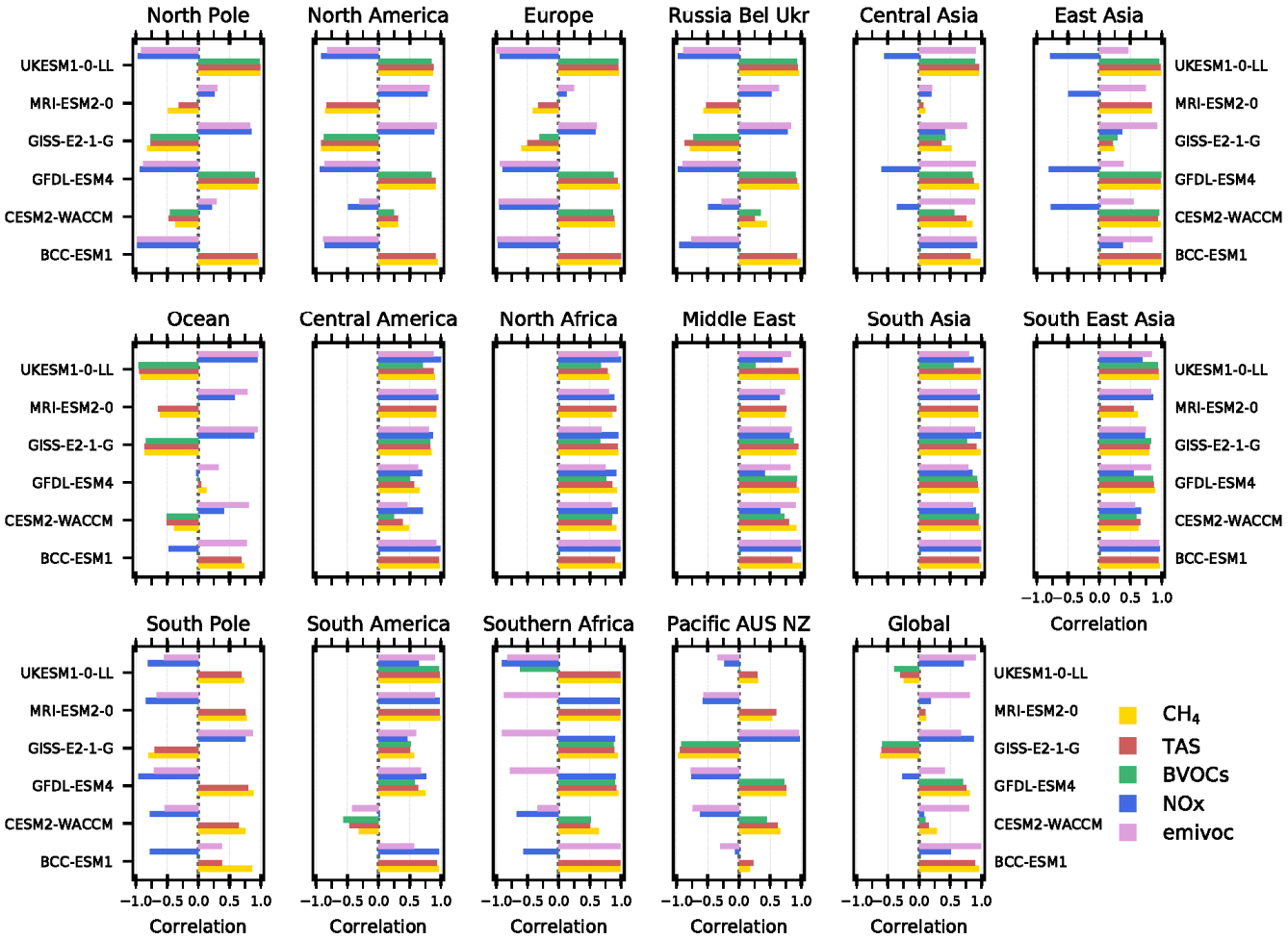

Figure 13 – Correlation coefficients calculated when comparing future annual mean surface O_3 concentrations against individual variables of surface CH_4 concentrations, surface air temperature (TAS), emissions of biogenic volatile organic compounds (BVOCs), NOx (NO + NO_2) concentrations and anthropogenic emissions of non-methane volatile organic compounds (NMVOCs) from individual CMIP6 models over the period 2015 to 2100 in the ssp370 scenario.

5.2 Surface $PM_{2.5}$

Relatively small global changes in annual mean surface $PM_{2.5}$ are predicted for all CMIP6 models across all scenarios (Figure 14), with an increase in ssp370 and a reduction in the others. Small reductions in $PM_{2.5}$ are predicted for all scenarios across Europe (0.3 to 3 µg m^{-3}) and North America (0.0 to 1.3 µg m^{-3}) due to the reduction in aerosol and aerosol precursor emissions. Differences in $PM_{2.5}$ between scenarios are highlighted across a number of regions.

For the weak climate and air pollutant mitigation scenario ssp370, increases in annual mean surface $PM_{2.5}$ are predicted across South Asia (7.34 +/- 34.14 µg m^{-3} by 2050 and 43.13 +/- 3.10 µg m^{-3} by 2100), South East Asia (32.70 +/- 54.73 µg m^{-3} by 2100), Southern Africa (1.69 +/- 43.75 µg m^{-3} by 2100), Central (32.83 +/- 3.25 µg m^{-3} by 2100) and South America (32.91 +/- 3.6 µg m^{-3} by 2100). The increases in $PM_{2.5}$ are driven mainly by the increase in aerosol and aerosol precursor emissions in this scenario (Fig. 2), shown by the positive correlations between emissions and surface $PM_{2.5}$ in CMIP6 models across these regions (Figure 16). However, there is a degree of uncertainty associated with all of these future predictions indicated by the large diversity across the CMIP6 models. Some of the largest predicted increases in surface $PM_{2.5}$ occur across South Asia in ssp370, a region already with high present day $PM_{2.5}$ concentrations. The increase in $PM_{2.5}$ peak in 2050 across this region, which coincides with the increase of SO_2, BC and OC emissions, before declining to 2100 when emissions reduce. Over East Asia, annual mean $PM_{2.5}$ concentrations are simulated to remain at or near 2005-2014 values until the latter half of the 21st Century when the decrease in emissions reduce $PM_{2.5}$ concentrations by 2.58 +/- 2.76 µg m^{-3}. The impact of reductions in NTSLCFs on top of the ssp370 scenario act to constrain any increases of $PM_{2.5}$ concentrations to near present day values across most regions. However, substantial reductions in $PM_{2.5}$ concentrations of 5.6 +/- 2.01 µg m^{-3} and 5.93 +/- 12.14 µg m^{-3} below

2005-2014 values are achieved by 2050 across East and South Asia respectively, by implementing these measures. Due to the short lifetime of aerosols in the atmosphere $PM_{2.5}$ concentrations respond rapidly to the large cuts in emissions that occur in ssp370-lowNTCF and show the benefits to targeting these emissions, although there could be a potential climate impact (Allen et al., 2020).

Reductions in annual mean surface $PM_{2.5}$ are simulated across all regions for ssp126, ssp245 and ssp585. Differences exist in the magnitude and timing of $PM_{2.5}$ reductions across regions linked to the changes in emissions. The largest reductions in $PM_{2.5}$ occur over South Asia in 2100 and range from 1~~2~~1.1 +/- ~~1~~2.~~8~~9 µg m^{-3} in ssp126 to ~~9~~8.~~6~~1 +/- ~~1~~2.9 µg m^{-3} in ssp585, a substantial benefit to regional air quality. Similar benefits to $PM_{2.5}$ are achieved over East Asia by 2100 although the more rapid improvements occur over this region in the first part of the 21st Century.

The response of $PM_{2.5}$ concentrations is more variable, with a larger diversity across CMIP6 models within regions that are close to natural aerosol emission sources. This is particularly noticeable over North Africa where the variability across CMIP6 models in dust emissions from the Saharan source region (Fig. S8~~7~~) results in an uncertain $PM_{2.5}$ response across this region. A similar response is also exhibited across the Middle East and Central Asia. The potential influence of BVOCs on SOA formation (Fig. S22~~15~~ and S26~~18~~) could also be contributing to the diversity in the CMIP6 model responses across the South America and Southern Africa regions.

The CMIP6 models show that future reductions in aerosols and aerosol precursors will lead to a decrease in surface $PM_{2.5}$ concentrations across most world regions and a benefit to regional air quality (and human health), consistent with that from CMIP5. However, if emissions are not controlled over economically developing regions such as South America, Asia and Africa then surface $PM_{2.5}$ is anticipated to increase and worsen future regional air quality. Targeting emission reductions of ~~NT~~SLCFs in the short-term shows the potential for rapid improvements in surface $PM_{2.5}$ and air quality.

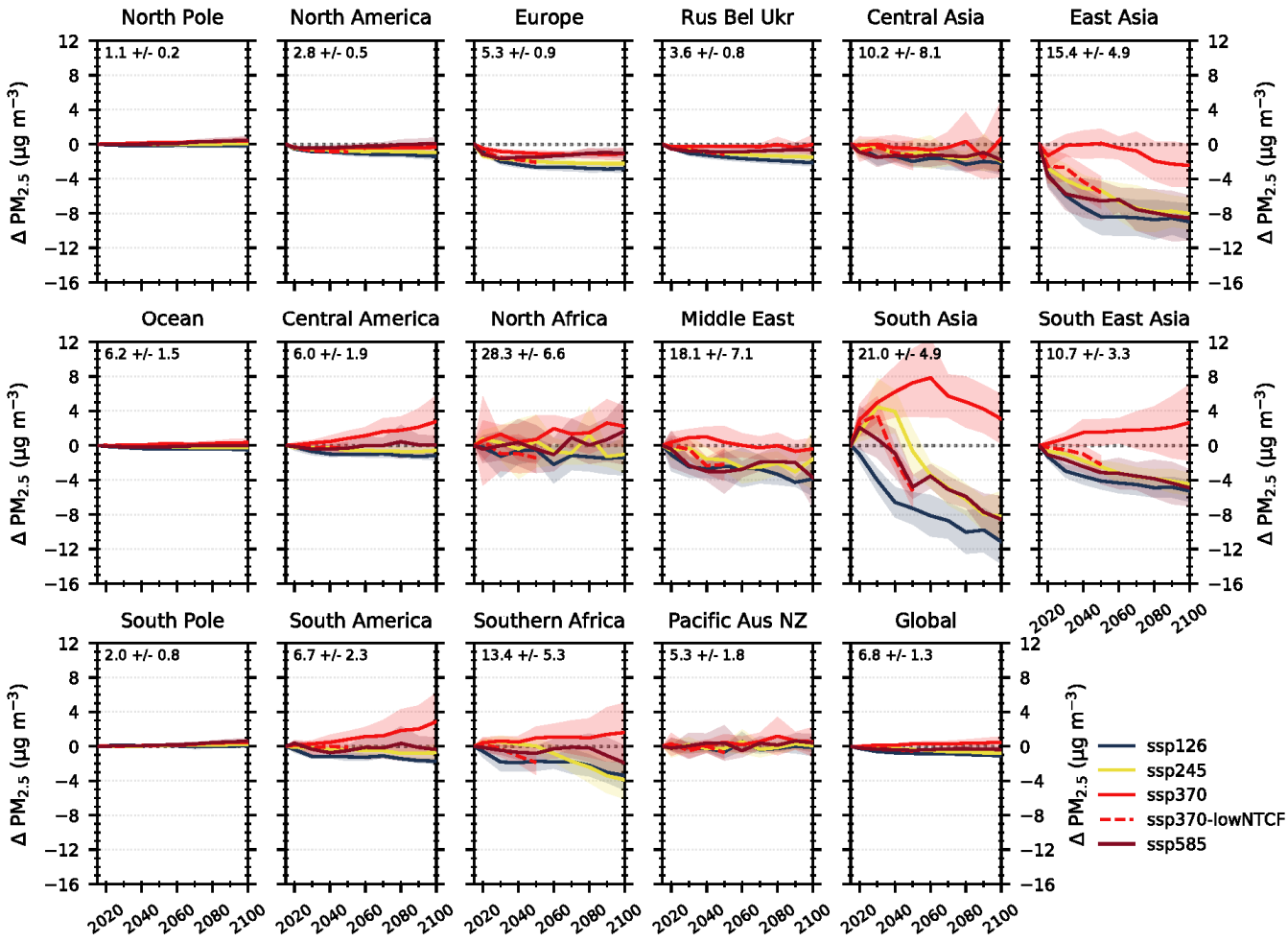

Figure 1~~3~~4 – Future global and regional changes in annual mean surface $PM_{2.5}$, relative to 2005-2014 mean, for the different SSPs used in CMIP6. Each line represents a multi-model mean across the region with shading representing the +/- 1 standard deviation in the mean. See Table 1 for details of models contributing to each scenario. The multi-model regional mean value (+/- 1 standard deviation) for the year 2005-2014 is shown in the top left corner of each panel.

In a similar analysis to that for surface O_3, a more detailed comparison has been undertaken of four CMIP6 models predicting changes in annual and seasonal surface $PM_{2.5}$ in 2050 and 2095 under ssp370 (Figure 1~~5~~4). In addition, an analysis of the relationships, in terms of correlation coefficients, between future annual mean surface $PM_{2.5}$ and other variables (total surface precipitation, surface air temperature and emissions of BVOCs, SO_2, BC and organic aerosol) has been undertaken for CMIP6 models in the ssp370 scenario (Figure 16). Small reductions in annual mean surface $PM_{2.5}$ concentrations (<2 μg m^{-3}) are simulated consistently by all CMIP6 models across North America and Europe in ssp370, with larger reductions simulated in DJF than JJA. ~~-~~The reductions in annual mean $PM_{2.5}$ over Europe and North America are mainly attributed to decreases in the BC and SO_4 components (Fig. S24 and S25), as indicated by the strong correlations with BC and SO_2 emissions across CMIP6 models (Figure 16). However, by 2095 a small increase (up to 2 μg m^{-3}) is simulated in JJA by UKESM1-0-LL and CESM2-WACCM over North America, which could be attributed to changes in climate due to the strong positive correlations in both models for temperature, precipitation and BVOCs (Figure 16).

South Asia, the region with the largest simulated future change in annual mean surface $PM_{2.5}$ of up to 12 μg m^{-3}, shows fairly good agreement between three CMIP6 models (UKESM1-0-LL, GFDL-ESM4 and CESM2-WACCM) as predictions in 2050 and 2095 are all within the range of each of the individual models. The future increases in annual mean surface $PM_{2.5}$ appear to be strongly driven by emission changes as there are strong positive correlations between these variables across South Asia in all models (Figure 16). ~~-~~Across South Asia, all models simulate a larger increase in DJF mean surface $PM_{2.5}$ concentrations, of up to 18 μg m^{-3} by 2050, than occurs in JJA, and reflects the seasonality shown in the model evaluation. The MIROC-ES2L model predicts smaller future increases in surface $PM_{2.5}$ than the other models across South Asia of up to 5 μg m^{-3} in both 2050 and 2095. This is a result of smaller changes in the BC, OA and sulphate aerosol components in the MIROC-ES2L model despite increases in aerosols and aerosol precursor emissions across South Asia in ssp370 (Figure S24~~16~~-S26~~18~~).

Disagreements in both the sign and magnitude of simulated future annual and seasonal mean surface $PM_{2.5}$ changes between CMIP6 models are also exhibited across East Asia. Small regional annual mean increases are predicted in 2050 due to $PM_{2.5}$ increases in JJA from~~or~~ all models apart from GFDL-ESM4~~,~~, ~~attributed to a~~A larger reduction in the SO_4 component is simulated over East Asia by GFDL-ESM4 than in other models ~~across this region~~ (Fig S25~~17~~), resulting in an overall decrease in $PM_{2.5}$. In 2095 most models~~, apart from CESM2-WACCM~~, simulate a reduction in $PM_{2.5}$ concentrations in both seasons across East Asia, apart from CESM2-WACCM due to the increase in JJA. All models simulate continual reductions out to 2100 for SO_4 across this region, whereas BC increases in the near-term before decreasing out to 2100. For OA, CESM2-WACCM shows larger increases over East Asia in both 2050 and 2095 compared to the other models, which show a smaller increase in 2050 and a reduction by 2095 (Fig. S26~~18~~). CESM2-WACCM includes a more complex treatment of SOA formation, showing a strong response to climate and historical trends in OA (Tilmes et al., 2019)~~,~~. Positive correlations are shown for CESM2-WACCM between surface $PM_{2.5}$ and emissions of BVOC and temperature (Fig. 16), which are not present in other models and could explain the ~~multi-model~~ differences between this model and others across East Asia. The discrepancies in CMIP6 models are not as obvious over South Asia as the effect of the increase in OA over South Asia in CESM2-WACCM is masked by coincident increases in other components across other models, as indicated by the strong correlations with emissions here. CESM2-WACCM also shows larger simulated increases in $PM_{2.5}$ over South America, Central America, Southern Africa and South East Asia than other models, which can be attributed to the larger increase in the OA fraction (Fig. S26) ~~in this model~~and the strong correlations in this model with changes in temperature and emissions (BVOCs and SO_2). ~~However, o~~Over Southern Africa UKESM1-0-LL shows a reduction in future $PM_{2.5}$, in contrast to ~~the~~ other models~~.~~, ~~This can again be attributed~~ due to a reduction in the BC, OA ~~fraction~~and dust aerosol components ~~in UKESM1~~ (Fig. S24, S26 and S27~~18~~)~~,~~. UKESM1-0-LL exhibits particularly strong negative correlations for surface $PM_{2.5}$ when compared

with temperature and precipitation. These relationships over Southern Africa are quite different to other CMIP6 models, which is also highlighted in the model evaluation over this region (Fig. 8) and indicates that climate change influences aerosol concentrations differently over this region in this model (Figure 16). In addition, there is a slight positive correlation of $PM_{2.5}$ with BVOC emissions in UKESM1-0-LL over Southern Africa. Future ~~related to potential changes in land use and a reduction in~~ biogenic emissions (including monoterpenes) reduce here ~~across Southern Africa~~ in ssp370 (Fig. S22~~15~~), potentially due to land-use vegetation change as UKESM1-0-LL has dynamic vegetation coupled to BVOC emissions (Table S1). This could also reduce $PM_{2.5}$ concentrations over this region because monoterpene emissions are the main precursor to SOA formation in ~~this~~ UKESM1-0-LL~~model~~ (Mulcahy et al., 2019).

The decadal annual and seasonal mean $PM_{2.5}$ response is variable across individual CMIP6 models over regions close to natural sources of particulate matter (North Africa, Central Asia and Pacific, Australia and New Zealand). Over these regions there is a large range in both the sign and magnitude of the annual and seasonal $PM_{2.5}$ response, which can be mainly attributed to the dust fraction (Fig. S27~~19~~) and the fact that this aerosol source has a large inter-annual variability in its emission strength. There is also a lack of consistency across CMIP6 models in the correlations of $PM_{2.5}$ with any individual driver, indicating the variability of aerosol sources in these regions within models. Interestingly, the CMIP6 models do not agree in the sign and magnitude of future changes to dust concentrations in ssp370 (Fig. S27~~19~~).

Across the ocean and North Pole regions all the CMIP6 models tend to simulate a small increase in $PM_{2.5}$ concentrations, which can be attributed to increases in sea salt concentrations (Fig. S28~~0~~). A strong increase in sea salt concentrations ~~all models~~ is simulated in all models across the Southern Ocean (and other oceans), potentially driven by changes to meteorological conditions (reflected by the positive correlations of $PM_{2.5}$ with the climate variables temperatures and precipitation in Fig. 16), which increase wind speed and sea salt emissions. As ssp370 is a scenario with a large climate change signal, the increases in $PM_{2.5}$ across the North Pole, particularly in 2100, can be attributed to the melting of sea ice increasing sea salt emissions, which again is reflected in the positive correlations of $PM_{2.5}$ with climate variables over this region. However, the magnitude of this response is different in the CMIP6 models due to the underlying ECS and the response of Arctic surface temperatures within the individual model.

The differences in the simulated future $PM_{2.5}$ changes across the CMIP6 models in ssp370 highlight that it is important to consider how natural sources of aerosol respond in a future climate in addition to that from changes in anthropogenic emissions. Particular differences between models have been shown for dust, sea salt and also organic (secondary) aerosols, which should be explored further. In addition, the different representations of aerosols within individual models e.g. organic aerosols, are an important consideration as they can make a large difference to any future regional prediction of $PM_{2.5}$.

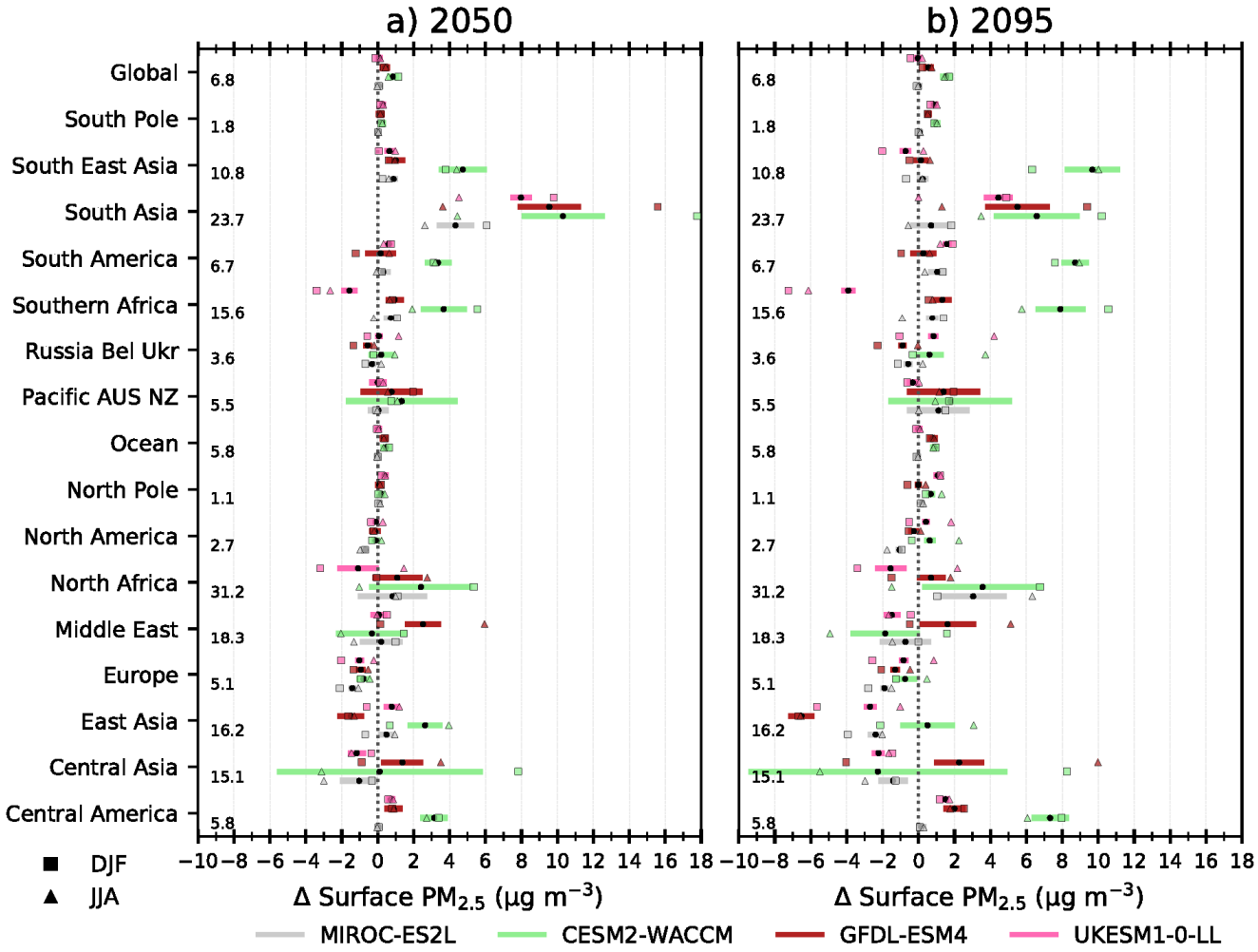

765 **Figure 154 – Future global and regional changes in the decadal annual and seasonal mean surface $PM_{2.5}$, relative to the 2005-2014 mean, for the ssp370 pathway used in CMIP6. Each black circle represents the decadal annual mean response for an individual model in a) 2045-2055 and b) 2090-2100, with the coloured bars showing the standard deviation across the decadal annual mean. The DJF and JJA seasonal mean response averaged over the 10 relevant period are shown by squares and triangles respectively. The multi-model regional mean over the period 2005- 2014 is given towards the left of each panel.**

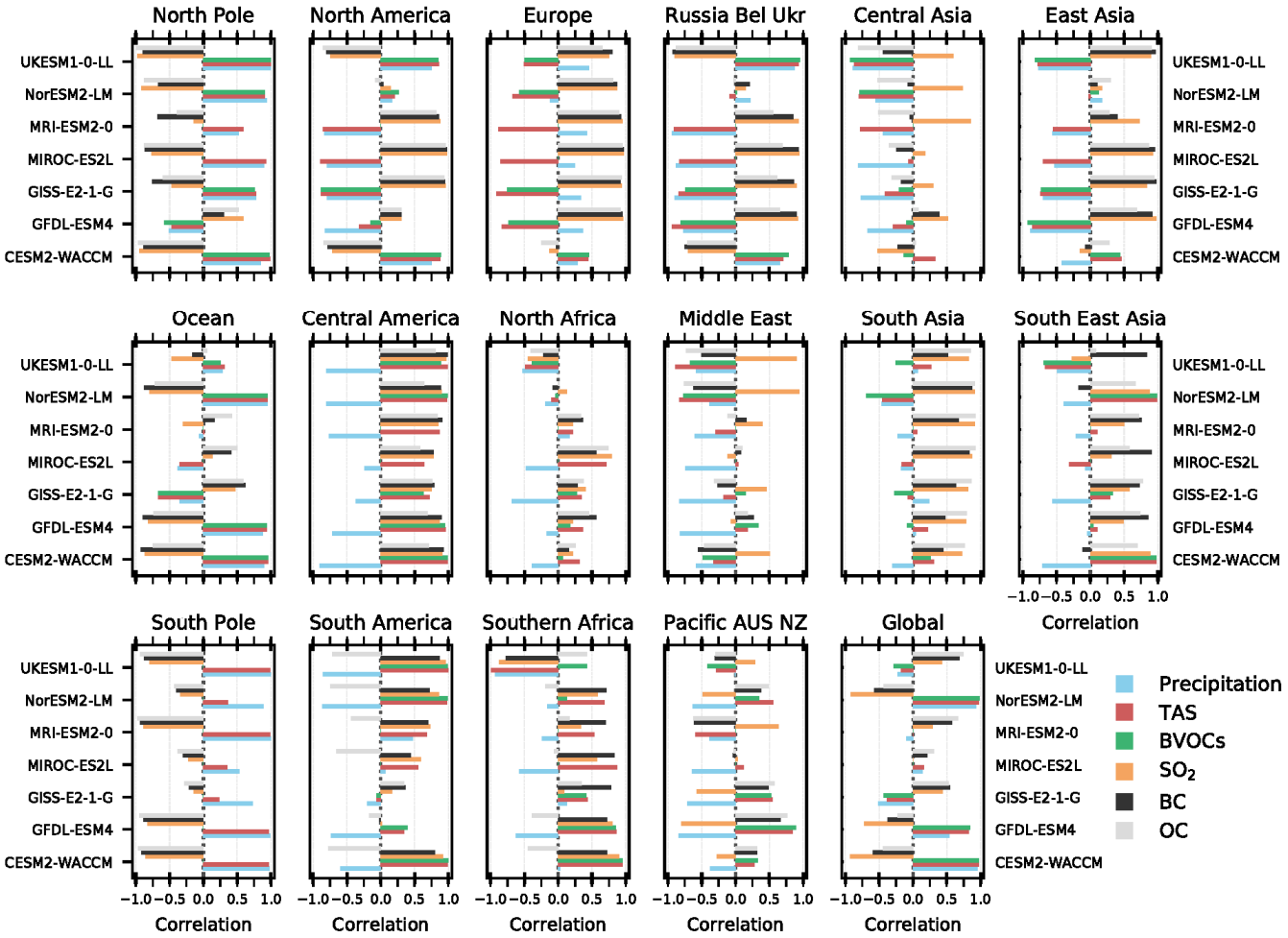

Figure 16 – Correlation coefficients calculated when comparing future annual mean surface $PM_{2.5}$ concentrations against individual variables of precipitation, surface air temperature (TAS), emissions of biogenic volatile organic compounds (BVOCs) and emissions of SO_2, black carbon (BC) and organic carbon (OC) from individual CMIP6 models (that had data out to 2100) over the period 2015 to 2100 in the ssp370 scenario.

6 Conclusions

In this study we have provided an initial analysis of the historical and future changes in air pollutants (O_3 and $PM_{2.5}$) from the latest generation of Earth system and climate models that have submitted results from experiments conducted as part of CMIP6. Data was available from the historical experiments of ~~5~~6 CMIP6 models for surface O_3 and 1~~0~~1 models for surface $PM_{2.5}$. Historical changes in regional concentrations of O_3 and $PM_{2.5}$ are presented over the period 1850 to 2014 using data from all models. A present day model evaluation of the CMIP6 models was conducted against surface observations of O_3 and $PM_{2.5}$ obtained from the TOAR and GASSP databases respectively. An additional comparison was performed for simulated $PM_{2.5}$ concentrations against the MERRA-2 aerosol reanalysis product. An assessment is then made of the changes in surface O_3 and $PM_{2.5}$ simulated by the CMIP6 models across different future scenarios, ranging from weak to strong air pollutant and climate mitigation.

The ~~5~~6 CMIP6 models simulate present day (2005-2014) surface O_3 concentrations that are elevated in the Northern Hemisphere summer, with lower values throughout the year across the Southern Hemisphere. However, a large model diversity is shown across the continental Northern Hemisphere due to the large simulated seasonal cycles in certain models. Compared to surface O_3 measurements, CMIP6 models ~~consistently~~ overestimate~~predict~~ observed annual mean values and in both summer and winter across most regions by up to 16 ppb (a similar result to previous multi-model evaluations of global chemistry-climate models in (Young et al., (2018)). An exception to this is at observation locations across Antarctica where CMIP6 models tend to underestimate~~predict~~ observed values by 5 ppb.

Large surface $PM_{2.5}$ concentrations are simulated in CMIP6 models near dust and anthropogenic emission source regions. Model diversity across the CMIP6 models is largest near the dust source regions due to their sensitivity to meteorological variability, whereas across other regions the CMIP6 models are relatively similar in their simulation of $PM_{2.5}$ concentrations. Evaluating the approximate $PM_{2.5}$ calculated from CMIP6 models (excluding nitrate aerosols) against ground based $PM_{2.5}$ observations shows an ~~consistent~~ underestimation~~prediction~~ across most regions of up to 10 μg m^{-3}. The underestimation of observations by models is larger in the northern hemisphere winter than summer, in part due to the absence of nitrate aerosols within most CMIP6 models and also due to underrepresentation of other aerosol processes within ~~the~~ global models (a similar result to other multi-model assessments). To improve the spatial coverage and consistency of the $PM_{2.5}$ evaluation with CMIP6 models an additional comparison was made to the MERRA-2 aerosol reanalysis product. A similar, but slightly smaller, underestimation of $PM_{2.5}$ concentrations over Europe and North America was found in the comparison of CMIP6 models and MERRA-2, providing further confidence in the~~is~~ result from the ground-based comparison. CMIP6 models overestimated the monthly $PM_{2.5}$ concentrations in MERRA-2 over South and East Asia by up 15 μg m^{-3}, ~~contrary~~in contrast to the evaluation using ground based observations. Mean ~~A~~annual ~~mean~~ cycles simulated by CMIP6 models and MERRA-2 tend to agree across other regions for which there are no suitable ground-based observations. The comparison of surface O_3 and $PM_{2.5}$ simulated by CMIP6 models to observations shows similar biases to previous generations of global composition-climate models. Further studies are required (e.g. global sensitivity or process studies) to explore uncertainties in models and the differences with observations.

Across the historical period (1850-2014), the CMIP6 models simulated a global annual increase in surface O_3 of between 7 and 14 ppb, with a larger increase in JJA than DJF. A global multi-model mean increase of 11.7~~5~~ +/- 2.3~~2~~ ppb was simulated by the CMIP6 models which agrees well with the change previously simulated by CMIP5 models. A large diversity in the historical change of surface O_3 was simulated by CMIP6 models across South Asia and other Northern Hemisphere regions. CMIP6 models predicted larger historical changes in surface O_3 than those from an emission-only driven parameterisation, indicating a potential climate change impact (Wu et al., 2008; Bloomer et al., 2009; Weaver et al., 2009; Rasmussen et al., 2013; Colette et al., 2015) on surface O_3 over the historical period. Small global increases in surface $PM_{2.5}$ are simulated over the historical period by CMIP6 models, with larger regional changes of up to 12 μg m^{-3} on an annual mean basis and up to 18 μg m^{-3} in DJF across East and South Asia. The largest diversity in the response of CMIP6 models occurs over Asian regions, with large interannual variabilities near dust source regions. CMIP6 models simulate the peak in $PM_{2.5}$ concentrations in the 1980s across Europe and North America, prior to simulating the observed decline in concentrations to present day (Leibensperger et al., 2012; Tørseth et al., 2012; Turnock et al., 2015), ~~resulting from~~attributed to the implementation of air pollutant emission controls over these regions.

The CMIP6 models predict surface O_3 to increase across most regions in the weak mitigation scenarios (ssp370 and ssp585), particularly over South and East Asia (up to 1~~0~~6 ppb by 2100) due to a combination of increases in air pollutant emissions, increases in global CH_4 abundances and climate change. Discrepancies exist in the regional surface O_3 response in ssp370 between individual CMIP6 models due to differences in the future response of chemistry (NOx), climate (temperature) and biogenic precursor emissions. Benefits to regional air quality from large reductions in surface O_3 are possible across all regions for scenarios that contain strong climate and air pollutant mitigation measures, including those targeting CH_4.

CMIP6 models predict surface $PM_{2.5}$ concentrations to decreases across all regions in both the middle-of-the-road (ssp245) and strong mitigation scenarios (ssp126) by up to 12 μg m^{-3} due to the reduction in anthropogenic aerosols and aerosol precursor emissions, yielding a benefit to regional air quality. Whereas for the weak climate and air pollutant mitigation scenario (ssp370), annual and seasonal mean surface $PM_{2.5}$ is simulated to increase across a number of regions. Implementing mitigation measures specifically targeting ~~NT~~SLCFs on top of the ssp370 scenario shows immediate improvements in $PM_{2.5}$ concentrations, restricting any changes to below present day values. The largest change in regional mean $PM_{2.5}$ concentrations, and also largest diversity across CMIP6 models, is predicted in ssp370 across South Asia, an area with already poor air quality.

Disagreements in the prediction of future changes to regional surface $PM_{2.5}$ concentrations between individual CMIP6 models can ~~mainly~~ be attributed to differences in the complexity of the aerosol schemes implemented within models, in particular the formation mechanisms of organic aerosols and emission of BVOCs over certain regions~~. Additionally~~, along with the strength of the climate change signal (temperature and precipitation) ~~within~~ simulated by models and ~~how~~ the~~is~~ ~~can have important~~ impact~~s~~ this has on natural aerosol emissions via Earth system couplings ~~leading to discrepancies between models~~.

The results from CMIP6 provide an opportunity to assess the simulation of historical and future changes in air pollutants within the latest generation of Earth system and climate models using up to date scenarios of future socio-economic development. Large changes in air pollutants were simulated over the historical period, primarily in response to changes in anthropogenic emissions. Future regional concentrations of air pollutants depend on the particular trajectory of climate and air pollutant mitigation that the world follows, with important consequences for regional air quality and human health. Substantial benefits can be achieved across most world regions by implementing measures to mitigate the extent of climate change, as well as from large reductions in air pollutants emissions, including CH_4 which is particularly important for controlling O_3. In future scenarios which do not mitigate climate change and air pollutant emissions, the regional concentrations of air pollutants are anticipated to increase. Important differences between individual CMIP6 models have been identified in terms of how they ~~treat the~~simulate air pollutants from the interaction of chemistry (O_3 and NOx), climate (temperature and precipitation) and natural precursor emissions (BVOCs) in the future. Further research and understanding is necessary of these processes to improve the robustness of regional predictions of air pollutants on climate change timescales (decadal to centennial).

Data Availability

CMIP6 data is archived at the Earth System Grid Federation and is freely available to download. A list of the model datasets used in this study are provided in Table 1.

Author Contributions

S.T.T. conducted the analysis and wrote the paper with contributions from R.J.A. T.W. and J.Z. performed BCC-ESM1 simulations. L.E. and S.T. performed CESM2-WACCM simulations. P.N. and M.M. performed CNRM-ESM2-1 simulations. L.W. H. and ~~V.N.~~J.G.J. performed GFDL-ESM4 simulations. S.B. and K.T. performed GISS-E2-1-G~~H~~ simulations. M.A and P.G. performed HadGEM3-GC31-LL simulations. T.T. performed MIROC6-ES2L simulations. D.N. performed MPI-ESM1.2-HAM simulations. M.D. and N.O. performed MRI-ESM2-0 simulations. D.O. and M.S. performed NorESM2-LM simulations. A.S. and F.M.O'C. performed UKESM1-0-LL simulations. All co-authors have been involved in providing comments and editing the manuscript.

Competing Interests

The author declares that there are no conflicts of interest.

Acknowledgements

S.T.T. and F.M.O'C. would like to acknowledge that support for this work came from the BEIS and DEFRA Met Office Hadley Centre Climate Programme (GA01101). S.T.T. would also like to acknowledge the UK-China Research and Innovation Partnership Fund through the Met Office Climate Science for Service Partnership (CSSP) China as part of the Newton Fund. FMO'C also acknowledge the EU Horizon 2020 Research Programme CRESCENDO project, grant agreement number

641816. T.T. was supported by the supercomputer system of the National Institute for Environmental Studies, Japan, and JSPS KAKENHI Grant Number JP19H05669. K.T. and S.B. acknowledge resources supporting this work were provided by the NASA High-End Computing (HEC) Program through the NASA Center for Climate Simulation (NCCS) at Goddard Space Flight Center. M.D. and NO were supported by the Japan Society for the Promotion of Science (grant numbers: JP18H03363, JP18H05292, and JP20K04070) and the Environment Research and Technology Development Fund (JPMEERF20172003, JPMEERF20202003, and JPMEERF20205001) of the Environmental Restoration and Conservation Agency of Japan.

For making their measurement data available to be used in this study we would like to acknowledge the providers who supplied their data to the GASSP database and TOAR database. David Neubauer acknowledges funding from the European Union's Horizon 2020 research and innovation programme project FORCeS under grant agreement No 821205 and a grant from the Deutsches Klimarechenzentrum (DKRZ) under project ID 1051. S.S was supported by Korea Meteorological Administration Research and Development Program "Development and Assessment of IPCC AR6 Climate change scenario" under grant (KMA2018-00321)

References

Aas, W., Mortier, A., Bowersox, V., Cherian, R., Faluvegi, G., Fagerli, H., Hand, J., Klimont, Z., Galy-Lacaux, C., Lehmann, C. M. B., Myhre, C. L., Myhre, G., Olivié, D., Sato, K., Quaas, J., Rao, P. S. P., Schulz, M., Shindell, D., Skeie, R. B., Stein, A., Takemura, T., Tsyro, S., Vet, R. and Xu, X.: Global and regional trends of atmospheric sulfur, Sci. Rep., 9(1), 953, doi:10.1038/s41598-018-37304-0, 2019.

Allen, R. J., Landuyt, W. and Rumbold, S. T.: An increase in aerosol burden and radiative effects in a warmer world, Nat. Clim. Chang., 6(3), 269–274, doi:10.1038/nclimate2827, 2016.

Allen, R. J., Turnock, S., Nabat, P., Neubauer, D., Lohmann, U., Olivie, D., Oshima, N., Michou, M., Wu, T., Zhang, J., Takemura, T., Schulz, M., Tsigaridis, K., Bauer, S., Emmons, L., Horowitz, L., Naik, V., van Noije, T., Bergman, T., Lamarque, J.-F., Zanis, P., Tegen, I., Westervelt, D. M., Le Sager, P., Good, P., Shim, S., O'Connor, F., Akritidis, D., Georgoulias, A. K., Deushi, M., Sentman, L., Fujimori, S. and Collins, W. J.: Climate and air quality impacts due to mitigation of non-methane near-term climate forcers, Atmos. Chem. Phys. Discuss., In review, doi:https://doi.org/10.5194/acp-2019-1209, 2020.

Apte, J. S., Marshall, J. D., Cohen, A. J. and Brauer, M.: Addressing Global Mortality from Ambient PM 2.5, Environ. Sci. Technol., 49, 8057–8066, doi:10.1021/acs.est.5b01236, 2015.

Bauer, S. E., Tsigaridis, K., Faluvegi, G., Kelley, M., Lo, K. K., Miller, R. L., Nazarenko, L., Schmidt, G. A. and Wu, J.: Historical (1850-2014) aerosol evolution and role on climate forcing using the GISS ModelE2.1 contribution to CMIP6, J. Adv. Model. Earth Syst., doi:10.1029/2019ms001978, 2020.

Bloomer, B. J., Stehr, J. W., Piety, C. A., Salawitch, R. J. and Dickerson, R. R.: Observed relationships of ozone air pollution with temperature and emissions, Geophys. Res. Lett., 36(9), 1–5, doi:10.1029/2009GL037308, 2009.

Boucher, O., Randall, P., Artaxo, P., Bretherton, C., Feingold, G., Forster, P., Kerminen, V.-M., Kondo, Y., Liao, H., Lohmann, U., Rasch, P., Satheesh, S. K., Sherwood, S., Stevens, B. and Zhang, X. Y.: Clouds and Aerosols. In: Climate Change 2013: The Physical Science Basis. Contribution of Working Group I to the Fifth Assessment Report of the Intergovernmental Panel on Climate Change, Cambridge University Press., 2013.

Buchard, V., Randles, C. A., da Silva, A. M., Darmenov, A., Colarco, P. R., Govindaraju, R., Ferrare, R., Hair, J., Beyersdorf, A. J., Ziemba, L. D., Yu, H., Buchard, V., Randles, C. A., Silva, A. M. da, Darmenov, A., Colarco, P. R., Govindaraju, R., Ferrare, R., Hair, J., Beyersdorf, A. J., Ziemba, L. D. and Yu, H.: The MERRA-2 Aerosol Reanalysis, 1980 Onward. Part II: Evaluation and Case Studies, J. Clim., 30(17), 6851–6872, doi:10.1175/JCLI-D-16-0613.1, 2017.

Butt, E. W., Turnock, S. T., Rigby, R., Reddington, C. L., Yoshioka, M., Johnson, J. S., Regayre, L. A., Pringle, K. J., Mann, G. W. and Spracklen, D. V.: Global and regional trends in particulate air pollution and attributable health burden over the past 50 years, Environ. Res. Lett., 12(10), doi:10.1088/1748-9326/aa87be, 2017.

Checa-Garcia, R., Hegglin, M. I., Kinnison, D., Plummer, D. A. and Shine, K. P.: Historical Tropospheric and Stratospheric Ozone Radiative Forcing Using the CMIP6 Database, Geophys. Res. Lett., 45(7), 3264–3273, doi:10.1002/2017GL076770, 2018.

Chin, M., Diehl, T., Tan, Q., Prospero, J. M., Kahn, R. A., Remer, L. A., Yu, H., Sayer, A. M., Bian, H., Geogdzhayev, I. V., Holben, B. N., Howell, S. G., Huebert, B. J., Hsu, N. C., Kim, D., Kucsera, T. L., Levy, R. C., Mishchenko, M. I., Pan, X., Quinn, P. K., Schuster, G. L.,

Streets, D. G., Strode, S. A., Torres, O. and Zhao, X.-P.: Multi-decadal aerosol variations from 1980 to 2009: a perspective from observations and a global model, Atmos. Chem. Phys., 14(7), 3657–3690, doi:10.5194/acp-14-3657-2014, 2014.

Cohen, A. J., Brauer, M., Burnett, R., Anderson, H. R., Frostad, J., Estep, K., Balakrishnan, K., Brunekreef, B., Dandona, L., Dandona, R., Feigin, V., Freedman, G., Hubbell, B., Jobling, A., Kan, H., Knibbs, L., Liu, Y., Martin, R., Morawska, L., Pope, C. A., Shin, H., Straif, K., Shaddick, G., Thomas, M., van Dingenen, R., van Donkelaar, A., Vos, T., Murray, C. J. L. and Forouzanfar, M. H.: Estimates and 25-year trends of the global burden of disease attributable to ambient air pollution: an analysis of data from the Global Burden of Diseases Study 2015., Lancet (London, England), 389(10082), 1907–1918, doi:10.1016/S0140-6736(17)30505-6, 2017.

Colette, A., Andersson, C., Baklanov, A., Bessagnet, B., Brandt, J., Christensen, J. H., Doherty, R., Engardt, M., Geels, C., Giannakopoulos, C., Hedegaard, G. B., Katragkou, E., Langner, J., Lei, H., Manders, A., Melas, D., Meleux, F., Rouïl, L., Sofiev, M., Soares, J., Stevenson, D. S., Tombrou-Tzella, M., Varotsos, K. V and Young, P.: Is the ozone climate penalty robust in Europe?, Environ. Res. Lett., 10(8), 084015, doi:10.1088/1748-9326/10/8/084015, 2015.

Collins, J. W., Lamarque, J. F., Schulz, M., Boucher, O., Eyring, V., Hegglin, I. M., Maycock, A., Myhre, G., Prather, M., Shindell, D. and Smith, J. S.: AerChemMIP: Quantifying the effects of chemistry and aerosols in CMIP6, Geosci. Model Dev., 10(2), 585–607, doi:10.5194/gmd-10-585-2017, 2017.

Danabasoglu, G.: NCAR CESM2-WACCM model output prepared for CMIP6 AerChemMIP, , doi:10.22033/ESGF/CMIP6.10023, 2019a.

Danabasoglu, G.: NCAR CESM2-WACCM model output prepared for CMIP6 CMIP, , doi:10.22033/ESGF/CMIP6.10024, 2019b.

Danabasoglu, G.: NCAR CESM2-WACCM model output prepared for CMIP6 ScenarioMIP, , doi:10.22033/ESGF/CMIP6.10026, 2019c.

Doherty, R. M., Wild, O., Shindell, D. T., Zeng, G., MacKenzie, I. A., Collins, W. J., Fiore, A. M., Stevenson, D. S., Dentener, F. J., Schultz, M. G., Hess, P., Derwent, R. G. and Keating, T. J.: Impacts of climate change on surface ozone and intercontinental ozone pollution: A multi-model study, J. Geophys. Res. Atmos., 118(9), 3744–3763, doi:10.1002/jgrd.50266, 2013.

Dunne, J. P., Horowitz, L. W., Adcroft, A. J., Ginoux, P., Held, I. M., John, J. G., Krasting, J. P., Malyshev, S., Naik, V., Paulot, F., Shevliakova, E., Stock, C. A., Zadeh, N., Balaji, V., Blanton, C., Dunne, K. A., Dupuis, C., Durachta, J., Dussin, R., Gauthier, P. P. G., Griffies, S. M., Guo, H., Hallberg, R. W., Harrison, M., He, J., Hurlin, W., McHugh, C., Menzel, R., Milly, P. C. D., Nikonov, S., Paynter, D. J., Ploshay, J., Radhakrishnan, A., Rand, K., Reichl, B. G., Robinson, T., Schwarzkopf, D. M., Sentman, L. T., Underwood, S., Vahlenkamp, H., Winton, M., Wittenberg, A. T., Wyman, B., Zeng, Y. and Zhao, M.: The GFDL Earth System Model version 4.1 (GFDL-ESM4.1): Model 1 description and simulation characteristics, J. Adv. Model. Earth Syst., Submitted, 2020.

Emmons, L. K., Schwantes, R. H., Orlando, J. J., Tyndall, G., Kinnison, D., Lamarque, J., Marsh, D., Mills, M. J., Tilmes, S., Bardeen, C., Buchholz, R. R., Conley, A., Gettelman, A., Garcia, R., Simpson, I., Blake, D. R., Meinardi, S. and Pétron, G.: The Chemistry Mechanism in the Community Earth System Model Version 2 (CESM2), J. Adv. Model. Earth Syst., 12(4), 1–21, doi:10.1029/2019ms001882, 2020.

Eyring, V., Bony, S., Meehl, G. A., Senior, C. A., Stevens, B., Stouffer, R. J. and Taylor, K. E.: Overview of the Coupled Model Intercomparison Project Phase 6 (CMIP6) experimental design and organization, Geosci. Model Dev., 9(5), 1937–1958, doi:10.5194/gmd-9-1937-2016, 2016.

Fagerli, H. and Aas, W.: Trends of nitrogen in air and precipitation: Model results and observations at EMEP sites in Europe, 1980–2003, Environ. Pollut., 154(3), 448–461 [online] Available from: http://www.sciencedirect.com/science/article/pii/S0269749108000523 (Accessed 9 December 2013), 2008.

Fiore, A. M., Jacob, D. J., Field, B. D., Streets, D. G., Fernandes, S. D. and Jang, C.: Linking ozone pollution and climate change: The case for controlling methane, Geophys. Res. Lett., 29(19), 25–1, doi:10.1029/2002GL015601, 2002.

Fiore, A. M., Naik, V., Spracklen, D. V, Steiner, A., Unger, N., Prather, M., Bergmann, D., Cameron-Smith, P. J., Cionni, I., Collins, W. J., Dalsøren, S., Eyring, V., Folberth, G. a, Ginoux, P., Horowitz, L. W., Josse, B., Lamarque, J.-F., MacKenzie, I. a, Nagashima, T., O'Connor, F. M., Righi, M., Rumbold, S. T., Shindell, D. T., Skeie, R. B., Sudo, K., Szopa, S., Takemura, T. and Zeng, G.: Global air quality and climate., Chem. Soc. Rev., 41(19), 6663–83, doi:10.1039/c2cs35095e, 2012.

Forster, P. M., Maycock, A. C., McKenna, C. M. and Smith, C. J.: Latest climate models confirm need for urgent mitigation, Nat. Clim. Chang., 1–4, doi:10.1038/s41558-019-0660-0, 2019.

Fortems-Cheiney, A., Foret, G., Siour, G., Vautard, R., Szopa, S., Dufour, G., Colette, A., Lacressonniere, G. and Beekmann, M.: A 3 °C global RCP8.5 emission trajectory cancels benefits of European emission reductions on air quality, Nat. Commun., 8(89), 1–5, doi:10.1038/s41467-017-00075-9, 2017.

Fowler, D., Pilegaard, K., Sutton, M. A., Ambus, P., Raivonen, M., Duyzer, J., Simpson, D., Fagerli, H., Fuzzi, S., Schjoerring, J. K., Granier, C., Neftel, A., Isaksen, I. S. A., Laj, P., Maione, M., Monks, P. S., Burkhardt, J., Daemmgen, U., Neirynck, J., Personne, E., Wichink-Kruit,

R., Butterbach-Bahl, K., Flechard, C., Tuovinen, J. P., Coyle, M., Gerosa, G., Loubet, B., Altimir, N., Gruenhage, L., Ammann, C., Cieslik, S., Paoletti, E., Mikkelsen, T. N., Ro-Poulsen, H., Cellier, P., Cape, J. N., Horváth, L., Loreto, F., Niinemets, Ü., Palmer, P. I., Rinne, J., Misztal, P., Nemitz, E., Nilsson, D., Pryor, S., Gallagher, M. W., Vesala, T., Skiba, U., Brüggemann, N., Zechmeister-Boltenstern, S., Williams, J., O'Dowd, C., Facchini, M. C., de Leeuw, G., Flossman, A., Chaumerliac, N. and Erisman, J. W.: Atmospheric composition change: Ecosystems–Atmosphere interactions, Atmos. Environ., 43(33), 5193–5267, doi:10.1016/j.atmosenv.2009.07.068, 2009.

Gao, Y., Fu, J. S., Drake, J. B., Lamarque, J.-F. and Liu, Y.: The impact of emission and climate change on ozone in the United States under representative concentration pathways (RCPs), Atmos. Chem. Phys., 13(18), 9607–9621, doi:10.5194/acp-13-9607-2013, 2013.

Gettelman, A., Mills, M. J., Kinnison, D. E., Garcia, R. R., Smith, A. K., Marsh, D. R., Tilmes, S., Vitt, F., Bardeen, C. G., McInerny, J., Liu, H. L., Solomon, S. C., Polvani, L. M., Emmons, L. K., Lamarque, J. F., Richter, J. H., Glanville, A. S., Bacmeister, J. T., Phillips, A. S., Neale, R. B., Simpson, I. R., DuVivier, A. K., Hodzic, A. and Randel, W. J.: The Whole Atmosphere Community Climate Model Version 6 (WACCM6), J. Geophys. Res. Atmos., 124(23), 12380–12403, doi:10.1029/2019JD030943, 2019.

Gidden, M. J., Riahi, K., Smith, S. J., Fujimori, S., Luderer, G., Kriegler, E., van Vuuren, D. P., van den Berg, M., Feng, L., Klein, D., Calvin, K., Doelman, J. C., Frank, S., Fricko, O., Harmsen, M., Hasegawa, T., Havlik, P., Hilaire, J., Hoesly, R., Horing, J., Popp, A., Stehfest, E. and Takahashi, K.: Global emissions pathways under different socioeconomic scenarios for use in CMIP6: a dataset of harmonized emissions trajectories through the end of the century, Geosci. Model Dev., 12(4), 1443–1475, doi:10.5194/gmd-12-1443-2019, 2019.

Glotfelty, T., He, J. and Zhang, Y.: Impact of future climate policy scenarios on air quality and aerosol-cloud interactions using an advanced version of CESM/CAM5: Part I. model evaluation for the current decadal simulations, Atmos. Environ., 152, 222–239, doi:10.1016/J.ATMOSENV.2016.12.035, 2017.

Good, P.: MOHC HadGEM3-GC31-LL model output prepared for CMIP6 ScenarioMIP, , doi:10.22033/ESGF/CMIP6.10845, 2019.

Good, P., Sellar, A., Tang, Y., Rumbold, S., Ellis, R., Kelley, D., Kuhlbrodt, T. and Walton, J.: MOHC UKESM1.0-LL model output prepared for CMIP6 ScenarioMIP, , doi:10.22033/ESGF/CMIP6.1567, 2019.

Griffiths, P. T., Murray, L. T., Zeng, G., Archibald, A. T., Emmons, L. K., Galbally, I., Hassler, B., Horowitz, L. W., Keeble, J., Liu, J., Moeini, O., Naik, V., O'Connor, F. M., Shin, Y. M., Tarasick, D., Tilmes, S., Turnock, S. T., Wild, O., Young, P. J. and Zanis, P.: Tropospheric ozone in CMIP6 Simulations, Atmos. Chem. Phys. Discuss., (February), doi:https://doi.org/10.5194/acp-2019-1216, 2020.

Hajima, T. and Kawamiya, M.: MIROC MIROC-ES2L model output prepared for CMIP6 CMIP, , doi:10.22033/ESGF/CMIP6.902, 2019.

Hajima, T., Watanabe, M., Yamamoto, A., Tatebe, H., Noguchi, A., Abe, M., Ohgaito, R., Ito, A., Yamazaki, D., Ito, A., Takata, K., Ogochi, K. and Watanabe, S.: Description of the MIROC-ES2L Earth system model and evaluation of its climate – biogeochemical processes and feedbacks, Geosci. Model Dev. Discuss., 5(October), 2019.

Hoesly, R. M., Smith, S. J., Feng, L., Klimont, Z., Janssens-Maenhout, G., Pitkanen, T., Seibert, J. J., Vu, L., Andres, R. J., Bolt, R. M., Bond, T. C., Dawidowski, L., Kholod, N., Kurokawa, J., Li, M., Liu, L., Lu, Z., Moura, M. C. P., O'Rourke, P. R. and Zhang, Q.: Historical (1750–2014) anthropogenic emissions of reactive gases and aerosols from the Community Emissions Data System (CEDS), Geosci. Model Dev., 11(1), 369–408, doi:10.5194/gmd-11-369-2018, 2018.

Horowitz, L. W., Naik, V., Sentman, L. T., Paulot, F., Blanton, C., McHugh, C., Radhakrishnan, A., Rand, K., Vahlenkamp, H., Zadeh, N. T., Wilson, C., Ginoux, P., He, J., John, J. G., Lin, M., Paynter, D. J., Ploshay, J., Zhang, A. and Zeng, Y.: NOAA-GFDL GFDL-ESM4 model output prepared for CMIP6 AerChemMIP ssp370-lowNTCF, , Version 20180701, Earth System Grid Federation, doi:10.22033/ESGF/CMIP6.8693, 2018.

Horowitz, L. W., Naik, V., Paulot, F., Ginoux, P. A., Dunne, J. P., Mao, J., Schnell, J., Chen, X., He, J., John, J. G., Lin, M., Lin, P., Malyshev, S., Paynter, D., Shevliakova, E. and Zhao, M.: The GFDL Global Atmospheric Chemistry-Climate Model AM4.1: Model Description and Simulation Characteristics, J. Adv. Model. Earth Syst., Submitted, 2019.

Im, U., Christensen, J. H., Geels, C., Hansen, K. M., Brandt, J., Solazzo, E., Alyuz, U., Balzarini, A., Baro, R., Bellasio, R., Bianconi, R., Bieser, J., Colette, A., Curci, G., Farrow, A., Flemming, J., Fraser, A., Jimenez-Guerrero, P., Kitwiroon, N., Liu, P., Nopmongcol, U., Palacios-Peña, L., Pirovano, G., Pozzoli, L., Prank, M., Rose, R., Sokhi, R., Tuccella, P., Unal, A., Vivanco, M. G., Yarwood, G., Hogrefe, C. and Galmarini, S.: Influence of anthropogenic emissions and boundary conditions on multi-model simulations of major air pollutants over Europe and North America in the framework of AQMEII3, Atmos. Chem. Phys., 18(12), 8929–8952, doi:10.5194/acp-18-8929-2018, 2018.

Isaksen, I. S. A., Granier, C., Myhre, G., Berntsen, T. K., Dalsøren, S. B., Gauss, M., Klimont, Z., Benestad, R., Bousquet, P., Collins, W., Cox, T., Eyring, V., Fowler, D., Fuzzi, S., Jöckel, P., Laj, P., Lohmann, U., Maione, M., Monks, P., Prevot, A. S. H., Raes, F., Richter, A., Rognerud, B., Schulz, M., Shindell, D., Stevenson, D. S., Storelvmo, T., Wang, W.-C., van Weele, M., Wild, M. and Wuebbles, D.:

Atmospheric composition change: Climate–Chemistry interactions, Atmos. Environ., 43(33), 5138–5192 [online] Available from: http://www.sciencedirect.com/science/article/pii/S1352231009006943 (Accessed 9 December 2013), 2009.

Jacob, D. J. and Winner, D. a.: Effect of climate change on air quality, Atmos. Environ., 43(1), 51–63, doi:10.1016/j.atmosenv.2008.09.051, 2009.

John, J. G., Blanton, C., McHugh, C., Radhakrishnan, A., Rand, K., Vahlenkamp, H., Wilson, C., Zadeh, N. T., Gauthier, P. P. G., Dunne, J. P., Dussin, R., Horowitz, L. W., Lin, P., Malyshev, S., Naik, V., Ploshay, J., Silvers, L., Stock, C., Winton, M. and Zeng, Y.: NOAA-GFDL GFDL-ESM4 model output prepared for CMIP6 ScenarioMIP, , Version 20180701, Earth System Grid Federation, doi:10.22033/ESGF/CMIP6.1414, 2018.

Johnson, C. E., Collins, W. J., Stevenson, D. S. and Derwent, R. G.: Relative roles of climate and emissions changes on future tropospheric oxidant concentrations, J. Geophys. Res. Atmos., 104(D15), 18631–18645, doi:10.1029/1999JD900204, 1999.

Karset, I. H. H., Berntsen, T. K., Storelvmo, T., Alterskjær, K., Grini, A., Olivié, D., Kirkevåg, A., Seland, Ø., Iversen, T. and Schulz, M.: Strong impacts on aerosol indirect effects from historical oxidant changes, Atmos. Chem. Phys., 18(10), 7669–7690, doi:10.5194/acp-18-7669-2018, 2018.

Kirkevåg, A., Grini, A., Olivié, D., Seland, Ø., Alterskjær, K., Hummel, M., Karset, I. H. H., Lewinschal, A., Liu, X., Makkonen, R., Bethke, I., Griesfeller, J., Schulz, M. and Iversen, T.: A production-tagged aerosol module for Earth system models, OsloAero5.3 – extensions and updates for CAM5.3-Oslo, Geosci. Model Dev., 11(10), 3945–3982, doi:10.5194/gmd-11-3945-2018, 2018.

Kirtman, B., Power, S. B., Adedoyin, J. A., Boer, G. J., Bojariu, R., Camilloni, I., Doblas-Reyes, F. J., Fiore, A. M., Kimoto, M., Meehl, G. A., Prather, M., Sarr, A., Schar, C., Sutton, R., van Oldenborgh, G. J., Vecchi, G. and Wang, H. J.: Near-term Climate Change: Projections and Predictability. In: Climate Change 2013: The Physical Science Basis. Contribution of Working Group I to the Fifth Assessment Report of the Intergovernmental Panel on Climate Change, edited by T. F. Stocker, D. Qin, G.-K. Plattner, M. Tignore, S. K. Allen, J. Boschung, A. Nauels, Y. Xia, V. Bex, and P. M. Midgley, Cambridge University Press, Cambridge, United Kingdom and New York, NY, USA., 2013.

Krasting, J. P., John, J. G., Blanton, C., McHugh, C., Nikonov, S., Radhakrishnan, A., Rand, K., Zadeh, N. T., Balaji, V., Durachta, J., Dupuis, C., Menzel, R., Robinson, T., Underwood, S., Vahlenkamp, H., Dunne, K. A., Gauthier, P. P. G., Ginoux, P., Griffies, S. M., Hallberg, R., Harrison, M., Hurlin, W., Malyshev, S., Naik, V., Paulot, F., Paynter, D. J., Ploshay, J., Schwarzkopf, D. M., Seman, C. J., Silvers, L., Wyman, B., Zeng, Y., Adcroft, A., Dunne, J. P., Dussin, R., Guo, H., He, J., Held, I. M., Horowitz, L. W., Milly, P. C. D., Shevliakova, E., Stock, C., Winton, M., Xie, J. and Zhao, M.: NOAA-GFDL GFDL-ESM4 model output prepared for CMIP6 CMIP, , Version 20190726, Earth System Grid Federation, doi:10.22033/ESGF/CMIP6.1407, 2018.

Kuhlbrodt, T., Jones, C. G., Sellar, A., Storkey, D., Blockley, E., Stringer, M., Hill, R., Graham, T., Ridley, J., Blaker, A., Calvert, D., Copsey, D., Ellis, R., Hewitt, H., Hyder, P., Ineson, S., Mulcahy, J., Siahaan, A. and Walton, J.: The Low-Resolution Version of HadGEM3 GC3.1: Development and Evaluation for Global Climate, J. Adv. Model. Earth Syst., 10(11), 2865–2888, doi:10.1029/2018MS001370, 2018.

Lamarque, J.-F., Shindell, D. T., Josse, B., Young, P. J., Cionni, I., Eyring, V., Bergmann, D., Cameron-Smith, P., Collins, W. J., Doherty, R., Dalsoren, S., Faluvegi, G., Folberth, G., Ghan, S. J., Horowitz, L. W., Lee, Y. H., MacKenzie, I. A., Nagashima, T., Naik, V., Plummer, D., Righi, M., Rumbold, S. T., Schulz, M., Skeie, R. B., Stevenson, D. S., Strode, S., Sudo, K., Szopa, S., Voulgarakis, A. and Zeng, G.: The Atmospheric Chemistry and Climate Model Intercomparison Project (ACCMIP): overview and description of models, simulations and climate diagnostics, Geosci. Model Dev., 6(1), 179–206, doi:10.5194/gmd-6-179-2013, 2013.

Leibensperger, E. M., Mickley, L. J., Jacob, D. J., Chen, W.-T., Seinfeld, J. H., Nenes, a., Adams, P. J., Streets, D. G., Kumar, N. and Rind, D.: Climatic effects of 1950–2050 changes in US anthropogenic aerosols – Part 1: Aerosol trends and radiative forcing, Atmos. Chem. Phys., 12(7), 3333–3348, doi:10.5194/acp-12-3333-2012, 2012.

Lelieveld, J., Evans, J. S., Fnais, M., Giannadaki, D. and Pozzer, a: The contribution of outdoor air pollution sources to premature mortality on a global scale., Nature, 525(7569), 367–71, doi:10.1038/nature15371, 2015.

Li, K., Jacob, D. J., Liao, H., Shen, L., Zhang, Q. and Bates, K. H.: Anthropogenic drivers of 2013–2017 trends in summer surface ozone in China, Proc. Natl. Acad. Sci. U. S. A., 116(2), 422–427, doi:10.1073/pnas.1812168116, 2019.

Malley, C. S., Henze, D. K., Kuylenstierna, J. C. I., Vallack, H. W., Davila, Y., Anenberg, S. C., Turner, M. C. and Ashmore, M. R.: Updated Global Estimates of Respiratory Mortality in Adults ≥30 Years of Age Attributable to Long-Term Ozone Exposure, Environ. Health Perspect., 125(8), 087021, doi:10.1289/EHP1390, 2017.

van Marle, M. J. E., Kloster, S., Magi, B. I., Marlon, J. R., Daniau, A.-L., Field, R. D., Arneth, A., Forrest, M., Hantson, S., Kehrwald, N. M., Knorr, W., Lasslop, G., Li, F., Mangeon, S., Yue, C., Kaiser, J. W. and van der Werf, G. R.: Historic global biomass burning emissions

for CMIP6 (BB4CMIP) based on merging satellite observations with proxies and fire models (1750–2015), Geosci. Model Dev., 10(9), 3329–3357, doi:10.5194/gmd-10-3329-2017, 2017.

Michou, M., Nabat, P., Saint-Martin, D., Bock, J., Decharme, B., Mallet, M., Roehrig, R., Séférian, R., Sénési, S. and Voldoire, A.: Present-day and historical aerosol and ozone characteristics in CNRM CMIP6 simulations, J. Adv. Model. Earth Syst., 2019MS001816, doi:10.1029/2019MS001816, 2019.

Mortier, A., Gliss, J., Schulz, M., Aas, W., Andrews, E., Bian, H., Chin, M., Ginoux, P., Hand, J., Holben, B., Hua, Z., Kipling, Z., Kirkevåg, A., Laj, P., Lurton, T., Myhre, G., Neubauer, D., Olivié, D., von Salzen, K., Takemura, T. and Tilmes, S.: Evaluation of climate model aerosol trends with ground-based observations over the last two decades – an AeroCom and CMIP6 analysis, Atmos. Chem. Phys., 1–36, doi:10.5194/acp-2019-1203, 2020.

Mulcahy, J. P., Johnson, C., Jones, C. G., Povey, A. C., Scott, C. E., Sellar, A., Turnock, S. T., Woodhouse, M. T., Abraham, N. L., Andrews M., Bellouin, N., Browse, J., Carslaw, K. S., Dalvi, M., Folberth, G., Grosvenor, D., Hardacre, C., Johnson, B., Jones, A., Kipling, Z., Mann, G., Mollard, J., Schutgens, N., O'Connor, F., Palmieri, J., Reddington, C., Richardson, M., Stier, P., Woodward, S. and Yool, A.: Description and evaluation of aerosol in UKESM1 and HadGEM3-GC3.1 CMIP6 historical simulations, Geosci. Model Dev., submited(March), 2019.

Myhre, G., Shindell, D., Breon, F.-M., Collins, W., Fuglestvedt, J., Huang, J., Koch, D., Lamarque, J.-F., Lee, D., Mendoza, B., Nakajima, T., Robock, A., Stephens, G., Takemura, T. and Zhang, H.: Anthropogenic and Natural Radiative Forcing. In: Climate Change 2013: The Physical Science Basis. Contribution of Working Group I to the Fifth Assessment Report of the Intergovernemental Panel on Cliamte Change, edited by T. F. Stocker, D. Qin, G.-K. Plattner, M. Tignore, S. K. Allen, J. Boschung, A. Nauels, Y. Xia, V. Bex, and P. M. Midgley, Cambridge University Press, Cambridge, United Kingdom and New York, NY, USA., 2013.

NASA Goddard Institute For Space Studies (NASA/GISS): NASA-GISS GISS-E2.1H model output prepared for CMIP6 CMIP, , doi:10.22033/ESGF/CMIP6.1421, 2018.

Neal, L. S., Dalvi, M., Folberth, G., Mcinnes, R. N., Agnew, P., O 'connor, F. M., Savage, N. H. and Tilbee, M.: A description and evaluation of an air quality model nested within global and regional composition-climate models using MetUM, Geosci. Model Dev, 10, 3941–3962, doi:10.5194/gmd-10-3941-2017, 2017.

Neubauer, D., Ferrachat, S., Siegenthaler-Le Drian, C., Stoll, J., Folini, D. S., Tegen, I., Wieners, K.-H., Mauritsen, T., Stemmler, I., Barthel, S., Bey, I., Daskalakis, N., Heinold, B., Kokkola, H., Partridge, D., Rast, S., Schmidt, H., Schutgens, N., Stanelle, T., Stier, P., Watson-Parris, D. and Lohmann, U.: HAMMOZ-Consortium MPI-ESM1.2-HAM model output prepared for CMIP6 AerChemMIP, , doi:10.22033/ESGF/CMIP6.1621, 2019.

Norwegian Climate Center (NCC): NCC NorESM2-LM model output prepared for CMIP6 CMIP historical, [online] Available from: http://cera-www.dkrz.de/WDCC/meta/CMIP6/CMIP6.CMIP.NCC.NorESM2-LM.historical, 2018.

O'Neill, B. C., Kriegler, E., Riahi, K., Ebi, K. L., Hallegatte, S., Carter, T. R., Mathur, R. and van Vuuren, D. P.: A new scenario framework for climate change research: the concept of shared socioeconomic pathways, Clim. Change, 122(3), 387–400, doi:10.1007/s10584-013-0905-2, 2014.

O'Neill, B. C., Tebaldi, C., van Vuuren, D. P., Eyring, V., Friedlingstein, P., Hurtt, G., Knutti, R., Kriegler, E., Lamarque, J.-F., Lowe, J., Meehl, G. A., Moss, R., Riahi, K. and Sanderson, B. M.: The Scenario Model Intercomparison Project (ScenarioMIP) for CMIP6, Geosci. Model Dev., 9(9), 3461–3482, doi:10.5194/gmd-9-3461-2016, 2016.

Oshima, N., Yukimoto, S., Deushi, M., Koshiro, T., Kawai, H., Tanaka, T. Y. and Yoshida, K.: Global and Arctic effective radiative forcing of anthropogenic gases and aerosols in MRI-ESM2.0, Prog. Earth Planet. Sci., Accepted, 2020.

Pan, X., Chin, M., Gautam, R., Bian, H., Kim, D., Colarco, P. R., Diehl, T. L., Takemura, T., Pozzoli, L., Tsigaridis, K., Bauer, S. and Bellouin, N.: A multi-model evaluation of aerosols over South Asia: common problems and possible causes, Atmos. Chem. Phys., 15(10), 5903–5928, doi:10.5194/acp-15-5903-2015, 2015.

Parrish, D. D., Lamarque, J. F., Naik, V., Horowitz, L., Shindell, D. T., Staehelin, J., Derwent, R., Cooper, O. R., Tanimoto, H., Volz-Thomas, A., Gilge, S., Scheel, H. E., Steinbacher, M. and Fröhlich, M.: Long-term changes in lower tropospheric baseline ozone concentrations: Comparing chemistry-climate models and observations at northern midlatitudes, J. Geophys. Res., 119(9), 5719–5736, doi:10.1002/2013JD021435, 2014.

Pozzer, A., Meij, A. De, Pringle, K. J., Tost, H., Doering, U. M., Aardenne, J. Van and Lelieveld, J.: Distributions and regional budgets of aerosols and their precursors simulated with the EMAC chemistry-climate model, Atmos. Chem. Phys., 12, 961–987, doi:10.5194/acp-12-961-2012, 2012.

Pozzoli, L., Janssens-Maenhout, G., Diehl, T., Bey, I., Schultz, M. G., Feichter, J., Vignati, E. and Dentener, F.: Re-analysis of tropospheric

sulfate aerosol and ozone for the period 1980–2005 using the aerosol-chemistry-climate model ECHAM5-HAMMOZ, Atmos. Chem. Phys., 11(18), 9563–9594, doi:10.5194/acp-11-9563-2011, 2011.

Provençal, S., Buchard, V., da Silva, A. M., Leduc, R., Barrette, N., Elhacham, E. and Wang, S.-H.: Evaluation of PM2.5 surface concentration simulated by Version 1 of the NASA's MERRA Aerosol Reanalysis over Israel and Taiwan., Aerosol air Qual. Res., 17(1), 253–261, doi:10.4209/aaqr.2016.04.0145, 2017.

Randles, C. A., da Silva, A. M., Buchard, V., Colarco, P. R., Darmenov, A., Govindaraju, R., Smirnov, A., Holben, B., Ferrare, R., Hair, J., Shinozuka, Y., Flynn, C. J., Randles, C. A., Silva, A. M. da, Buchard, V., Colarco, P. R., Darmenov, A., Govindaraju, R., Smirnov, A., Holben, B., Ferrare, R., Hair, J., Shinozuka, Y. and Flynn, C. J.: The MERRA-2 Aerosol Reanalysis, 1980 Onward. Part I: System Description and Data Assimilation Evaluation, J. Clim., 30(17), 6823–6850, doi:10.1175/JCLI-D-16-0609.1, 2017.

Rao, S., Klimont, Z., Leitao, J., Riahi, K., Van Dingenen, R., Reis, L. A., Calvin, K., Dentener, F., Drouet, L., Fujimori, S., Harmsen, M., Luderer, G., Heyes, C., Strefler, J., Tavoni, M. and Van Vuuren, D. P.: A multi-model assessment of the co-benefits of climate mitigation for global air quality, Environ. Res. Lett., 11(12), 124013, doi:10.1088/1748-9326/11/12/124013, 2016.

Rao, S., Klimont, Z., Smith, S. J., Dingenen, R. Van, Dentener, F., Bouwman, L., Riahi, K., Amann, M., Bodirsky, B. L., Van Vuuren, D. P., Reis, L. A., Calvin, K., Drouet, L., Fricko, O., Fujimori, S., Gernaat, D., Havlik, P., Harmsen, M., Hasegawa, T., Heyes, C., Hilaire, J., Luderer, G., Masui, T., Stehfest, E., Strefler, J., Van Der Sluis, S. and Tavoni, M.: Future air pollution in the Shared Socio-economic Pathways, Glob. Environ. Chang., 42, 346–358, doi:10.1016/j.gloenvcha.2016.05.012, 2017.

Rasmussen, D. J., Hu, J., Mahmud, A. and Kleeman, J. M.: The Ozone Climate Penalty: past, present and future, Environ. Sci. Technol., 47(24), 14258–14266, doi:10.1109/TMI.2012.2196707.Separate, 2013.

Reddington, C. L., Carslaw, K. S., Stier, P., Schutgens, N., Coe, H., Liu, D., Allan, J., Browse, J., Pringle, K. J., Lee, L. A., Yoshioka, M., Johnson, J. S., Regayre, L. A., Spracklen, D. V., Mann, G. W., Clarke, A., Hermann, M., Henning, S., Wex, H., Kristensen, T. B., Leaitch, W. R., Pöschl, U., Rose, D., Andreae, M. O., Schmale, J., Kondo, Y., Oshima, N., Schwarz, J. P., Nenes, A., Anderson, B., Roberts, G. C., Snider, J. R., Leck, C., Quinn, P. K., Chi, X., Ding, A., Jimenez, J. L. and Zhang, Q.: The global aerosol synthesis and science project (GASSP): Measurements and modeling to reduce uncertainty, Bull. Am. Meteorol. Soc., 98(9), 1857–1877, doi:10.1175/BAMS-D-15-00317.1, 2017.

Reis, L. A., Drouet, L., van Dingenen, R. and Emmerling, J.: Future global air quality indices under different socioeconomic and climate assumptions, Sustain., 10(10), 1–27, doi:10.3390/su10103645, 2018.

Riahi, K., Van Vuuren, D. P., Kriegler, E., Edmonds, J., O 'neill, B. C., Fujimori, S., Bauer, N., Calvin, K., Dellink, R., Fricko, O., Lutz, W., Popp, A., Cuaresma, J. C., Kc, S., Leimbach, M., Jiang, L., Kram, T., Rao, S., Emmerling, J., Ebi, K., Hasegawa, T., Havlik, P., Humpenöder, F., Aleluia, L., Silva, D., Smith, S., Stehfest, E., Bosetti, V., Eom, J., Gernaat, D., Masui, T., Rogelj, J., Strefler, J., Drouet, L., Krey, V., Luderer, G., Harmsen, M., Takahashi, K., Baumstark, L., Doelman, J. C., Kainuma, M., Klimont, Z., Marangoni, G., Lotze-Campen, H., Obersteiner, M., Tabeau, A. and Tavoni, M.: The Shared Socioeconomic Pathways and their energy, land use, and greenhouse gas emissions implications: An overview, Glob. Environ. Chang., 42, 153–168, doi:10.1016/j.gloenvcha.2016.05.009, 2017.

Ridley, J., Menary, M., Kuhlbrodt, T., Andrews, M. and Andrews, T.: MOHC HadGEM3-GC31-LL model output prepared for CMIP6 CMIP, , doi:10.22033/ESGF/CMIP6.419, 2018.

Schultz, M. G., Schröder, S., Lyapina, O., Cooper, O., Galbally, I., Petropavlovskikh, I., Von Schneidemesser, E., Tanimoto, H., Elshorbany, Y., Naja, M., Seguel, R., Dauert, U., Eckhardt, P., Feigenspahn, S., Fiebig, M., Hjellbrekke, A.-G., Hong, Y.-D., Christian Kjeld, P., Koide, H., Lear, G., Tarasick, D., Ueno, M., Wallasch, M., Baumgardner, D., Chuang, M.-T., Gillett, R., Lee, M., Molloy, S., Moolla, R., Wang, T., Sharps, K., Adame, J. A., Ancellet, G., Apadula, F., Artaxo, P., Barlasina, M., Bogucka, M., Bonasoni, P., Chang, L., Colomb, A., Cuevas, E., Cupeiro, M., Degorska, A., Ding, A., Fröhlich, M., Frolova, M., Gadhavi, H., Gheusi, F., Gilge, S., Gonzalez, M. Y., Gros, V., Hamad, S. H., Helmig, D., Henriques, D., Hermansen, O., Holla, R., Huber, J., Im, U., Jaffe, D. A., Komala, N., Kubistin, D., Lam, K.-S., Laurila, T., Lee, H., Levy, I., Mazzoleni, C., Mazzoleni, L., McClure-Begley, A., Mohamad, M., Murovic, M., Navarro-Comas, M., Nicodim, F., Parrish, D., Read, K. A., Reid, N., Ries, L., Saxena, P., Schwab, J. J., Scorgie, Y., Senik, I., Simmonds, P., Sinha, V., Skorokhod, A., Spain, G., Spangl, W., Spoor, R., Springston, S. R., Steer, K., Steinbacher, M., Suharguniyawan, E., Torre, P., Trickl, T., Weili, L., Weller, R., Xu, X., Xue, L. and Zhiqiang, M.: Tropospheric Ozone Assessment Report: Database and Metrics Data of Global Surface Ozone Observations, Elem Sci Anth, 5(0), 58, doi:10.1525/elementa.244, 2017.

Seferian, R.: CNRM-CERFACS CNRM-ESM2-1 model output prepared for CMIP6 CMIP, , doi:10.22033/ESGF/CMIP6.1391, 2018.

Seferian, R.: CNRM-CERFACS CNRM-ESM2-1 model output prepared for CMIP6 AerChemMIP, , doi:10.22033/ESGF/CMIP6.1389, 2019.

Séférian, R., Nabat, P., Michou, M., Saint-Martin, D., Voldoire, A., Colin, J., Decharme, B., Delire, C., Berthet, S., Chevallier, M., Sénési, S., Franchisteguy, L., Vial, J., Mallet, M., Joetzjer, E., Geoffroy, O., Guérémy, J., Moine, M., Msadek, R., Ribes, A., Rocher, M., Roehrig, R., Salas-y-Mélia, D., Sanchez, E., Terray, L., Valcke, S., Waldman, R., Aumont, O., Bopp, L., Deshayes, J., Éthé, C. and Madec, G.: Evaluation of CNRM Earth System Model, CNRM-ESM2-1: Role of Earth System Processes in Present-Day and Future Climate, J. Adv. Model. Earth Syst., 2019MS001791, doi:10.1029/2019MS001791, 2019.

Sellar, A. A., Jones, C. G., Mulcahy, J., Tang, Y., Yool, A., Wiltshire, A., O'Connor, F. M., Stringer, M., Hill, R., Palmieri, J., Woodward, S., Mora, L., Kuhlbrodt, T., Rumbold, S., Kelley, D. I., Ellis, R., Johnson, C. E., Walton, J., Abraham, N. L., Andrews, M. B., Andrews, T., Archibald, A. T., Berthou, S., Burke, E., Blockley, E., Carslaw, K., Dalvi, M., Edwards, J., Folberth, G. A., Gedney, N., Griffiths, P. T., Harper, A. B., Hendry, M. A., Hewitt, A. J., Johnson, B., Jones, A., Jones, C. D., Keeble, J., Liddicoat, S., Morgenstern, O., Parker, R. J., Predoi, V., Robertson, E., Siahaan, A., Smith, R. S., Swaminathan, R., Woodhouse, M. T., Zeng, G. and Zerroukat, M.: UKESM1: Description and evaluation of the UK Earth System Model, J. Adv. Model. Earth Syst., 2019MS001739, doi:10.1029/2019MS001739, 2019.

Shen, L., Mickley, L. J. and Murray, L. T.: Influence of 2000–2050 climate change on particulate matter in the United States: results from a new statistical model, Atmos. Chem. Phys., 17(6), 4355–4367, doi:10.5194/acp-17-4355-2017, 2017.

Shindell, D. T., Kuylenstierna, J. C. I., Vignati, E., van Dingenen, R., Amann, M., Klimont, Z., Anenberg, S. C., Muller, N., Janssens-Maenhout, G., Raes, F., Schwartz, J., Faluvegi, G., Pozzoli, L., Kupiainen, K., Höglund-Isaksson, L., Emberson, L., Streets, D., Ramanathan, V., Hicks, K., Oanh, N. T. K., Milly, G., Williams, M., Demkine, V. and Fowler, D.: Simultaneously mitigating near-term climate change and improving human health and food security., Science, 335(6065), 183–9, doi:10.1126/science.1210026, 2012.

Silva, R. A., West, J. J., Lamarque, J. F., Shindell, D. T., Collins, W. J., Faluvegi, G., Folberth, G. A., Horowitz, L. W., Nagashima, T., Naik, V., Rumbold, S. T., Sudo, K., Takemura, T., Bergmann, D., Cameron-Smith, P., Doherty, R. M., Josse, B., MacKenzie, I. A., Stevenson, D. S. and Zeng, G.: Future global mortality from changes in air pollution attributable to climate change, Nat. Clim. Chang., 7(9), 647–651, doi:10.1038/nclimate3354, 2017.

Silva, R. a, West, J. J., Zhang, Y., Anenberg, S. C., Lamarque, J.-F., Shindell, D. T., Collins, W. J., Dalsoren, S., Faluvegi, G., Folberth, G., Horowitz, L. W., Nagashima, T., Naik, V., Rumbold, S., Skeie, R., Sudo, K., Takemura, T., Bergmann, D., Cameron-Smith, P., Cionni, I., Doherty, R. M., Eyring, V., Josse, B., MacKenzie, I. a, Plummer, D., Righi, M., Stevenson, D. S., Strode, S., Szopa, S. and Zeng, G.: Global premature mortality due to anthropogenic outdoor air pollution and the contribution of past climate change, Environ. Res. Lett., 8, 034005, doi:10.1088/1748-9326/8/3/034005, 2013.

Solazzo, E., Bianconi, R., Hogrefe, C., Curci, G., Tuccella, P., Alyuz, U., Balzarini, A., Baró, R., Bellasio, R., Bieser, J., Brandt, J., Christensen, J. H., Colette, A., Francis, X., Fraser, A., Vivanco, M. G., Jiménez-Guerrero, P., Im, U., Manders, A., Nopmongcol, U., Kitwiroon, N., Pirovano, G., Pozzoli, L., Prank, M., Sokhi, R. S., Unal, A., Yarwood, G. and Galmarini, S.: Evaluation and error apportionment of an ensemble of atmospheric chemistry transport modeling systems: multivariable temporal and spatial breakdown, Atmos. Chem. Phys., 17(4), 3001–3054, doi:10.5194/acp-17-3001-2017, 2017.

Tachiiri, K. and Kawamiya, M.: MIROC MIROC-ES2L model output prepared for CMIP6 ScenarioMIP, , doi:10.22033/ESGF/CMIP6.936, 2019.

Takemura, T.: Distributions and Climate Effects of Atmospheric Aerosols from the preindustrial era to 2100 along Representative Concentration Pathways (RCPs) simulated using the GLobal Aerosol Model SPRINTARS, Atmos. Chem. Phys., 12, 11555–11572 [online] Available from: http://www.atmos-chem-phys.net/12/11555/2012/acp-12-11555-2012.pdf, 2012.

Tang, Y., Rumbold, S., Ellis, R., Kelley, D., Mulcahy, J., Sellar, A., Walton, J. and Jones, C.: MOHC UKESM1.0-LL model output prepared for CMIP6 CMIP, , doi:10.22033/ESGF/CMIP6.1569, 2019.

Taylor, K. E., Stouffer, R. J. and Meehl, G. A.: An Overview of CMIP5 and the Experiment Design, Bull. Am. Meteorol. Soc., 93(4), 485–498, doi:10.1175/BAMS-D-11-00094.1, 2012.

Tegen, I., Neubauer, D., Ferrachat, S., Siegenthaler-Le Drian, C., Bey, I., Schutgens, N., Stier, P., Watson-Parris, D., Stanelle, T., Schmidt, H., Rast, S., Kokkola, H., Schultz, M., Schroeder, S., Daskalakis, N., Barthel, S., Heinold, B. and Lohmann, U.: The global aerosol–climate model ECHAM6.3–HAM2.3 – Part 1: Aerosol evaluation, Geosci. Model Dev., 12(4), 1643–1677, doi:10.5194/gmd-12-1643-2019, 2019.

Tilmes, S., Hodzic, A., Emmons, L. K., Mills, M. J., Gettelman, A., Kinnison, D. E., Park, M., Lamarque, J. -F., Vitt, F., Shrivastava, M., Campuzano Jost, P., Jimenez, J. and Liu, X.: Climate forcing and trends of organic aerosols in the Community Earth System Model (CESM2), J. Adv. Model. Earth Syst., 2019MS001827, doi:10.1029/2019MS001827, 2019.

Tørseth, K., Aas, W., Breivik, K., Fjæraa, a. M., Fiebig, M., Hjellbrekke, a. G., Lund Myhre, C., Solberg, S. and Yttri, K. E.: Introduction to the European Monitoring and Evaluation Programme (EMEP) and observed atmospheric composition change during 1972–2009, Atmos.

Chem. Phys., 12(12), 5447–5481, doi:10.5194/acp-12-5447-2012, 2012.

Tsigaridis, K., Daskalakis, N., Kanakidou, M., Adams, P. J., Artaxo, P., Bahadur, R., Balkanski, Y., Bauer, S. E., Bellouin, N., Benedetti, A., Bergman, T., Berntsen, T. K., Beukes, J. P., Bian, H., Carslaw, K. S., Chin, M., Curci, G., Diehl, T., Easter, R. C., Ghan, S. J., Gong, S. L., Hodzic, A., Hoyle, C. R., Iversen, T., Jathar, S., Jimenez, J. L., Kaiser, J. W., Kirkevåg, A., Koch, D., Kokkola, H., Lee, Y. H., Lin, G., Liu, X., Luo, G., Ma, X., Mann, G. W., Mihalopoulos, N., Morcrette, J.-J., Müller, J.-F., Myhre, G., Myriokefalitakis, S., Ng, N. L., O'Donnell, D., Penner, J. E., Pozzoli, L., Pringle, K. J., Russell, L. M., Schulz, M., Sciare, J., Seland, Ø., Shindell, D. T., Sillman, S., Skeie, R. B., Spracklen, D., Stavrakou, T., Steenrod, S. D., Takemura, T., Tiitta, P., Tilmes, S., Tost, H., van Noije, T., van Zyl, P. G., von Salzen, K., Yu, F., Wang, Z., Zaveri, R. A., Zhang, H., Zhang, K., Zhang, Q. and Zhang, X.: The AeroCom evaluation and intercomparison of organic aerosol in global models, Atmos. Chem. Phys., 14(19), 10845–10895, doi:10.5194/acp-14-10845-2014, 2014.

Turnock, S. T., Spracklen, D. V., Carslaw, K. S., Mann, G. W., Woodhouse, M. T., Forster, P. M., Haywood, J., Johnson, C. E., Dalvi, M., Bellouin, N. and Sanchez-Lorenzo, a.: Modelled and observed changes in aerosols and surface solar radiation over Europe between 1960 and 2009, Atmos. Chem. Phys., 15, 9477–9500, doi:10.5194/acp-15-9477-2015, 2015.

Turnock, S. T., Wild, O., Dentener, F. J., Davila, Y., Emmons, L. K., Flemming, J., Folberth, G. A., Henze, D. K., Jonson, J. E., Keating, T. J., Kengo, S., Lin, M., Lund, M., Tilmes, S. and O'Connor, F. M.: The impact of future emission policies on tropospheric ozone using a parameterised approach, Atmos. Chem. Phys., 18(12), 8953–8978, doi:10.5194/acp-18-8953-2018, 2018.

Turnock, S. T., Wild, O., Sellar, A. and O'Connor, F. M.: 300 years of tropospheric ozone changes using CMIP6 scenarios with a parameterised approach, Atmos. Environ., 213, 686–698, doi:10.1016/J.ATMOSENV.2019.07.001, 2019.

United Nations: Paris Agreement, 2016.

Voldoire, A.: CNRM-CERFACS CNRM-ESM2-1 model output prepared for CMIP6 ScenarioMIP, , doi:10.22033/ESGF/CMIP6.1395, 2019.

van Vuuren, D. P., Kriegler, E., O'Neill, B. C., Ebi, K. L., Riahi, K., Carter, T. R., Edmonds, J., Hallegatte, S., Kram, T., Mathur, R. and Winkler, H.: A new scenario framework for Climate Change Research: scenario matrix architecture, Clim. Change, 122(3), 373–386, doi:10.1007/s10584-013-0906-1, 2014.

Weaver, C. P., Liang, X. Z., Zhu, J., Adams, P. J., Amar, P., Avise, J., Caughey, M., Chen, J., Cohen, R. C., Cooter, E., Dawson, J. P., Gilliam, R., Gilliland, A., Goldstein, A. H., Grambsch, A., Grano, D., Guenther, A., Gustafson, W. I., Harley, R. A., He, S., Hemming, B., Hogrefe, C., Huang, H. C., Hunt, S. W., Jacob, D. J., Kinney, P. L., Kunkel, K., Lamarque, J. F., Lamb, B., Larkin, N. K., Leung, L. R., Liao, K. J., Lin, J. T., Lynn, B. H., Manomaiphiboon, K., Mass, C., Mckenzie, D., Mickley, L. J., O'Neill, S. M., Nolte, C., Pandis, S. N., Racherla, P. N., Rosenzweig, C., Russell, A. G., Salathé, E., Steiner, A. L., Tagaris, E., Tao, Z., Tonse, S., Wiedinmyer, C., Williams, A., Winner, D. A., Woo, J. H., Wu, S. and Wuebbles, D. J.: A preliminary synthesis of modeled climate change impacts on U.S. regional ozone concentrations, Bull. Am. Meteorol. Soc., 90(12), 1843–1863, doi:10.1175/2009BAMS2568.1, 2009.

Westervelt, D. M., Horowitz, L. W., Naik, V., Tai, A. P. K., Fiore, A. M. and Mauzerall, D. L.: Quantifying PM2.5-meteorology sensitivities in a global climate model, Atmos. Environ., 142, 43–56, doi:10.1016/J.ATMOSENV.2016.07.040, 2016.

Wild, O. and Prather, M. J.: Global tropospheric ozone modeling: Quantifying errors due to grid resolution, J. Geophys. Res. Atmos., 111(11), 1–14, doi:10.1029/2005JD006605, 2006.

Wild, O., Fiore, A. M., Shindell, D. T., Doherty, R. M., Collins, W. J., Dentener, F. J., Schultz, M. G., Gong, S., Mackenzie, I. A., Zeng, G., Hess, P., Duncan, B. N., Bergmann, D. J., Szopa, S., Jonson, J. E., Keating, T. J. and Zuber, A.: Modelling future changes in surface ozone: A parameterized approach, Atmos. Chem. Phys., 12(4), 2037–2054, doi:10.5194/acp-12-2037-2012, 2012.

Wild, O., Voulgarakis, A., O'Connor, F., Lamarque, J. F., Ryan, E. M. and Lee, L.: Global sensitivity analysis of chemistry-climate model budgets of tropospheric ozone and OH: Exploring model diversity, Atmos. Chem. Phys., 20(7), 4047–4058, doi:10.5194/acp-20-4047-2020, 2020.

de Wit, H. A., Hettelingh, J.-P. and Harmens, H.: Trends in ecosystem and health responses to long-range transported atmospheric pollutants (ICP Waters Report 125/2015). [online] Available from: https://www.unece.org/fileadmin/DAM/env/documents/2016/AIR/Publications/Trends_in_ecosystem_and_health_responses_to_long-range_transported_atmospheric_pollutants.pdf, 2015.

Wu, S., Mickley, L. J., Leibensperger, E. M., Jacob, D. J., Rind, D. and Streets, D. G.: Effects of 2000-2050 global change on ozone air quality in the United States, J. Geophys. Res. Atmos., 113(6), doi:10.1029/2007JD008917, 2008.

Wu, T., Lu, Y., Fang, Y., Xin, X., Li, L., Li, W., Jie, W., Zhang, J., Liu, Y., Zhang, L., Zhang, F., Zhang, Y., Wu, F., Li, J., Chu, M., Wang, Z., Shi, X., Liu, X., Wei, M., Huang, A., Zhang, Y. and Liu, X.: The Beijing Climate Center Climate System Model (BCC-CSM): the main

progress from CMIP5 to CMIP6, Geosci. Model Dev., 12(4), 1573–1600, doi:10.5194/gmd-12-1573-2019, 2019.

Wu, T., Zhang, F., Zhang, J., Jie, W., Zhang, Y., Wu, F., Li, L., Yan, J., Liu, X., Lu, X., Tan, H., Zhang, L., Wang, J. and Hu, A.: Beijing Climate Center Earth System Model version 1 (BCC-ESM1): Model description and evaluation of aerosol simulations, Geosci. Model Dev., 13(3), 977–1005, doi:10.5194/gmd-13-977-2020, 2020.

Young, P. J., Archibald, A. T., Bowman, K. W., Lamarque, J.-F., Naik, V., Stevenson, D. S., Tilmes, S., Voulgarakis, A., Wild, O., Bergmann, D., Cameron-Smith, P., Cionni, I., Collins, W. J., Dalsøren, S. B., Doherty, R. M., Eyring, V., Faluvegi, G., Horowitz, L. W., Josse, B., Lee, Y. H., MacKenzie, I. A., Nagashima, T., Plummer, D. A., Righi, M., Rumbold, S. T., Skeie, R. B., Shindell, D. T., Strode, S. A., Sudo, K., Szopa, S. and Zeng, G.: Pre-industrial to end 21st century projections of tropospheric ozone from the Atmospheric Chemistry and Climate Model Intercomparison Project (ACCMIP), Atmos. Chem. Phys., 13(4), 2063–2090, doi:10.5194/acp-13-2063-2013, 2013.

Young, P. J., Naik, V., Fiore, A. M., Gaudel, A., Guo, J., Lin, M. Y., Neu, J. L., Parrish, D. D., Rieder, H. E., Schnell, J. L., Tilmes, S., Wild, O., Zhang, L., Ziemke, J. R., Brandt, J., Delcloo, A., Doherty, R. M., Geels, C., Hegglin, M. I., Hu, L., Im, U., Kumar, R., Luhar, A., Murray, L., Plummer, D., Rodriguez, J., Saiz-Lopez, A., Schultz, M. G., Woodhouse, M. T. and Zeng, G.: Tropospheric Ozone Assessment Report: Assessment of global-scale model performance for global and regional ozone distributions, variability, and trends, Elem Sci Anth, 6(1), 10, doi:10.1525/elementa.265, 2018.

Yukimoto, S., Koshiro, T., Kawai, H., Oshima, N., Yoshida, K., Urakawa, S., Tsujino, H., Deushi, M., Tanaka, T., Hosaka, M., Yoshimura, H., Shindo, E., Mizuta, R., Ishii, M., Obata, A. and Adachi, Y.: MRI MRI-ESM2.0 model output prepared for CMIP6 AerChemMIP, , doi:10.22033/ESGF/CMIP6.633, 2019a.

Yukimoto, S., Koshiro, T., Kawai, H., Oshima, N., Yoshida, K., Urakawa, S., Tsujino, H., Deushi, M., Tanaka, T., Hosaka, M., Yoshimura, H., Shindo, E., Mizuta, R., Ishii, M., Obata, A. and Adachi, Y.: MRI MRI-ESM2.0 model output prepared for CMIP6 CMIP historical, , doi:10.22033/ESGF/CMIP6.6842, 2019b.

Yukimoto, S., Koshiro, T., Kawai, H., Oshima, N., Yoshida, K., Urakawa, S., Tsujino, H., Deushi, M., Tanaka, T., Hosaka, M., Yoshimura, H., Shindo, E., Mizuta, R., Ishii, M., Obata, A. and Adachi, Y.: MRI MRI-ESM2.0 model output prepared for CMIP6 ScenarioMIP, , doi:10.22033/ESGF/CMIP6.638, 2019c.

Yukimoto, S., Kawai, H., Koshiro, T., Oshima, N., Yoshida, K., Urakawa, S., Tsujino, H., Deushi, M., Tanaka, T., Hosaka, M., Yabu, S., Yoshimura, H., Shindo, E., Mizuta, R., Obata, A., Adachi, Y. and Ishii, M.: The meteorological research institute Earth system model version 2.0, MRI-ESM2.0: Description and basic evaluation of the physical component, J. Meteorol. Soc. Japan, 97(5), 931–965, doi:10.2151/jmsj.2019-051, 2019d.

Zhang, J., Wu, T., Shi, X., Zhang, F., Li, J., Chu, M., Liu, Q., Yan, J., Ma, Q. and Wei, M.: BCC BCC-ESM1 model output prepared for CMIP6 CMIP, , doi:10.22033/ESGF/CMIP6.1734, 2018.

Zhang, J., Wu, T., Shi, X., Zhang, F., Li, J., Chu, M., Liu, Q., Yan, J., Ma, Q. and Wei, M.: BCC BCC-ESM1 model output prepared for CMIP6 AerChemMIP, , doi:10.22033/ESGF/CMIP6.1733, 2019.